Geoarchaeological Case Studies at the Lower Guadiana Estuary:

Paleogeographic Development and Human-Environment Interactions at the Phoenician Site of Ayamonte (SW-Andalusia/Spain)

Dissertation

zur Erlangung des akademischen Grades

Doktor der Naturwissenschaften (Dr. rer. nat.)

am Fachbereich Geowissenschaften

der Freien Universität Berlin

vorgelegt von

Torsten Klein

Berlin 2018

Erstgutachterin:

Prof. Dr. Brigitta Schütt

Institut für Geographische Wissenschaften Fachbereich Geowissenschaften

Freie Universität Berlin

Malteserstr. 74-100

12249 Berlin

Zweitgutachterin:

Prof. Dr. Wiebke Bebermeier

Institut für Geographische Wissenschaften Fachbereich Geowissenschaften

Freie Universität Berlin

Malteserstr. 74-100

12249 Berlin

Tag der Disputation:

15.05.2018

Erklärung

Hiermit erkläre ich, dass ich die Dissertation „*Geoarchaeological Case Studies at the Lower Guadiana Estuary: Paleogeographic Development and Human-Environment Interactions at the Phoenician Site of Ayamonte (SW-Andalusia/Spain)*“ selbständig angefertigt und keine anderen als die von mir angegebenen Quellen und Hilfsmittel verwendet habe.

Ich erkläre weiterhin, dass die Dissertation bisher nicht in dieser oder in anderer Form in einem anderen Prüfungsverfahren vorgelegen hat.

Leipzig, 03.02.2018

Torsten Klein

Acknowledgements

This thesis was supported by the Cluster of Excellence Exc264 Topoi funded by the German Research Foundation (DFG).

I would like to express my great appreciation to my first supervisor, Prof. Dr. Brigitta Schütt, for giving me the chance to participate in this project and for the support throughout the years. Furthermore, I would like to thank my second supervisor, Prof. Dr. Wiebke Bebermeier, for the stimulating discussions and for supporting me. The work in and on Ayamonte would not have been possible without the help of Prof. Dr. Dirce Marzoli, German Archaeological Institute Madrid (DAI) and I want to thank her for that. In addition, I want to thank Elisabeth García Teyssandier, Benjamin Cabaco Encinas and Sarah Ißelhorst without whom fieldwork would not have been possible. I would like to thank the Junta of Andalucía and the municipality of Ayamonte for granting survey and drilling permission.

Furthermore, I would like to thank the other members of the working group Physical Geography at the FU Berlin who contributed to the thesis in one way or another: Dr. Jan Krause who provided me not only with artisanal support in the field, but also with logistic and administrative advice, Dr. Philip Hoelzmann, Manuela Scholz and Michaela Scholz for support in the Geomorphological Laboratory and all members of the working group.

I would like to express my sincere thanks to my friends and family, giving me inspiration and motivation.

Abstract

Recent excavations, under direction of the German Archaeological Institute Madrid, revealed extensive remains of Phoenician culture in the environs of the west-Andalusian city of Ayamonte, located at the mouth of the Guadiana River. Among others Phoenician tombs and the associated settlement were brought to light and provide information about the cultural landscape of the lowermost part of the Guadiana River around 3000 years ago.

The Guadiana River is one of the major streams draining the Iberian Peninsula and its lower estuary has been extensively studied in terms of ecological stress due to damming (e.g. the Alqueva dam) and postglacial sea-level rise, but geoarchaeological studies are rarely found. This study aims to answer geoarchaeological questions arising during intensive discussions about landscape sensitivity and human-environment interactions in the surrounding of the mentioned excavations. Geomorphological and sedimentological investigations are coupled with archaeological information.

Three selected landscape types with different research questions are presented in the form of detailed case studies: (a) the surroundings of the silted-up lagoonal-like environment of the "Estero de la Nao", (b) the terrestrial archives of adjacent slopes, close to the excavation and (c) the coastal marshland of the lower Guadiana Estuary.

The case studies reveal approximately 6000 years of rapid landscape change within the estuary and its environs. (a) The sedimentary archive of the lagoonal-like environment shows three important aspects of landscape development: (I) rapid siltation of a former open-water body, (II) indications on dredging activity in order to maintain an assumed anchorage in operation and (III) sedimentological traces of the tsunami generated from the Great Lisbon Earthquake in 1755. (b) Sedimentological results from adjacent slopes

confirm early settlement activity with a long-standing erosive history, accounted geomorphic phases of slope stability and slope instability as well as evidence of early ore mining activity. (c) Sedimentological and cartographic studies of the estuarine marshland reveal a rapid coastal evolution, allowing to design a paleogeographic scenario of the Late Holocene development of the lower Guadiana Estuary.

Zusammenfassung

Als 2007, im Zuge von Bauarbeiten in der westandalusischen Grenzstadt Ayamonte, einzelne phönizische Funde entdeckt wurden, erbrachten die darauffolgenden Rettungsgrabungen, geleitet vom Deutschen Archäologischen Institut Madrid, phönizische Gräber sowie eine zeitgleiche prähistorische Siedlung zum Vorschein. Die Hinterlassenschaften stellen bedeutende Informationen über die phönizische Kulturlandschaft dar.

Der Fluss Guadiana ist einer der großen Ströme, die die Iberische Halbinsel entwässern. Sein Mündungsbereich -ein gezeitenbeeinflusster Ästuar- ist ein intensiv untersuchter Raum und Forschungsobjekt zahlreicher ökologischer Studien sowie ein sehr gutes Geoarchiv zur Recherche des postglazialen Meeresspiegelanstieges. Studien mit einem geoarchäologischen Schwerpunkt in diesem Raum sind dagegen selten anzufinden. Die Beantwortung geoarchäologischer Forschungsfragen, die während intensiver Diskussionen über die landschaftliche Formung des Raumes sowie den Mensch-Umwelt-Interaktionen, geführt wurden, stellen die inhaltlichen Schwerpunkte dieser Arbeit dar. Zur Beantwortung der Forschungsfragen wurden, geomorphologische und kartographische Methoden mit archäologischen Informationen gekoppelt.

Die örtlichen Schwerpunkte der Untersuchungen liegen hierbei auf drei Landschaftsteilräumen in und um Ayamonte, die in einzelnen Fallstudien bearbeitet werden: (a) Die erste Fallstudie widmet sich den Sedimenten einer verlandeten lagunenartigen Bucht im rückwärtigen Hinterland der phönizischen Siedlung. (b) Fallstudie zwei beschäftigt sich mit den Erkenntnissen, die aus Hangsedimenten unweit der antiken Siedlung gewonnen werden konnten. (c) Die dritte Fallstudie ist im küstennahen Marschland verortet und bearbeitet den thematischen Schwerpunkt der spätholozänen Küstenveränderungen innerhalb des Guadianaästuars.

Die Ergebnisse belegen eine 6000 Jahre währende Geschichte raschen Landschaftswandels innerhalb des Ästuars aber auch der umliegenden Landschaftsteilräume. (a) Die Studie innerhalb der verlandeten lagunenartigen Bucht zeigt drei wichtige Aspekte landschaftlichen Wandels auf: (I) Zum einen belegen die Ergebnisse die teilweise Schiffbarkeit, jedoch auch die schnelle Verlandung des ehemals wasserführenden Raumes. (II) Des Weiteren zeigen die Resultate eines Bohrkerns, dass es womöglich anthropogene Eingriffe an einem Standort gegeben hat, an dem ein antiker Ankerplatz vermutet wird, mit dem Ziel diesen vor der voranschreitenden Verlandung zu bewahren und ihn somit weiter nutzbar zu halten. (III) Schlussendlich konnten außerdem Verwüstungsspuren innerhalb eines Kernes, die mit hoher Wahrscheinlichkeit von dem Tsunami, ausgelöst durch das verheerende Erdbeben am 1. November 1755, stammen, entdeckt und zugeordnet werden. (b) Ergebnisse der zweiten Studie liefern Hinweise auf die frühe Besiedlung des Standorts, sowie eine ausgeprägte Erosionsgeschichte mit deutlichen Aktivitäts- und Stabilitätsphasen. Ferner konnte mit geochemischen Methoden, der Nachweis frühzeitlicher Erzverhüttung erbracht werden. (c) Sedimentologische und kartographische Untersuchungen im küstennahem Marschland dokumentieren die sehr dynamische Küstenveränderung innerhalb des Ästuars und ermöglichen es aufschlussreiche Rekonstruktionsszenarien der letzten 6000 Jahre zu entwerfen.

I. List of Contents

II. List of Figures

III. List of Tables

1. Introduction

1.1 Project Background

Considering the numerous geoscientific studies during the past decades, the knowledge of prehistoric coastal landscape development along the southwest-Iberian coasts has been largely improved. However, little attention is paid to the areas along the Atlantic coast of southwest Iberia concerning the transformation of the natural space in a geoarchaeological context. Along the Mediterranean coast of southwest Iberia, various publications exist broaching the issue of the paleogeographies of prehistoric cities within these areas (many of them of Phoenician culture) and its geoarchaeological implications (Arteaga, 1988; Arteaga et al., 1989; Hoffmann and Schulz, 1987; Hoffmann and Schulz, 1988; Schubart et al., 1988; Schubart et al., 1989; Schulz, 2011). Although studies in the coastal areas west of the Strait of Gibraltar exist, those focus mainly on the mouths of the Guadalquivir and Guadalete Rivers (Arteaga et al., 2001; Arteaga and Roos, 2002; Borja et al., 1999; Caro Gómez et al., 2011; Dabrio et al., 1998; Dabrio et al., 2000; Lario et al., 2002; Zazo et al., 1998; Zazo et al., 2008a; Zazo et al., 2005). In addition to the investigations of these two coastal areas, there are many studies that are dedicated to the Holocene development at the Tinto-Odiel Estuary, located 40 km east of the city of Ayamonte. Here the focus is often set on the estuarine heavy metal load because of pre-historic mining (Avery, 1974; Borrego et al., 2004; Borrego et al., 2005; Borrego et al., 1999; Boulter, 1993; Cáceres et al., 2013; Davis Jr et al., 2000; Morral, 1990; Rufo et al., 2007; Ruiz et al., 2008). Studies on the Guadiana Estuary are numerically less represented and are mainly focused on the structure of the delta sediments offshore (González et al., 2004; Lobo et al., 2003; Lobo et al., 2005; Mendes et al., 2004; Mendes et al., 2010), the processes during post-glacial sea level rise (Boski et al., 2008; Boski et al., 2002; Delgado et al., 2012a; Fletcher et al., 2007; Sampath et al., 2015; Sampath et al., 2011) or the effects due to modern constructions such as jetties and dams (González et al., 2001; Morales et al., 2006).

With the discovery of a Phoenician necropolis in Ayamonte and a settlement with subsequent excavations (Teyssandier and Marzoli, 2014), the German Archaeological Institute (DAI) and the DFG funded Cluster of Excellence 264 'Topoi' initiated a common project focusing on the paleogeography and geoarchaeology of the west-Andalusian city and its surroundings. Mainly because of its location in the outer west of the Phoenician expansion area, the newly discovered necropolis is to be examined especially under aspects of marginality (Bebermeier et al., 2016). Particular emphasis is given to the aspects of environmental and spatial marginality. This doctoral thesis is written within the Research Group A-1 Ancient *Colonizations of marginal habitats* and aims to contribute to a better understanding of human-environment interactions triggered by the prehistoric use of the settlement site on the banks of the Guadiana Estuary.

1.2 Structure and Objectives

This doctoral thesis is structured into 5 chapters. Chapter 1 provides information about the project background, the central research aims as well as the strategy of the thesis. The regional setting chapter (Chapter 2) introduces the study area with increasing scale considerations. It provides information on geology, geomorphology, geotectonics, soils and hydrology. In addition, it provides a brief overview on the archaeological research of the area (Chapter 2.4). Chapter 3 introduces materials and methods applied in this thesis and provides information on field work, sediment analysis and the applied dating approach. In chapter 4 three case studies with different case-specific research questions and research goals are presented:

a. Case study 1 (Chapter 4.1): "Sedimentological evidence of an assumed ancient anchorage in the hinterland of a Phoenician settlement (Guadiana Estuary/SW-Spain)", authored in cooperation with Wiebke Bebermeier, Jan Krause, Dirce Marzoli and Brigitta Schütt, published in Quaternary International, Volume 407, Part A, 2 July 2016, Pages 110–125, Progress in Quaternary Archive Studies of the Iberian Peninsula
b. Case study 2 (Chapter 4.2): "Human-Environment Interactions at the Phoenician Site of Ayamonte (Huelva/Spain): – Insights from Terrestrial Borehole Data"
c. Case study 3 (Chapter 4.3): "Rapid Late Holocene Estuarine Changes and Anthropogenic Activities at the Guadiana Estuary (SW-Spain) Recorded in Sedimentary and Cartographic Archives"

The final chapter 5 combines the results from the case studies and integrates them into the geoarchaeological framework. The chapter deals with the main research questions of the research project: How beneficial or unfavorable were the environmental requirements for the settlement space and to which extent did the environmental impact influence the settlement. Furthermore, the chapter synthesizes the roles of global and regionally active triggers on landscape development with particular attention to the dependency on scales.

Of particular interest is the settlement dynamics with subsequent varying economic utilization of the area and its effects. Based on the presented case studies (chapter 4) the goal of this thesis is to contribute to a better understanding of the human-landscape relationships in the surroundings of the city of Ayamonte. Consequently, the aim of this thesis is to evaluate the interplay between the natural environment and human activity. In order to achieve these goals, three different case studies have been conducted focusing on two main research questions: (i) Did early human activities impact the landscape and the environment in the vicinity of the newly discovered

Phoenician settlement of Ayamonte and (ii) did the site and its surroundings, in spite of its seemingly spatially marginal position with respect to the Mediterranean commercial areas, provide conditions favorable to settlements for early cultures?

2. Regional Setting

2.1 The Guadiana River – Driving Force of a Mining Region

The Guadiana River is a transboundary river between Portugal and Spain. It is one of the major watercourses draining the Iberian Peninsula. Its total length is c. 720 km and the drainage catchment includes an area of c. 67,000 km² (Lobo et al., 2003). In some parts the final 200 km of the stream form the international border between the Portuguese Republic and the Kingdom of Spain (Fig. 1).

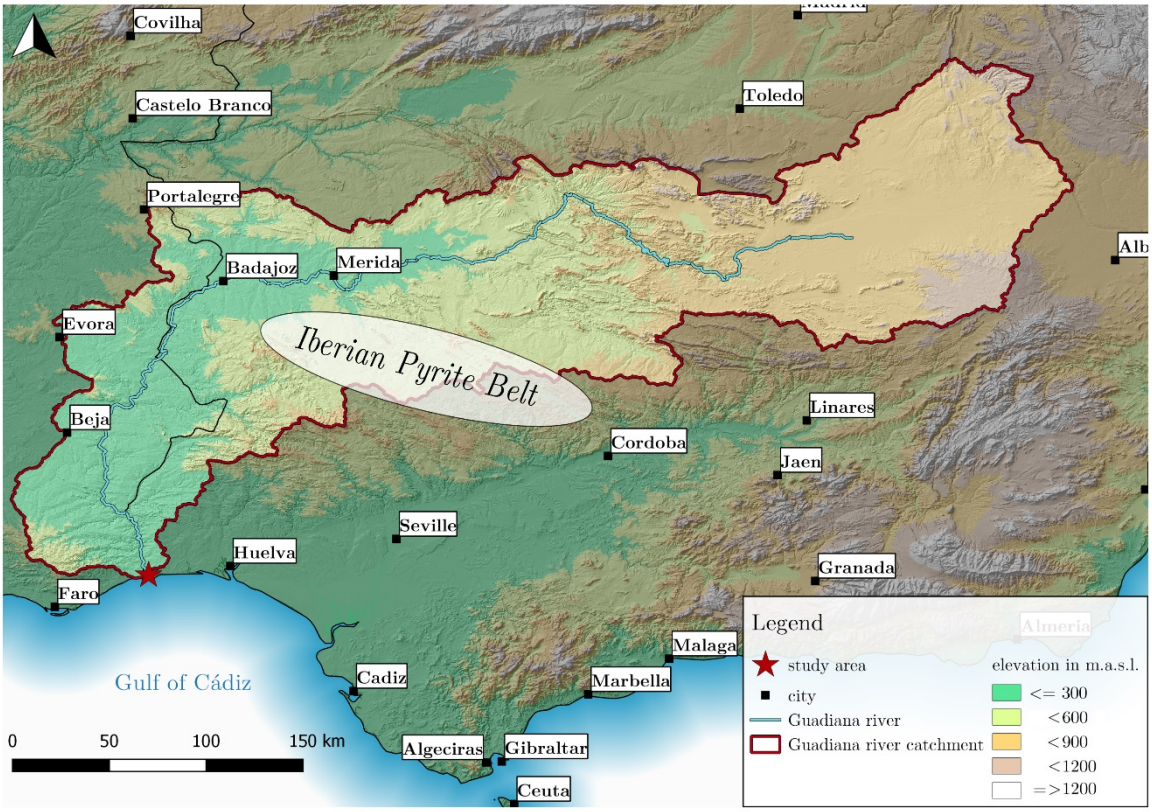

Figure 1: Guadiana River catchment area and the general location if the Iberian Pyrite Belt (Map layout: own design; coordinate reference system: WGS84/ Pseudo-Mercator; data source: Centro Nacional de Información Geográfica [http://centrodedescargas.cnig.es/CentroDescargas/index.jsp], access: 23.01.2018).

The Guadiana River drains the eastern reach of the Iberian Pyrite Belt, one of the largest metal-rich sulfide deposits in the world (Tornos, 2008; van Geen et al., 1997). The deposits of the Iberian Pyrite Belt were formed during late Paleozoic by precipitation from hydrothermal fluids during a period of intense submarine volcanism

(Boulter, 1993). Besides sulfur and iron, the deposits contain large amounts of copper, lead, zinc, gold and silver (Strauss et al., 1977). Earliest mineral extraction in southwest Iberia is documented for the Tinto-Odiel Estuary (42 km east of Ayamonte) and dates back to the 3rd millennium BCE (Pérez Macías, 1996; Salkied, 1987). Large scale mining of silver deposits commenced approx. 1200 BCE by the Phoenicians (Carretero et al., 2011; Nocete et al., 2011; Ruiz et al., 2008). At the time of the Roman Empire mining for copper and silver intensified, while they remained untouched during post-Roman times (Strauss et al., 1977). In the 18th and 19th century, due to the need for copper, intensive mining recommenced (Rothenberg and Blanco Freijeiro, 1981; Strauss et al., 1977). Metallogenic maps of the region around Ayamonte (see chapter 4.1 and Fig. 18C) show, that large metalliferous sources do not occur in the surrounding area (IGME, 1983). Most of mineral deposits are located within a distance more than 50 km to the northeast. Further information on mineral resources of the region is dealt with in case study I (chapter 4.1).

2.2 The Coasts of the Huelva Province

On a larger scale, the regional focus is set on the area of the Guadiana Estuary. This natural environment is situated in the Spanish province of Huelva, located in southwest Andalusia (Fig. 2A). The mouth of the Guadiana River is situated at the border between the Republic of Portugal and the Spanish Kingdom (Fig. 2B).

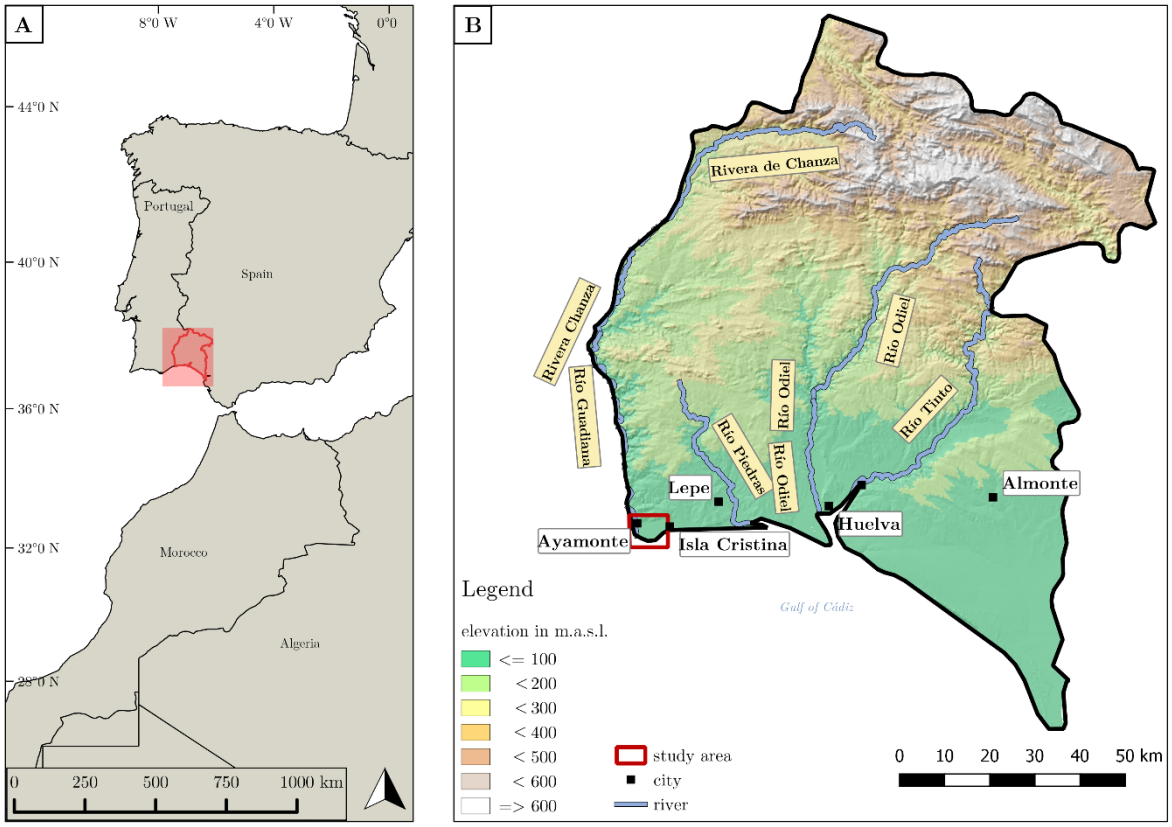

Figure 2: Location of the Huelva province; B – The Huelva province and the study area (red rectangle) (Map layout: own design; coordinate reference system: WGS84/ Pseudo-Mercator; data source: Centro Nacional de Información Geográfica [http://centrodedescargas.cnig.es/CentroDescargas/index.jsp], access: 23.01.2018).

The province of Huelva is delimited by the provinces Algarve and Lower Alentejo (both Portugal) to the west, the Spanish province of Badajoz to the north, the Spanish provinces of Seville and Cádiz to the east and the Atlantic Ocean (Gulf of Cádiz) to the south. The province is drained mainly by five great streams: the Guadiana River, Odiel River, Tinto River, Guadalquivir and Piedras River (Fig. 2B and Fig. 3).

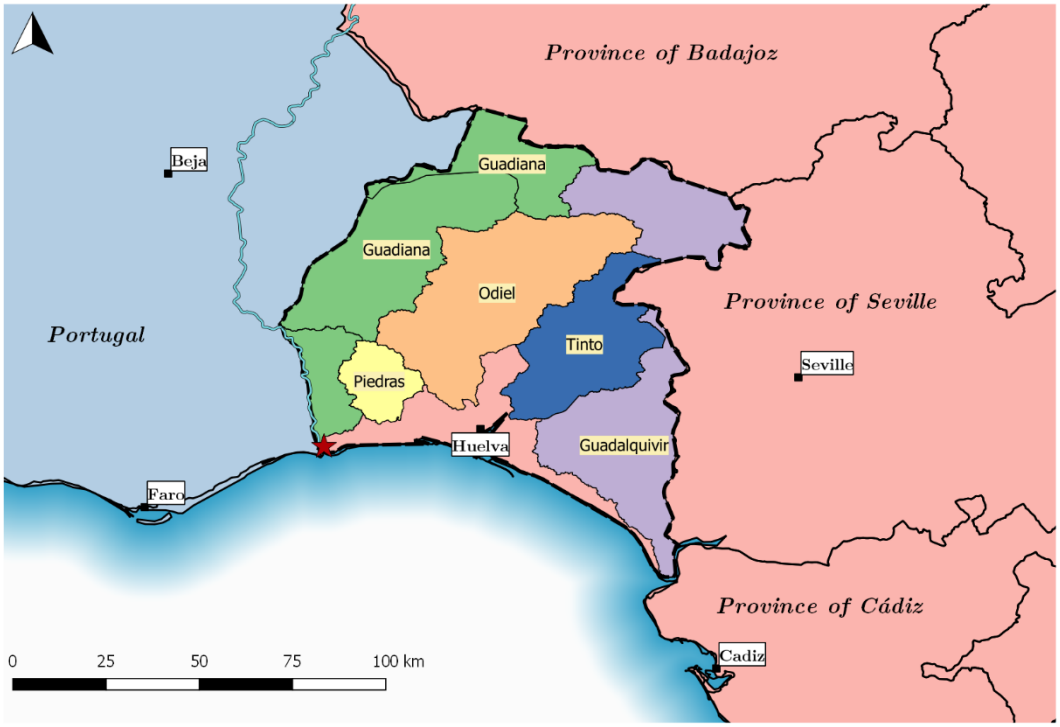

Figure 3: Main river catchments in the Huelva Province and the names of the surrounding provinces. The study area is marked by the red star (Map layout: own design; coordinate reference system: WGS84/ Pseudo-Mercator; data source: Centro Nacional de Información Geográfica [http://centrodedescargas.cnig.es/CentroDescargas/index.jsp], access: 23.01.2018).

Geomorphologically the coasts of the Huelva province represent the contact between the most western sector of the Guadalquivir Basin and the Atlantic Ocean. In this area two geological units are cropping out (Fig. 4): (a) the South Portuguese Zone, belonging to the Iberian Massif, which constitutes the socket of the Guadalquivir basin, and (b), the Neogene formations and Quaternary basin fill (Ríos, 1983). The Guadalquivir Basin was formed during the Neogene, because of the collision of the Baetic System with the ancient Iberian Massif edge. During that time, the basin was flooded by the sea and sediments were deposited, mostly originating from erosion of the surrounding Baetic Cordillera and the Iberian Massif. The gradual rise of the relief of the entire region produced broad areas on which a river network developed with extensive plains and river terraces (Ríos, 1983).

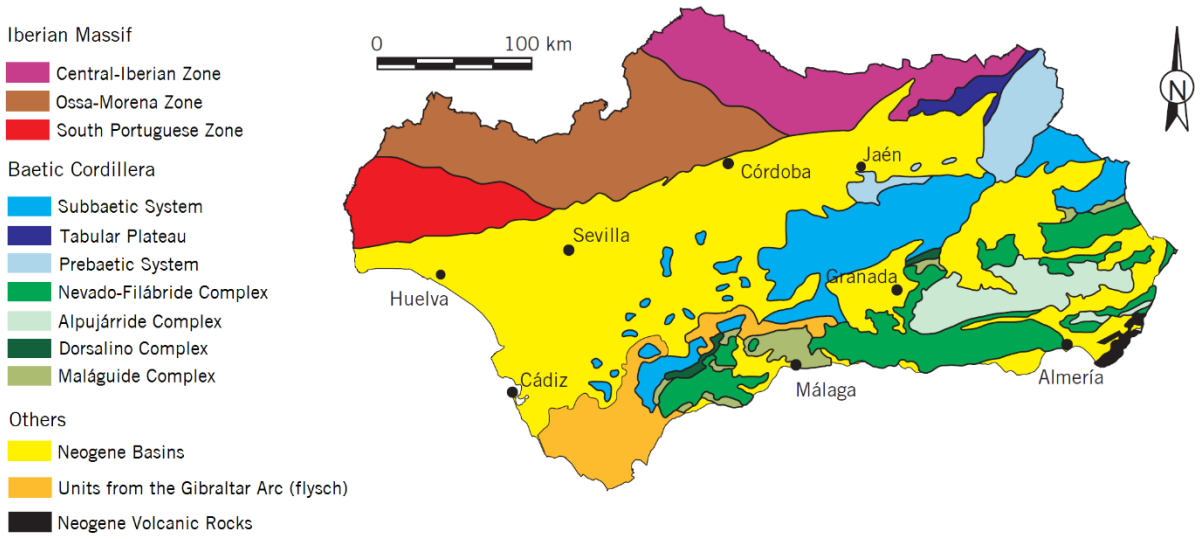

Figure 4: Geological units of Andalusia (modified after Megía and Muñoz, 2006).

As a result of the geological characteristics of the terrain and the low morphological rigidity of the coastal relief, a dynamic coast, in which many morphological changes occurred in relatively short periods of time, characterize today's landscape (Vera et al., 2004).

The main coastal changes occurred during the Holocene, due to pronounced sea-level rise which peaked about 6,500 years ago (Boski et al., 2002). Subsequently, coastal erosion, represented by extensive cliff areas, and coastal deposition, visible at the river mouths, forming spits and marshlands, form the recent coastline of the Huelva province (Rodríguez-Ramírez et al., 1996).

The coastal morphodynamic systems predominating the Huelva coast are: (I) marsh areas, (II) coastal spit bars and (III) dune systems. Marshes represent the transition between a river and the sea. In General, they are large flat areas and are affected by the action of the tides. Coastal spits and barrier islands are formed by longshore currents, transporting and depositing large amounts of sediment. Due to changes in flow energy and direction the parallel transported sediments are deposited at bays and river mouths (Dabrio et al., 2000). The development of active dune systems is triggered by the availability of unconsolidated, easily transportable coastal material. The dunes

at the Huelva coasts occur in different shapes. The internal structure with cross stratifications indicating alternating wind directions (Zazo et al., 1998).

2.3 The Guadiana Estuary

The study area comprises the eastern parts of the lower Guadiana Estuary (Fig. 5). Therefor the study sites of this thesis are exclusively located on Spanish territory, marking the Guadiana River as the superordinate western border of the investigated areas. While the western side of the lower estuary comprises a large littoral spit and large aeolian dunes, the eastern estuarine flank comprises an area of old barrier islands transformed into elongate spits, separated by salt marsh areas draining directly into the sea via a high-density channel network (Morales, 1997).

Figure 5: The Guadiana Estuary into the Atlantic; left half of the photograph: the study area and Ayamonte (Spain), right half of the photograph: Vila Real de Santo (Portugal). The viewing direction is oriented to the south (Source: Neg. 1402-291-D80 [L. Alves und B. Cabaco Encinas] in Teyssandier and Marzoli, 2014).

The final 50 km of the river are under major tidal influence and follow an almost perpendicular course relative to the coast. In this section, the river is incised into Hercynian bedrock, consisting of Carboniferous shales (IGME, 1983). The fluvial incision occurred during Pleistocene lowstands followed by the Holocene transgression (Boski et al., 2002). On its final 5 km the Guadiana River cuts a slightly wider valley into the Cretaceous and Jurassic limestones. Morales (1997) distinguishes between two major physiographic domains: a) the estuarine valley, characterized by the complex interaction between fluvial and marine hydrodynamics and sedimentary processes, and b) a prograding deltaic complex of barrier sands and marshes around the mouth of the main estuary channel dominated by wave activity (Fig. 6).

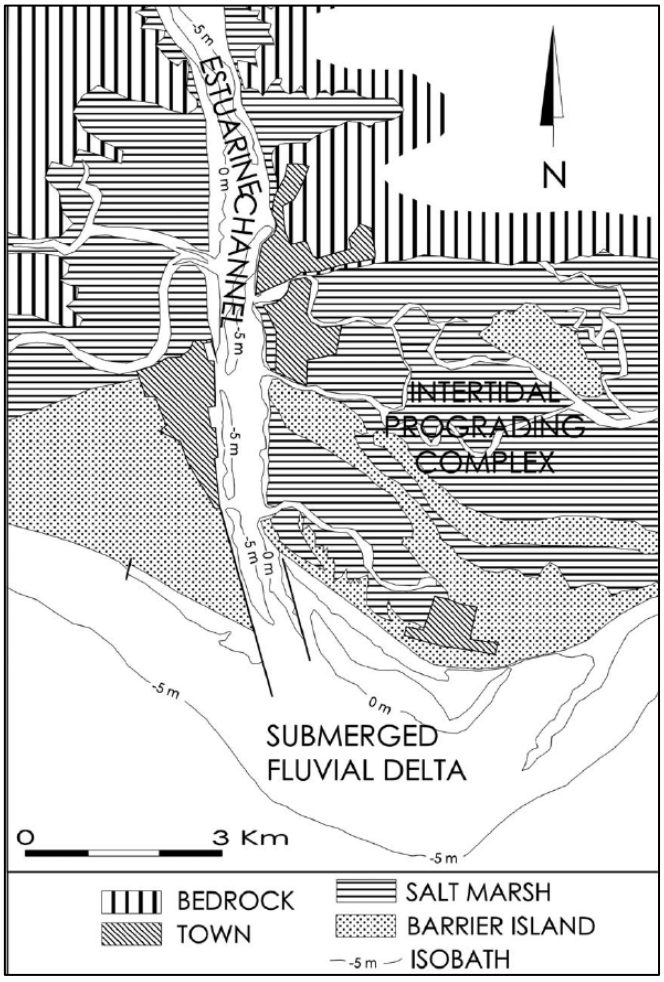

Figure 6: Morphosedimentary zones in the marine domain of the estuary (Morales et al., 2006).

Coastal alterations along the Gulf of Cádiz are closely related to sea-level changes. The most significant sea-level fluctuations occurred in the Holocene. From the beginning of the Holocene to 7500 cal BP, the average sea-level rise within the western parts of the Gulf of Cádiz was about 7 mm*a^{-1} (Boski et al., 2008). Since then, the average rate of sea-level rise reduced to about 0.9 mm*a^{-1} (Boski et al., 2008), a value much lower than the present sea-level rise of about 1.5 mm*a^{-1}(Dias and Taborda, 1992). After the Mid-Holocene shift in sea-level rise, the eustatic effects became less important and non-eustatic changes determined the coastline evolution.

2.3.1 Climate

The region is characterized by a Mediterranean climate with hot, dry summers and mild, wet winters (Csa-climate) (Köppen and Geiger, 1930-1939). The average annual temperature is 17.5 °C with a minimum in January (11.4 °C) and a maximum in August (24.4 °C) (Fig. 7). The precipitation varies by 75 mm between the driest month of July and the most precipitous month of December. The annual precipitation varies between 450 and 1,000 mm with a high interannual variability (mean annual precipitation: 483 mm; Loureiro, 1983).

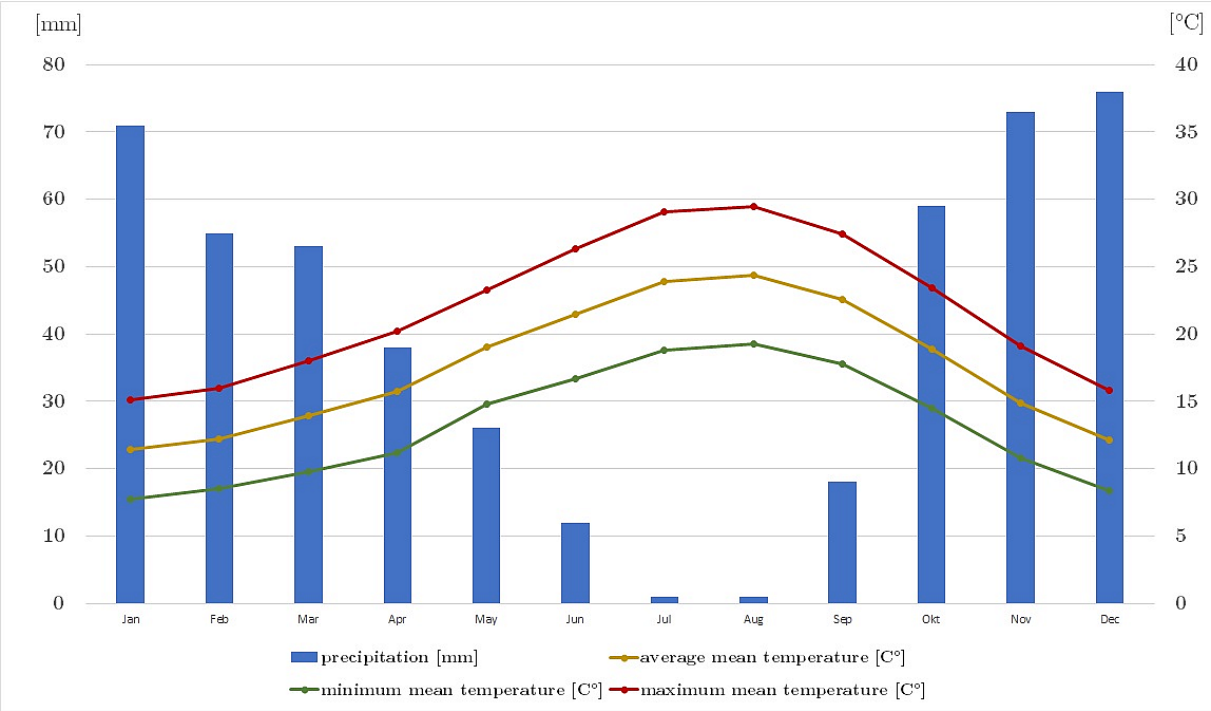

Figure 7: Climate diagram of the Vila Real de Santo António weather station (Portugal) (Data Source: Loureiro, 1983; reference period: 1930-1961).

2.3.2 Vegetation

Like in many other ibero-mediterranean regions, in the surroundings of Ayamonte agricultural and pastoral activities generated a landscape of parkland character, containing scattered oaks (*Quercus suber, Quercus rotundifolia*) above grazed vegetation of annual plants and low shrubs (Fig. 10; Capelo, 1996 and Fletcher, 2005).

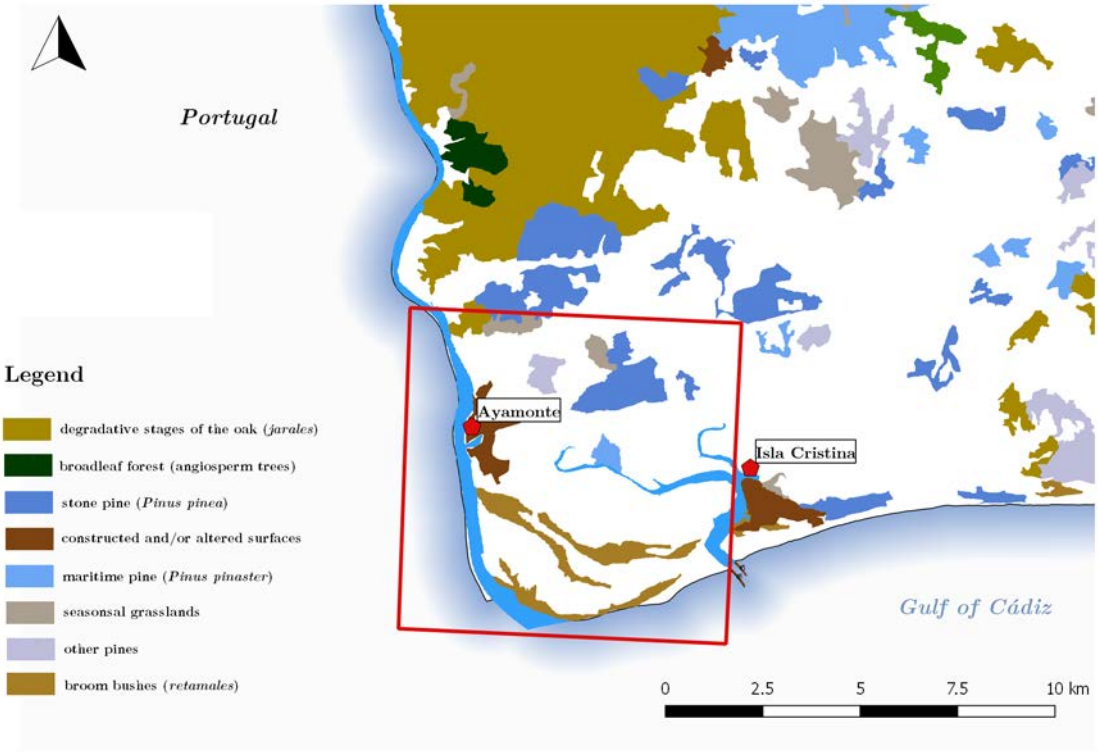

Figure 8: Map of the natural vegetation zones of the study area, acquired from the Atlas of Andalusia (volume II) by the Ministry of Environment. It is a fusion of the Forest Map of Spain and the updated Map of Plant Coverage of Andalusia of 1999, which highlights the forest resources of Andalusia (WMS-URL: http://www.juntadeandalucia.es/medioambiente/mapwms/REDIAM_Vegetacion_Natural_Andalucia?; coordinate reference system: WGS84/ Pseudo-Mercator).

Much of the vegetation of the Huelva Province littoral has been modified. The halophytic vegetation of the saltmarshes is dominated by succulent plants of the family *Chenopodiaceae*. Along the coastal strips, there are extensive agroforestry plantations of *Pinus pinaster* and *Eucalyptus*. In the environs of Ayamonte, traditional dry orchards of almond, olive, fig and carob are present. However, their economic value has been replaced by irrigated *Citrus* agriculture (Fletcher, 2005, Fig. 11).

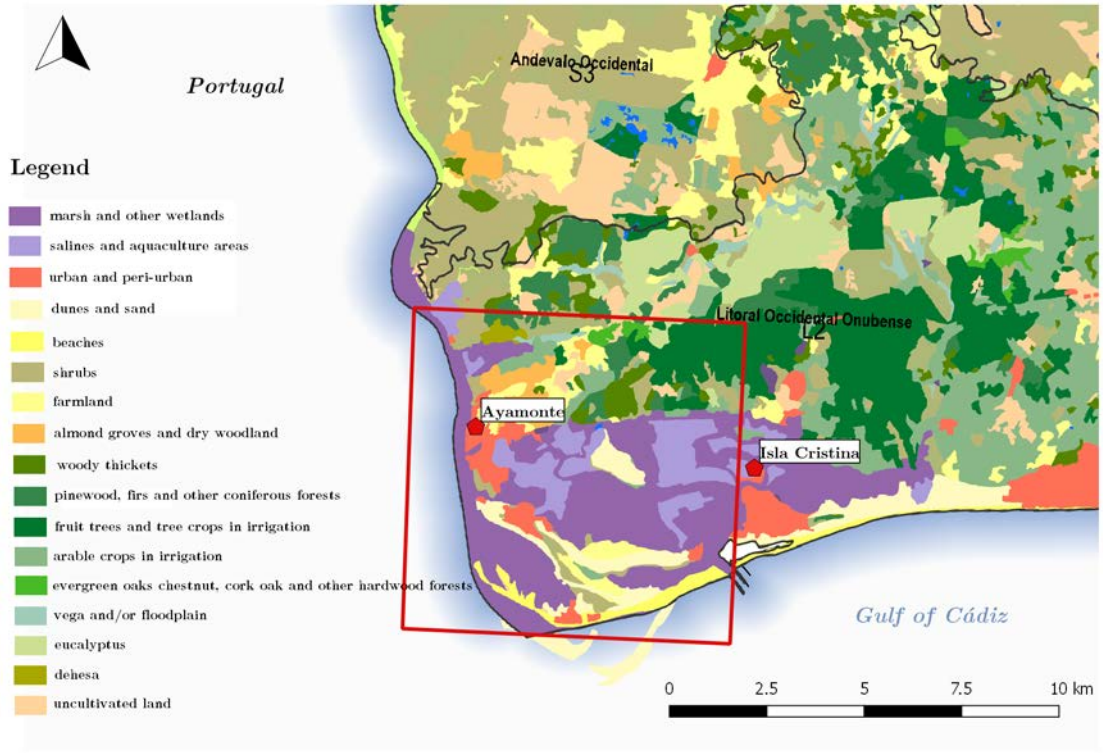

Figure 9: Map of the landscape units within the study area. Derived from the Atlas of Andalusia (volume II) by the Ministry of Public Works and Transport as well as the Ministry of Environment (WMS-URL: http://www.juntadeandalucia.es/medioambiente/mapwms/REDIAM_Paisajes_Andalucia?; coordinate reference system: WGS84/ Pseudo-Mercator).

Besides arboreal vegetation, the study area is dominated by shrubs of sclerophyllous types and aromatic types. The composition and characteristics of these shrublands is mainly controlled by grazing and cutting. Density and growth of these scrubs (spanish: *mattoral*) decrease with anthropogenic pressure (Fletcher, 2005). Typical representatives in the area are *Quercus coccifera, Juniperus, Pistacia lentiscus, Olea, Myrtus, Cistus* and *Rosmarinus*.

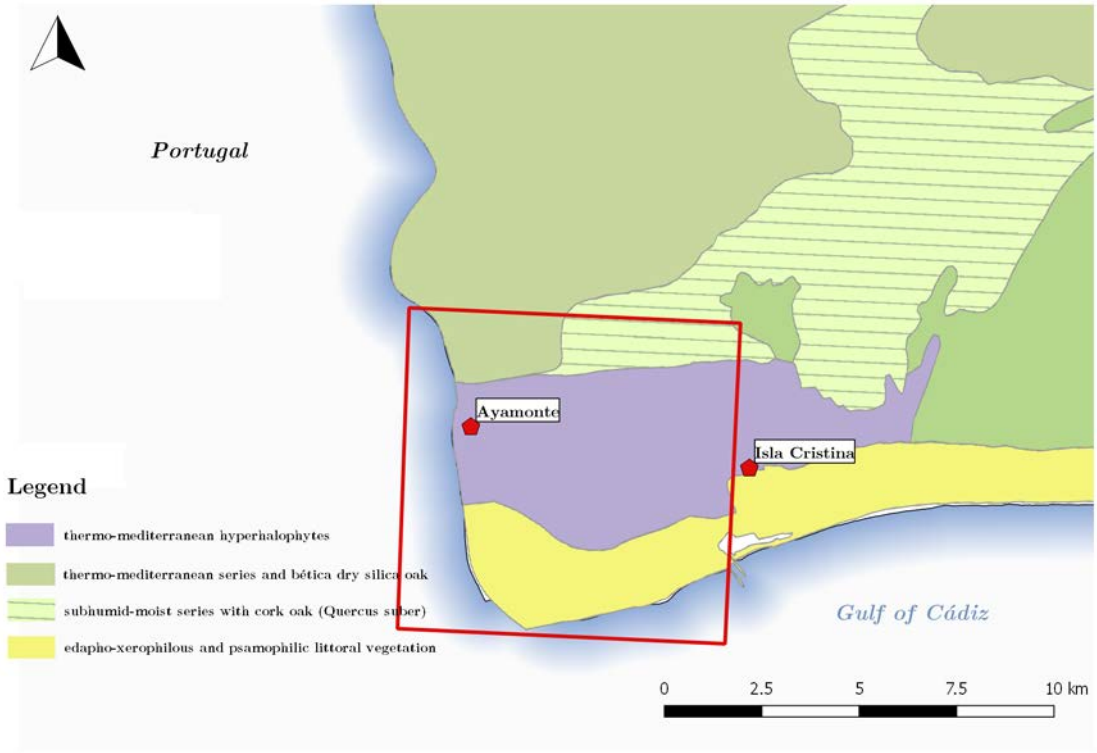

Figure 10: Map of vegetation series, elaborated from the Atlas of Andalusia (volume II) of the Ministry of Public Works and Transport as well as the Ministry of Environment of the Junta de Andalucía (WMS-URL: http://www.juntadeandalucia.es/medioambiente/mapwms/REDIAM_Series_Vegetacion_Andalucia?; coordinate reference system: WGS84/ Pseudo-Mercator).

The large area of estuarine wetlands is populated by halophytic vegetation such as *Arthrocnemum*, *Atriplex* and *Limoniastrum*. Grasses such as *Puccinellia maritima*, *Parapholis filiformis* and *Hordeum marinum* are also important components of saltmarsh vegetation (Fig. 12).

2.3.3 Relief

The relief of the study area is bisected. The southern parts are dominated by tidal forms (creeks and marshes), coastal detritic forms (barrier islands, dunes) and anthropogenically shaped areas (salines, aquaculture). The northern part, delimited from the south by an old paleocliff, is characterized by glacis, vegas, floodplains, hills and volcanic systems (Fig. 13). A more detailed review of the local geomorphology is given in chapter 4.3.

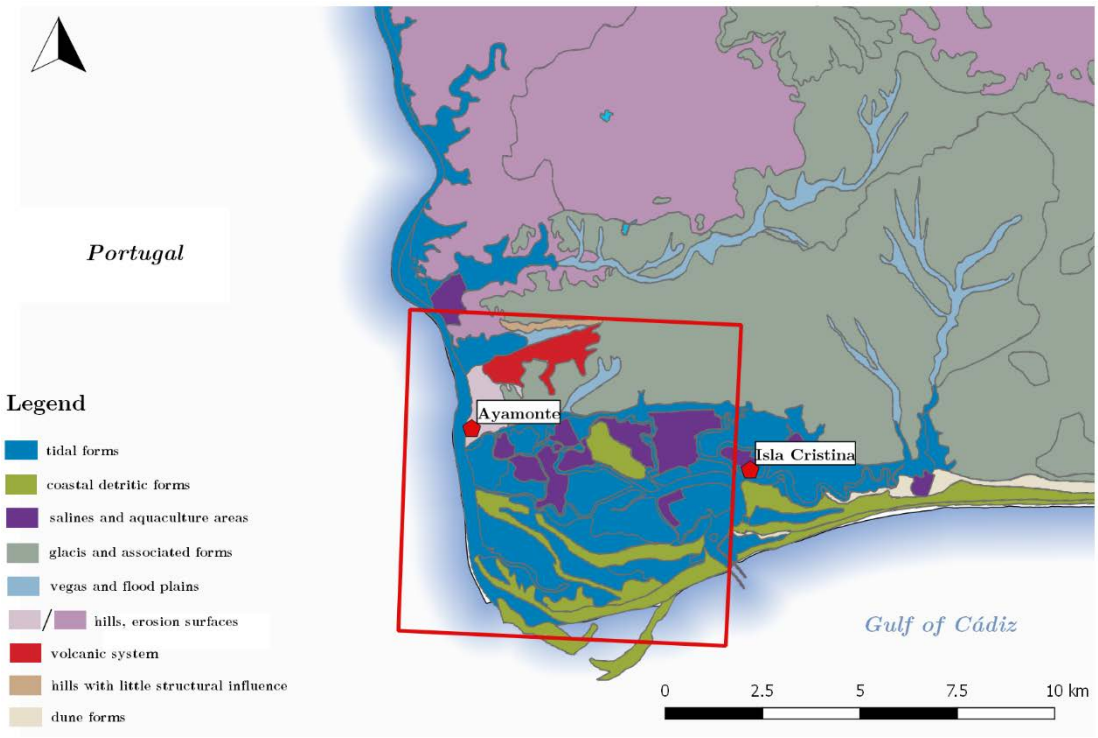

Figure 11: Geomorphological map of the study area, acquired from the Atlas of Andalusia (volume II) by the Ministry of Public Works and Transport as well as the Ministry of Environment of the Junta de Andalucía. Scale 1: 400,000. Developed from the Geological Map of the Magna series at scale 1: 50,000, adjusted with Landsat satellite images (WMS-URL: http://www.juntadeandalucia.es/medioambiente/mapwms/REDIAM_Geomorfologico_Andalucia?; coordinate reference system: WGS84/ Pseudo-Mercator).

2.3.4 Geotectonic and Geological Setting

Bedrock in the area around Ayamonte is highly heterogeneous (Fig. 14). While north of the study area carboniferous schists and fossiliferous graywackes dominate (Vidal et al., 1993), the parent material in the area of interest is composed of Triassic dolomites, with dikes of dolerites, indicating post-sedimentary magmatic activities. Tectonically the southwestern coast of Spain is located closely to the Africa-Eurasia plate boundary, which is a source area of high-magnitude earthquakes. Quaternary tectonics are dominated by E-W and NNW-SSE trending fault systems (Lobo et al., 2003); tsunami sediments resulting from the 1755 Great Lisbon Earthquake have been identified in coastal embayments of the Guadiana Estuary (Klein et al., 2016).

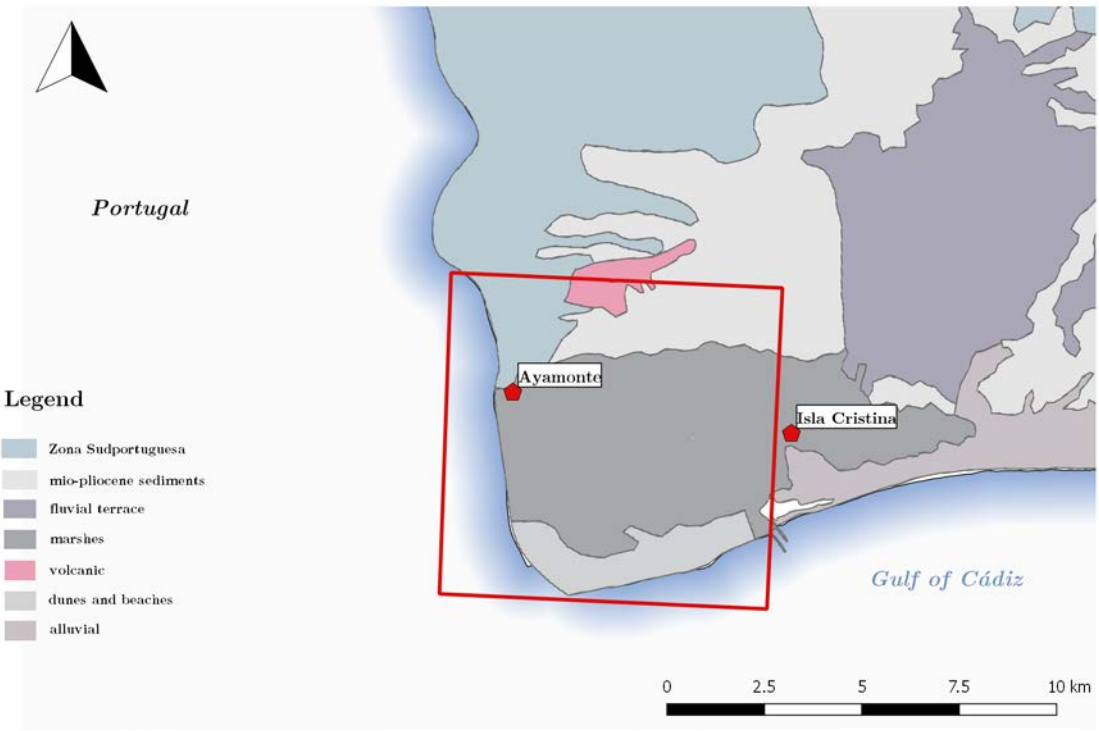

Figure 12: Geostructural units of the study area. (Geological map of Andalusia elaborated for the Atlas of Andalusia (volume II) by the Ministry of Public Works and Transport as well as the Ministry of Environment of the Junta de Andalucía. Developed from the Geological Map 1: 400,000, adjusted with satellite images (WMS-URL: http://www.juntadeandalucia.es/medioambiente/mapwms/REDIAM_Geologico_Andalucia?; coordinate reference system: WGS84/ Pseudo-Mercator).

While the shallow subsurface of lagoonal-like depressions (spanish: *"esteros"*) is dominated by gray, organic and silt rich mud (Fig. 15; Klein et al., 2016), the slopes are covered by shallow Quaternary sands and gravel (IGME, 1983).

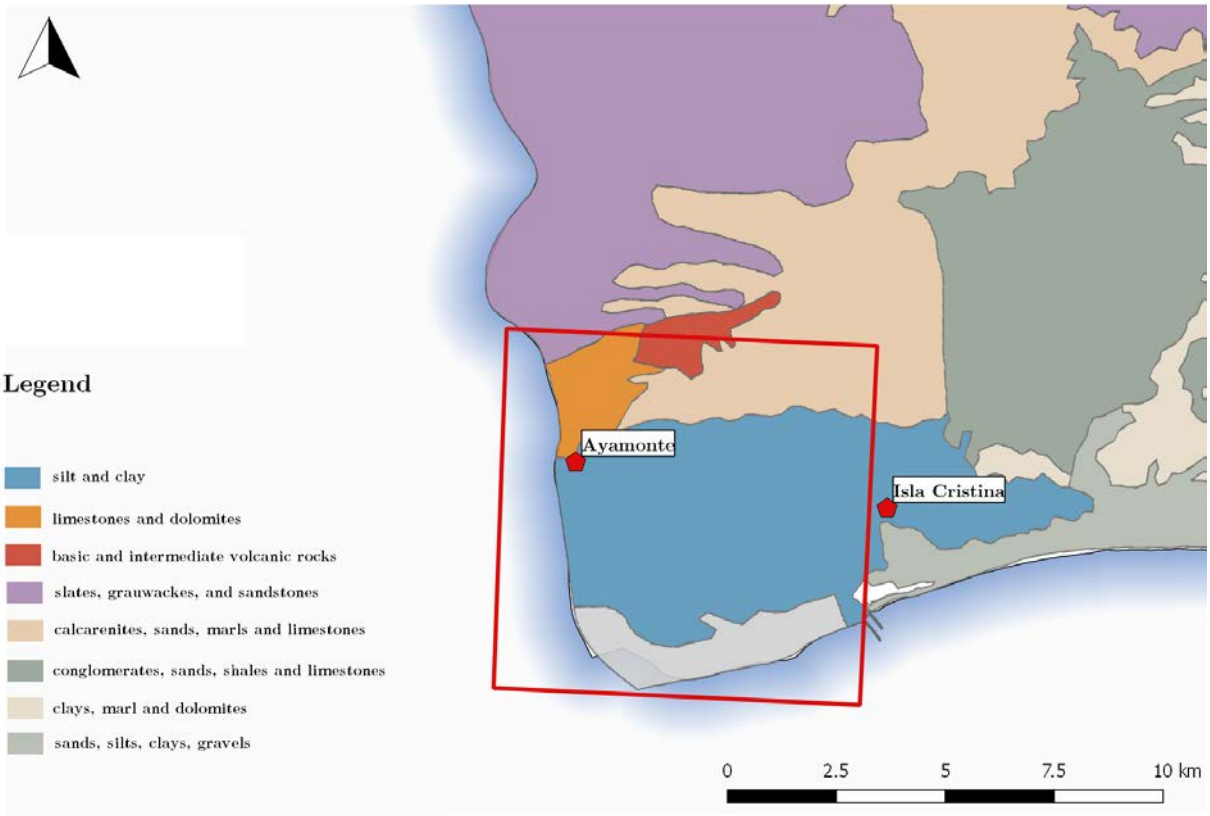

Figure 13: Lithology map of the study area. (Elaborated from the Atlas of Andalusia (volume II) of the Ministry of Public Works and Transport as well as the Ministry of Environment of the Junta de Andalucía (Scale 1: 400,000). Developed based on the 1: 400,000 Geological Map, adjusted with satellite images, and revised with the national geological mapping of the Magna series at a scale of 1: 50,000. it identifies the lithological units according to the intrinsic physical and chemical characteristics of the rocks, regardless of their chronological character (WMS-URL: http://www.juntadeandalucia.es/medioambiente/mapwms/REDIAM_Litologico_Andalucia?; coordinate reference system: WGS84/ Pseudo-Mercator).

2.3.5 Soils

The soils of the study area are mainly comprised of gleyic solonchaks, regosols and arenosols. Soil types, which are restricted to the area of the recent saltmarsh. However, planosols, regosols and lithosols, as well as luvisols occur within the area of interest. The urban area of Ayamonte is dominated by calcic cambisols and calcic luvisols. Eutric planosols, gleyic and plinthic luvisol occur within the large area of the Miocene Ridge east of the city of Ayamonte. The slopes of the northern edge of the study area are characterized by eutric regosols, cambisol and lithosols (CSIC-IARA, 1989; Fig. 8).

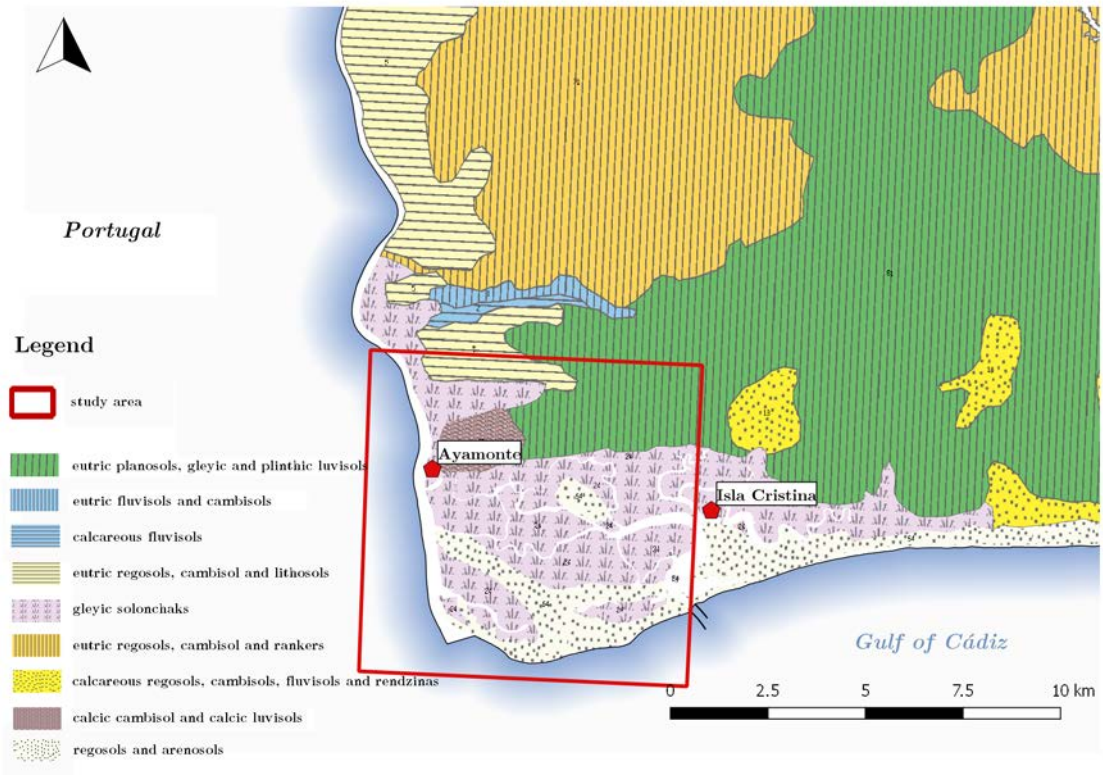

Figure 14: Soil types of the study area (Map of Soils of Andalusia at scale 1: 400,000 elaborated in 2005 by the Ministry of Environment from the map published in 1989 by the Ministry of Agriculture and the Council of Scientific Research. Digitized and readjusted based on the Landsat-TM satellite orthoimagery. Soils appear in cartographic units and are characterized by associations grouped at the second order level following the classification criteria of the F.A.O. (1974) and the 1985 European Union Soil Map. (WMS-URL: http://www.juntadeandalucia.es/medioambiente/mapwms/REDIAM_Suelos_Andalucia?; coordinate reference system: WGS84/ Pseudo-Mercator).

Concerning the crop yield, the study area is characterized by predominantly marginal and unproductive soils. However, on the Miocene ridge, soils of moderate land use capacity occur. There are only few areas characterized by good/moderate land use capacities, also restricted to the area of the Miocene ridge extending eastward from the city of Ayamonte (Fig. 9).

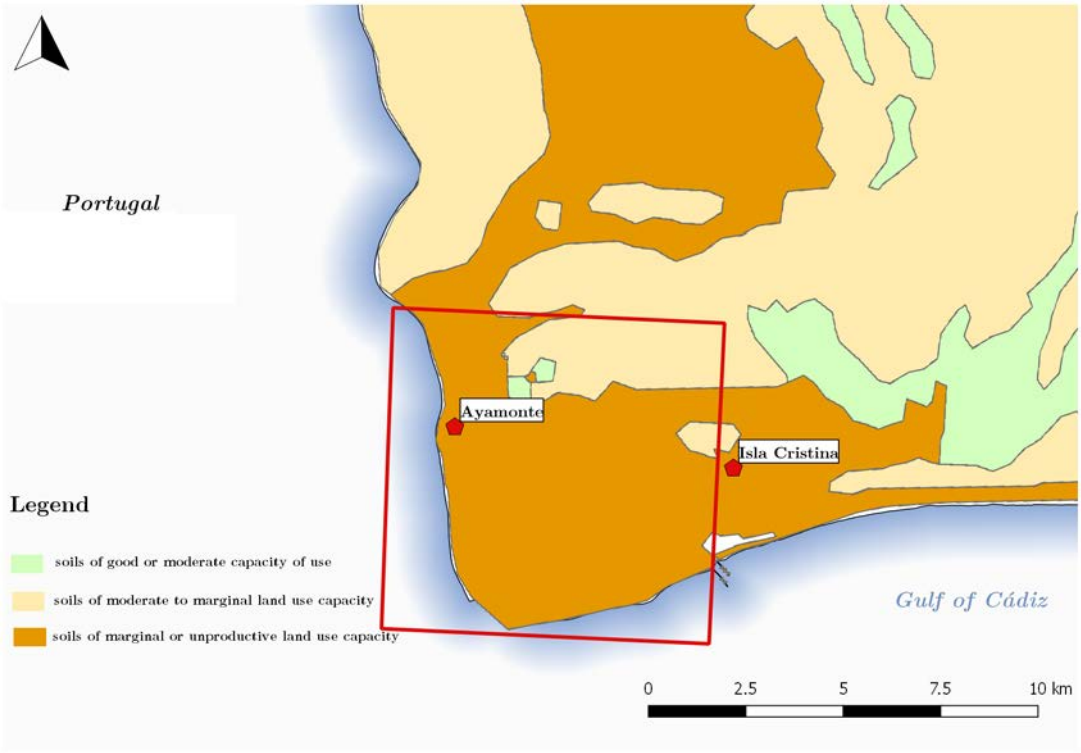

Figure 15: Map of soil use capacity of the study area. Classified in 4 main groups: land with excellent capacity of use, land of good or moderate capacity of use, lands of moderate to marginal capacity of use and marginal or unproductive lands. The red square marks the greater study area (WMS-URL: http://www.juntadeandalucia.es/medioambiente/mapwms/REDIAM_Capacidad_Uso_Andalucia; coordinate reference system: WGS84/ Pseudo-Mercator).

2.3.6 Hydrodynamic Setting

The Guadiana Estuary is characterized by a semidiurnal mesotidal regime, with a mean tidal range of 2.0 m (Morales, 1997). The tidal wave moves from east to west along the coast producing minor currents. Waves originating from southwest directions predominate, while waves from southeast directions are more energetic (Costa, 1994). Pires (1998) reports of the appearance of 5.3 m high waves within a 100-year recurrence interval hitting the coasts of the Huelva province. The generally prevailing wave height is about 0.92 m classifying the coastline as mixed-energetic and tide dominated (Borrego et al., 1995; Costa, 1994). Strong seasonal changes in river discharge characterize the Guadiana River. Summer discharge can be as low as 10 $m^{3}*s^{-1}$, while

winter discharge can exceed 3,000 m^3*s^{-1} (González et al., 2004). The interannual variability is likewise high (Morales, 1997).

2.3.7 Sediment Supply

Morales et al. (2001) assess that the Guadiana River is in an advanced state of infilling and undergoes deltaic progradation, which is favored by a high sediment supply and the narrow bedrock-controlled morphology of the estuary (Fletcher, 2005). The Guadiana Estuary is being supplied by sediments from two different sources: fluvial and marine. Although data on sediment supply is missing, it is estimated, that the Guadiana River, together with the Guadalquivir River, is the major supplier of fluvial material into the Gulf of Cádiz (Lobo et al., 2003). However, some of the sediment is being transported from the estuary towards the coasts located further to the east, because of longshore drift. González et al. (2001) estimate the sediment volume at the Guadiana Estuary mouth being transported longshore from west to east between 100,000 and 300,000 m^3/year. The sandy sediments, originating from the Portuguese coasts are transported to the east. Some of the sand- and gravel sized sediments are trapped in the estuarine system of the Guadiana River, but most of the sediment bypasses the river mouth (Morales, 1997).

2.3.8 Ecology, Land Use and Anthropogenic Pressure

The Guadiana Estuary is a natural system of high ecological value. Many species, such as birds, fish, molluscs and crustaceans use the area as a refuge and breeding place (Chícharo et al., 2007). The saltmarsh area developed on accreted sediments on both sides of the infilled estuary is occupied by halophyte vegetation, adapted to high salinity and periodic flooding (Fletcher, 2005). Until mid-20th century cereal cultivation was the main agricultural activity in the study area. Nowadays modern saltpans (especially in use at the Portuguese estuary margin), aquaculture and especially touristic infrastructure dominate the landscape appearance (Sampath, 2008). The latter is an extremely important source of income for the region, as it is estimated that more

than one million tourists visit the area of Isla Canela for recreational purposes between May and September (Rodríguez-Ramírez et al., 2003). Large parts of the salt marsh area at the Spanish estuary margin is highly altered for touristic urbanization processes.

Throughout the 20th century large scale changes in the shorelines have been observed. Intense damming reduces the total amount of river discharge significantly, altering sedimentation processes to the coastal areas (González et al., 2001). More than 40 dams cover 75 % of the Guadiana drainage area (Morales, 1997). In February 2002, the Alqueva Dam was inaugurated, creating the largest artificial lake in Western Europe, reducing the total amount of river discharge.

2.4 Archaeological Research

2.4.1 General Settlement History of the Guadiana Estuary Area

Verifiable colonization of the Guadiana Estuary starts around 7000 yrs BP, when simultaneously the mean-sea-level reached the approximate today's position (Arteaga, 1988; Arteaga et al., 1989; Hoffmann and Schulz, 1988; Jurado et al., 1997). Neolithic finds within the greater research area are known from the aeolian complexes in the surroundings of the modern city of Cádiz (Kunst, 2001). Some lithic tools associated to Neolithic times document the settlement activities. The megalithic tomb in Villablanca, 10 km northeast of Ayamonte, indicates an advanced stage of Neolithic culture (Kunst, 1988).

Remains of Chalcolithic fortifications are located in the hinterland of the Guadiana Estuary and in the vicinity of the city of Huelva (Kunst, 1988). Except for the Odiel River and Tinto River there is almost no direct evidence for Chalcolithic mining activities at the Iberian Peninsula (Kunst, 2001). However, there is a noticeable concentration of Chalcolithic settlements upstream the rivers close to numerous copper deposits of the region (Kunst, 1988).

The Bronze Age-settlements of the lower Guadiana River are characterized by a wide range of stone box graves. In contrast this richness is faced by an almost complete lack of settlement sites (Schubart, 1975). The only Bronze Age-settlement near Ayamonte was discovered close to the modern town of Odeleite, located 10 km northwest of the Guadiana Estuary. In comparison to the scattering of pre-Bronze Age sites, the locations of Bronze Age-settlements concentrate along the Guadiana River (Kunst, 1988).

Findings in Castro Marim (ancient *"Baesuris"*), a settlement on top of a hill right of the Guadiana River in 3 km distance from Ayamonte, dates back to the transition of Late Bronze Age and Iron Age and gives some hints for an indigenous population which was verifiable in contact with Phoenician traders (Arruda, 2000b).

Archeological findings of Roman times are abundant within the research area. The majority of the sites are located directly along the Guadiana River, respectively in the vicinity of the modern sand and barrier beaches and dunes. This may indicate that the dune system and beach barriers of Isla Canela (left of the Guadiana River mouth) already existed during Late Roman times. The densely settled areas along the banks of the Guadiana River, as well as along the banks of its major tributaries indicate stable fluvial dynamics at least since Roman times (Kunst, 1988).

2.4.2 Phoenicians at the Gulf of Cádiz

The Phoenician period on the Iberian Peninsula started around the 1st millennium BC and was characterized by an apparently systematical colonization of the coastal strips of modern Spain (Niemeyer, 1982; Schubart and Maaß-Lindemann, 2004). The Phoenician colony in modern Ayamonte was located in the most western parts of the Phoenician diaspora. The Phoenician colonies were exclusively located along the coastal strip of the Mediterranean Sea and Gulf of Cádiz, preferably located on ridges or peninsulas close to river mouths guaranteeing protection and access to the hinterland (Arruda, 2009; Arteaga, 1988; Aubet, 2001; Koch, 2001; Niemeyer, 1982).

The motivation of the Phoenicians to colonize the area, and their modes of contact with the indigenous community remain uncertain and are subject of a controversial debate (Arruda, 2009; Koch, 2001). However, although not located in close proximity to the coastline, numerous ore deposits in the hinterland of the Phoenician settlements along the coastal strip of the southwestern Iberian Peninsula are considered to be one of the main reasons for colonization (González de Canales et al., 2004; Mulhy, 1998). Although evidence of an export-oriented quarrying is missing, it is assumed that in particular the iron-, copper- and silver deposits were of particular economic importance (Schubart and Maaß-Lindemann, 2004). Next to the accessible ore deposits, available agricultural and marine resources as well as the availability of timber and slaves (indigenous Iberians) may have been factors of potential attraction (Arruda, 2009; Treumann, 2009).

2.4.3 Phoenicians at Ayamonte

Prior to the discovery of the Phoenician settlement and necropolis in the modern town of Ayamonte, the Guadiana Estuary was a *Terra Incognita* in terms of Phoenician settlement activities. The Phoenician findings in Ayamonte are manifold and include ceramics, remains of metallurgical furnaces, building structures and remains of a metal workshop (Fig. 16, Teyssandier and Marzoli, 2014). Based on these archeological finds the relatively large extent and significance of this Phoenician settlement during the 8th and 7th century BC can be derived. Both, the necropolis and the settlement are the most westerly evidences of Phoenician colonization and are therefore unique in their character (Teyssandier and Marzoli, 2014).

Figure 16: Grave with a fragmented urn containing the cremated remains of an adult man's corpse (Teyssandier and Marzoli, 2014).

3. Methods

3.1 General Approach

This study follows in many parts the research design of Brückner (2011). Prior to the field work analyzing topographic maps and satellite images helped identifying geoarchives suitable for answering the research questions. During one field campaign three different geoarchives were studied by applying percussion drilling.

3.2 Field Work

The fieldwork was conducted in October 2013. The study areas were mapped geomorphologically following Leser and Stäblein (1980). Fifteen sediment cores were obtained using a Wacker vibracoring device (BHF 30 S) with a 5-cm core diameter in open metal drill probes or in closed plastic tubes. The positions of the coring sites were measured with a handheld GPS device with 5 m horizontal accuracy.

Sediment description followed the guidelines form the German manual of soil mapping (Ad-Hoc-AG Boden, 2005). Sediment color was determined using the Munsell soil color chart. Furthermore, lithostratigraphic features (charcoal content, hydromorphic features, sorting) have been documented.

3.3 Laboratory Analyses

The collected sediments have been analyzed for magnetic susceptibility, carbon content, pH, electrical conductivity and elemental composition. The samples were sieved through a 2-mm sieve and dried at 105 °C. For the determination of carbon content and elemental composition, the samples were homogenized in a vibratory disc mill.

3.3.1 Carbon Determination

The carbon content of the sample (organic and inorganic) was determined using three methods: Total carbon contents (TC) was determined via LECO TruSpec CHN

analyzer. Total inorganic carbon contents (TIC) were determined using a Wösthoff Carmhograph C-16. Total organic carbon was calculated by subtraction of TIC from TC.

Not all samples were measured in this manner. The remaining samples, carbon contents have been estimated via loss-on-ignition.

a. LECO TruSpec CHN analyzer: Total carbon content is determined by detecting CO_2 flow by highly selective infrared and thermal conductivity (Leco, 2011). The detection limit is 0.01 mass-%.
b. Wösthoff Carmhograph C-16: Total inorganic carbon contents were determined by acid sample treatment and conductometrically detected by CO_2 flow (Blättermann et al., 2012). The detection limit is 0.01 mass-%.
c. Loss-on-ignition was measured according to Dean (1974). The samples have been oven-dried for twelve hours at 105 °C and heated afterwards to 550 °C and 880 °C in a muffle furnace.

3.3.2 pH and Electrical Conductivity

The pH value of a solution, as the negative decadic logarithm of hydrogen ion concentration, is an important geochemical parameter, affecting chemical, physical and biological properties of soils and sediments (Bates, 1973; Scheffer et al., 2010). Electrical conductivity is a measure of the concentration of ionizable dissolved substances and depends on the ion conductivity, ion concentration and temperature. It is an indicator for the salinity of a soil/sediment (Scheffer et al., 2010).

The pH value was determined using a Hanna handheld device (HI 98127) in 0.01 molar potassium chloride solution with 0.1 pH resolution with a sediment-solution ratio of 1:2. The electrical conductivity of the sediment samples was measured using a Hanna handheld device (HI 98301) with a ±2% accuracy in a solution with a sediment-distilled water ratio of 1:2 (Schneider, 2014).

3.3.3 Magnetic Susceptibility

The magnetic susceptibility is a basic parameter characterizing magnetic properties of physical matter such as rocks and sediments. It describes the magnetization of a material upon application of an external magnetic field. In principle, any material can be magnetized, as soon as it is exposed to an external, artificial field. The magnetic susceptibility is the measure that determines the magnitude of magnetization within a sample. Mainly ferrimagnetic or paramagnetic mineral concentrations affect the magnetic susceptibility. The magnetic susceptibility is a function of composition, form and size of the grains, as well as the concentration of the magnetizable material (Balsam et al., 2011; Knödel et al., 2005; Magiera et al., 2006).

The dimensionless magnetic volume susceptibility was measured using the Bartington Instruments MS2B and MS2C system at 4-cm intervals on closed plastic tubes and in 10 cm^3 sample containers following the methodology of Dearing (1994a).

3.3.4 X-ray Fluorescence (XRF)

A selection of sediment cores underwent x-ray fluorescence analyses, which is a rapid, non-consumptive, precise and reproducible method to determine the element composition of rocks and sediments (Pella, 1989; Ramsey et al., 1995; Vrebos and deVries, 2001). The method has been successfully applied on the identification of tsunamigenic deposits (Chagué-Goff et al., 2017; Cuven et al., 2013; Klein et al., 2016; Moreira et al., 2017; Werner et al., 2017) and deposits formed in prehistoric harbor basins (Finkler et al., 2017; Hadler, 2014; Klein et al., 2016; Rossi et al., 2015). More than 40 different elements were measured at the laboratory of the Geographical Institute of the Freie Universität Berlin using a portable XRF analyzer (Thermo Niton Xl3t 900 GOLDD) equipped with a CCD-camera, a semi-conductor detector with an Ag-anode. For the sediment cores from the case study of chapter 4.1, continuous core measurements were performed with a new device to mount portable energy-dispersive X-ray fluorescence spectrometers described by Hoelzmann et al. (2016). Each sample

was continuously measured for 120 seconds using four different filters to obtain mean relative concentrations per measured element (Fig. 17). The measuring interval was 1 cm so that 823 measurements with a total duration of 35 h were necessary for the approx. 9 m long sediment core Aya 05. For calibration a CRM lake sediment LKSD-2 (Lynch, 1990) was prepared in a sample cup and measured under identical measurement conditions. Only elements that show mean values larger than 4 times the 2σerror of the measurements (Al, Ca, Cl, Fe, K, Pb, Rb, S, Si, Sr, Ti, V, Zn) were taken into account for the analyses (Schwanghart et al., 2016).

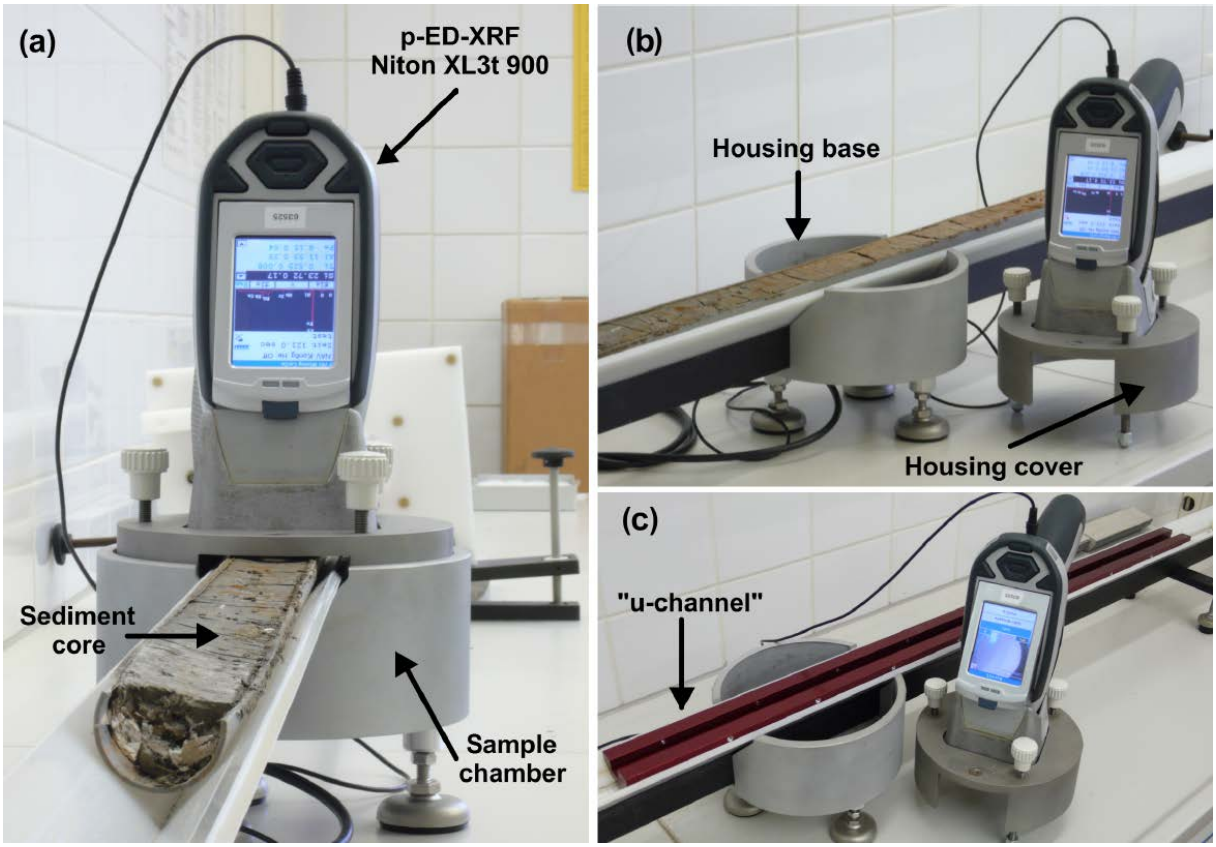

Figure 17: (a) p-ED-XRF spectrum analyzer fixed to the sample chamber to analyze a split sediment core; (b) view of the housing base with the lead-through for the split sediment core and the p-ED-XRF spectrum analyzer fixed to the housing cover; (c) same as (b) but with a "u-channel" often used in paleolimnological investigations (Hoelzmann et al., 2016).

The analysis of main elements and trace elements in geological materials is enabled by the behavior of atoms when they interact with radiation. Material stimulated by short wavelength radiation (e.g., X-rays) becomes ionized (Pella, 1989). If the energy of the

radiation is sufficient to dislodge an electron from an inner electron-level, the atom becomes unstable and an external electron replaces the missing internal electron. When this occurs, energy is released due to the reduced binding energy of the inner electrons. The emitted radiation is of lower energy and termed fluorescent radiation. The energy of the emitted photon is characteristic of a transition between distinct electron levels of a particular element, and can therefore be used to detect element abundancies within the sample (Benson, 1995; Cesareo, 2000; Shackley, 2011). X-Ray fluorescence is used in a wide range of applications, such as: environmental studies (e.g. Aranbarri et al., 2015; Kujau et al., 2010), ceramic and glass manufacturing (e.g. Freitas et al. 2018; Frahm, 2018), research in igneous, sedimentary, and metamorphic petrology and soil science (e.g. Acquafredda, 2018; Hupp and Donovan, 2018).

In the studies presented here, the element ratios Ca-Fe and Ca-Ti are of special interest. Calcium is used as an indicator for marine influence, brought into the sedimentary record by carbonate shells from marine macro- and microfauna (Hadler, 2014). On the other hand, titanium is a product of terrestrial weathering of minerals such as feldspar, quartz and mica (Angern et al., 1951; Stucki, 1988). Ca-Ti ratios are therefore reliable indicators of alterations between marine and terrigenous processes. Hadler (2014), Vött et al. (2011a) and Vött et al. (2011b) used a similar methodological approach for identifying tsunamites in ancient harbors. By calculating the Ca-Fe ratio it has been successfully attempted to delimit sedimentary units deposited under marine or terrestrial conditions. According to Vött et al. (2011a) low Ca-Fe ratios of sediments correlate with an increased terrestrial influence by subaerial decalcification and iron oxides formation, while high Ca-Fe ratios reflect prevailing marine conditions.

3.3.5 Inductively Coupled Plasma Optical Emission Spectrometry (ICP-OES)

ICP-OES measurements determine the element concentrations digested in a solution through the respective characteristic optical emission spectrum of each element (Hou and Jones, 2006). The measurements were conducted at the laboratory of the Physical

Geography at the Freie Universität Berlin using an ICP-OES Spectrometer Optima 2100 DV of Perkin Elmer.

Prior to ICP measurements, the samples were sieved (< 2 mm), dried at 50 °C and homogenized in an agate disk swing mill. *Aqua regia* dilutions of 1.0 g of dry sediment were produced with nitro-hydrochloric acid (7 ml HNO_3 65 %) and hydrochloric acid (21 ml of HCl 32 %) following DIN EN 13346 (2001). ICP-OES measurements were carried out for heavy metals, such as lead (Pb), chromium (Cr), zinc (Zn) and nickel (Ni). As a data quality control, a certified reference material (LGC6156; Portsmouth harbor sediment < 200 µm), duplicate dilutionsand blank reagents were used. The relative standard deviation from the reference material is calculated to Pb = 7 %, Cr = 5 %, Zn = 5 %, Ni = 5 %, and was aligned with the samples. Elemental composition was used to measure metal pollution within terrestrial and marine sediments.

3.3.6 Radiocarbon Dating

Samples of charred wood and organic bulk material were prepared for accelerator mass spectrometry dating (^{14}C) and measured at the Poznań Radiocarbon Laboratory, Poland. The samples consist of charcoal fragments, macroplant remains and bulk samples. Prior to the measurements the available dating material was isolated from sediment material. Alleged charcoal fragments were investigated under the optical microscope. The AMS dates were calibrated with OxCal 4.2 (Ramsey, 2009) and the IntCal 13 (Reimer et al., 2013) calibration curve with a confidence interval of 2σ

3.4 Secondary and Primary Data Analyses and Spatial Visualizations

The spatial data analyses and visualizations of secondary spatial information and primary results in the study area was conducted with ArcGIS 10.0-10.3, Grass GIS 7.0.4., Golden Software Strater 3, Quantum GIS 2.16.2. “Nødebo” and Inkscape 0.91. Furthermore, to primary results produced during the field and laboratory analyses, the

following secondary map material and data sets were taken into account for the production of map material and visualization of the results:

Digital elevation models:

- 1-arc second SRTM-data from USGS (2017)
- 200 m-, 25 m-, 5 m- and 0.5 m horizontal resolution LiDAR-data from CNIG (2017)

Topographical maps:

- Topographical detailed maps 1: 25,000 and 1: 50,000 from CNIG (2017)

Geological maps:

- Geological detailed map 1: 50,000 from (IGME, 1983)
- Geological maps depicted from the Web Mapping Service (WMS) of the IGME

Further thematic maps:

- Soil map of Andalusia depicted from the Web Mapping Service (WMS) of the Junta de Andalucia (2017)
- Map of soil use capacity depicted from the Web Mapping Service (WMS) of the Junta de Andalucia (2017)
- Map of vegetation series depicted from the Web Mapping Service (WMS) of the Junta de Andalucia (2017)
- Map of natural vegetation depicted from the Web Mapping Service (WMS) of the Junta de Andalucia (2017)
- Geomorphological map depicted from the Web Mapping Service (WMS) of the Junta de Andalucia (2017)
- Map of geostructural units depicted from the Web Mapping Service (WMS) of the Junta de Andalucia (2017)
- Lithology map depicted from the Web Mapping Service (WMS) of the Junta de Andalucia (2017)
- Map of landscapes depicted from the Web Mapping Service (WMS) of the Junta de Andalucia (2017)

Historical maps:

- See Table 5 in Chapter 4.3.3

4. Case Studies

4.1 Sedimentological Evidence of an Assumed Ancient Anchorage in the Hinterland of a Phoenician Settlement (Guadiana Estuary/SW-Spain)

Torsten Klein * [a, c], Wiebke Bebermeier [a, c], Jan Krause [a, c], Dirce Marzoli [b], Brigitta Schütt [a, c]

[a] Freie Universität Berlin, Department of Earth Sciences, Physical Geography, Malteserstr. 74-100, 12249 Berlin, Germany

[b] German Archaeological Institute (DAI) Madrid, Serrano 159, 28002 Madrid, Spain

[c] Excellence Cluster TOPOI, Research Area A – Spatial Environment and Conceptual Design, Hittorfstraße 18, 14195, Berlin, Germany

*Corresponding Author

published in 2016 in

Quaternary International, Volume 407, Part A, 2 July 2016, Pages 110-125

https://doi.org/10.1016/j.quaint.2015.12.038

4.2 Human-Environment Interactions at the Phoenician Site of Ayamonte (Huelva/Spain): – Insights from Terrestrial Borehole Data

Abstract

Archaeological findings indicate that in the south of the Iberian Peninsula the coastal range running parallel to the Atlantic coast and crossing the Guadiana Estuary has been populated continuously during Late Bronze Age/Early Iron Age. Most recent excavations document that from the 8th/7th century BCE onwards the ridge, where today the city of Ayamonte (Lower Andalusia/SW-Spain) is located, has already been populated by Phoenician colonists.

Identifying phases of geomorphic activity and stability and relate them to traces of human activities as one driving force constitute challenging tasks for geoarchaeological research. In this paper, Late Holocene terrestrial borehole data from two slope transects in the surrounding of the Phoenician site in Ayamonte are presented and set in relation to the regional archaeological context.

The sedimentological study is based on six sediment cores. Field data is supported by geochemical analyses and environmental magnetic data. The chronological framework was obtained from the analyses of fourteen radiocarbon samples.

Results show, that the extracted colluvial deposits cover the last 4000 years and record signals of human-environment interactions and intensive slope processes. Sediment characters and numerical dating suggest alternating phases of morphodynamics. While the sedimentological results suggest that the Early Modern Era and (Late) Bronze Age mark phases of increased erosion activities, indications of geomorphological stability during the Medieval Warm Period is given by the development of a buried topsoil. Lead concentrations indicate that prehistoric metallurgy can be traced back as early as Bronze Age and left a geochemical fingerprint in the slope deposits.

The landscape around Ayamonte was characterized by strong erosion processes during the Roman Era and the Early Modern Era, both epochs characterized by intense mining, strong deforestation and increased agricultural activities. During the Muslim domination of Iberia, the abandonment of mining activities seems to coincide with a phase of reduced erosion intensity. Furthermore, our study indicates that on-site smelting operations in the surroundings of Ayamonte took place already commencing during prehistory.

4.2.1 Introduction

The Phoenician settlement of Ayamonte (founded c. 8th century BC) is situated in close proximity to the Guadiana River and its lower estuary (Fig. 25). The site is located on top of a hill called "Cerro de las Flores" and had an outstanding strategic position in controlling the inlet of the Guadiana River into the Atlantic Ocean and permitting access to a hinterland rich in iron, copper and silver ores. The relative abundance of mineral resources in Southern Iberia has historically acted as a strategic resource for local and foreign civilizations (Arruda, 2009; Aubet, 2001; Moscati, 2001). Previous studies show, that the ancient site of Castro Marim, which is located at the opposite side of the Guadiana River (today situated on Portuguese territory) traces back to an indigenous foundation (Teyssandier and Marzoli, 2014), populated by Iberian tribes, maintaining intercultural contact to the Phoenician colonists (Arruda, 1997; Arruda, 2000a; Arruda, 2003; Arruda and Teixeira de Freitas, 2008). Most recent archaeological investigations document the importance of Ayamonte as Phoenician border town between different political spaces during the Late Bronze Age (LBA)/ Early Iron Age (EIA) (Teyssandier and Marzoli, 2014).

Figure 25: View from south to north over Ayamonte and the Guadiana River. The area of the Phoenician settlement is marked with the red ellipse. The excavation site of the necropolis is marked in pink (Source: 1517-043-D80 (L. Alves) in Teyssandier and Marzoli, 2014).

The aim of this study is to reconstruct phases of geomorphic activity and stability during the Late Holocene. Pursuing this goal, six sediment cores were extracted along two transects at two slopes near the Phoenician site of Ayamonte. Geoarchaeological, environmental magnetic and geochemical investigations as well as ^{14}C-datings, permit the deduction of cycles of sediment mobilization and storage. The initial results of this study contribute to the understanding of Late Holocene morphodynamics in the environs of the Guadiana Estuary. This study represents a complement to the studies, which are primarily devoted to the development of the Guadiana Estuary. Furthermore, this paper gives evidence on increased lead signatures in the terrestrial archives most likely caused by atmospheric deposition, from anthropogenic sources; inter alia resulting from mining and metallurgy.

4.2.2 Study Area

The Guadiana Estuary (37°10' N, 7°24' W) is situated in SW-Andalusia (resp. SE-Algarve-region), in the southernmost part of the international border between Portugal and Spain (Fig. 26). The Guadiana Estuary represents a wetland zone with salt marshes, lagoons and tidal creeks (Chícharo et al., 2007). During the Holocene sea level rise the coastal fluvial system has been transformed into an estuarine system, which is nowadays dominated by a mesotidal regime with a tidal range of 2.0 m (Borrego et al., 1995; Morales, 1997; Perillo, 1995a). Currents of predominantly east-west directions control coastal erosion and sedimentation processes (Goy et al., 1996).

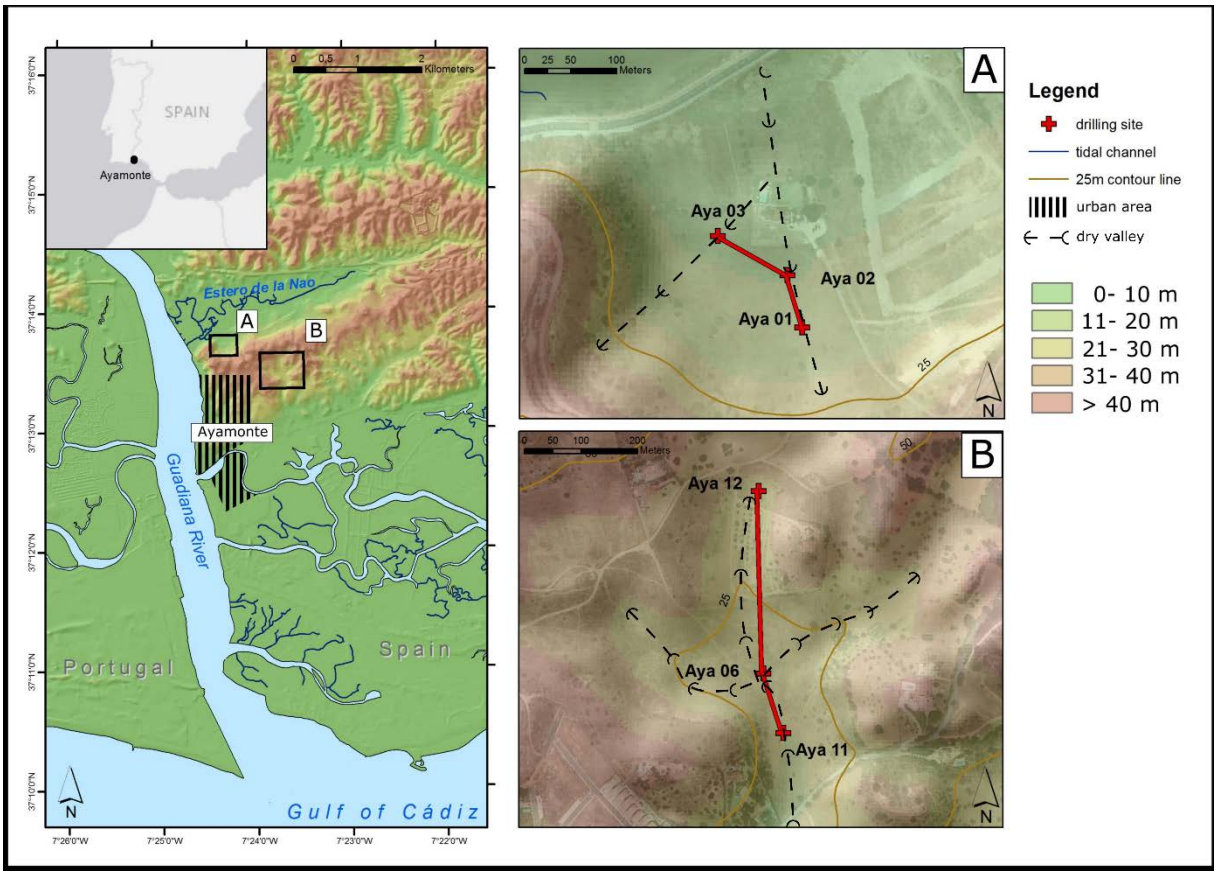

Figure 26: General map of the study area with study sites A and B (Map layout: own design; data sources: own data surveys and Centro Nacional de Información Geográfica [http://centrodedescargas.cnig.es/CentroDescargas/index.jsp], access: 23.01.2018; coordinate reference system: WGS84/Pseudo-Mercator]).

The Mediterranean climate is characterized by pronounced seasonality, with hot dry summers and mild winters during which the majority of rain falls. Mean January air temperatures of 9.9 °C contrast average August air temperatures of 23.3 °C (Rivas-Martínez et al., 1990). Annual temperature in Villa Real de Santo Antonio, about 4.5 km SSW of Ayamonte averages 16.3 °C and the mean annual rainfall remains below 500 mm (Loureiro, 1983).

The Guadiana River drains the eastern reach of the Iberian Pyrite Belt, one of the largest metal-rich sulfide deposits globally (van Geen et al., 1997). The deposits of the Iberian Pyrite Belt were formed during late Paleozoic by precipitation from hydrothermal fluids during a period of intense submarine volcanism (Boulter, 1993). Besides sulfur and iron, the deposits contain large amounts of copper, lead, zinc, gold and silver (Strauss et al., 1977). Earliest mineral extraction in southwest Iberia is documented for the Tinto-Odiel Estuary (42 km east of Ayamonte) and dates back to the 3rd millennium BCE, while large scale mining of silver deposits commenced approx. 1200 BCE by the Phoenicians (Ruiz et al., 2008). During Roman times mining for copper and silver intensified, while these deposits were almost untouched during post-Roman times (Strauss et al., 1977). During the 18th and 19th century due to the demand for copper, intensive mining started again (Strauss et al., 1977). Metallogenic maps of the Ayamonte region show, that in the close proximity important metalliferous sources do not occur (IGME, 1983). The majority of mineral deposits is located within a distance of more than 50 km to the northeast (Fig. 27A).

Bedrock in the area around Ayamonte is highly heterogeneous (Fig. 27B). While north of the study area carboniferous schists and fossiliferous graywackes dominate (Vidal et al., 1993), the parent material in the area of interest is composed of Triassic dolomites, with dikes of dolerites, indicating post-sedimentary magmatic activities. Tectonically the southwestern coast of Spain is located closely to the Africa-Eurasia plate boundary, which is a source area of high-magnitude earthquakes. Quaternary tectonics are

dominated by E-W and NNW-SSE trending fault systems (Lobo et al., 2003); tsunami sediments resulting from the 1755 Great Lisbon earthquake have been identified in coastal embayments of the Guadiana Estuary (Klein et al., 2016). While the shallow subsurface of lagoonal-like depressions (so called *"esteros"*) is dominated by gray, organic and silt rich mud (Klein et al., 2016), the slopes are covered by shallow Quaternary sands and gravel (IGME, 1983). Chromic cambisols with intense rubefication and strong iron oxide formation are the dominating soil type at both studied slopes. Incorporated extensive layers of rounded quartzite clasts refer to deposits of a Paleo-Guadiana. Today both studied slopes are used as pastures, while neighboring areas are (partially abandoned) terraced orange orchards.

The coring sites were chosen because of their proximity to the archaeological site. Both studied slopes are characterized by crestal convexity, a straight-line profile in the mid-section and a pronounced basal concavity, offering the possibility of intermittent sediment storage at the foot slopes.

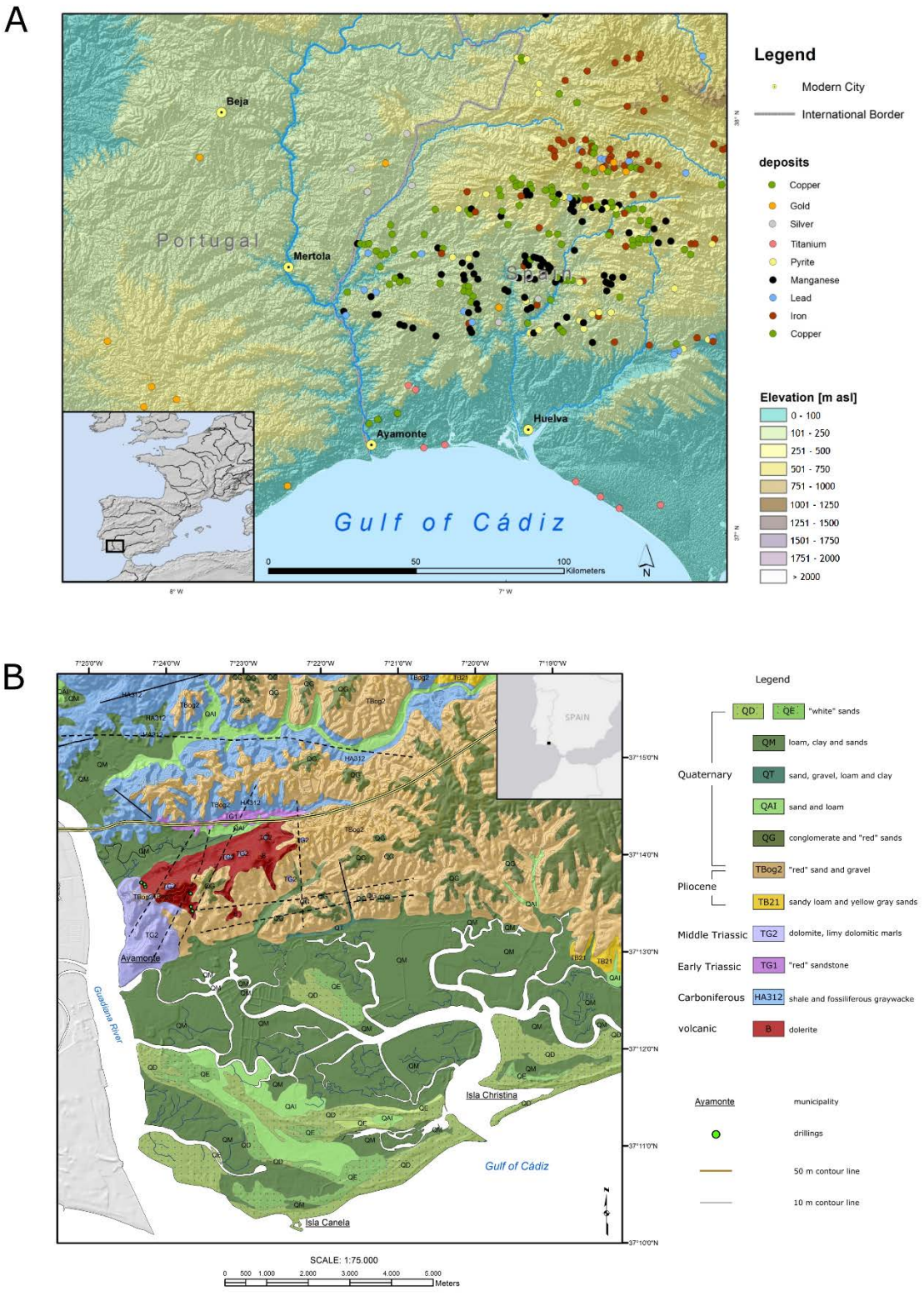

Figure 27: (A) Regional distribution of the most important ore deposits in the Huelva province (please note: except for gold and silver deposits, Portuguese ore deposits are not mapped); (B) Geological map of the study area; modified after IGME (1983) (Map layout: own design; data sources: IGME (1983) and Centro Nacional de Información Geográfica). [http://centrodedescargas.cnig.es/CentroDescargas/index.jsp], access: 23.01.2018; coordinate reference system: WGS84/Pseudo-Mercator)

Study site A is situated at the northern flank of an ENE-WSW striking solid rock ridge and is chosen to provide information on the downslope sediment transport towards the lower marsh lands. Sediment input from the marsh land can be excluded due to the coring sites' remoteness and elevation. The hoof-shaped depression close to the wetlands of the Estero de la Nao is located 600 m west of the Guadiana Riverbank and 1.5 km north of the city center of Ayamonte (Fig. 26 A). Information on the character of the slope deposits were gained by three sediment cores (Aya 01-Aya 03) located in c. 200 m distance to the recent wetlands of the Estero de la Nao. The three drillings are located at a north-exposed slope with two flat cut small-scale valleys. While Aya 01 and Aya 02 are situated within one valley, Aya 03 represents a different dry-valley.

Three merging dry valleys located 1.5 km west of the Guadiana Riverbank and the city center of Ayamonte characterize the study site B. Three drillings (Aya 12, Aya 06, Aya 11) were conducted at the central valley and in the confluence of the valleys, providing information on phases of slope stability and instability (Fig. 26 B). While the uppermost core Aya 12 represents a midslope position, Aya 06 and Aya 11 represent the confluence of the tributary valleys, resp. the downslope positions. Thus, it is expected to obtain information from the central valley and information from additional material of the two adjacent tributary valleys. Due to the spatial circumstances, the results should be subjected to critical scrutiny. Study site B is hydrologically decoupled from study site A and characterized by a basin like shape within the confluence area.

4.2.3 Methods

In early fall 2013 a field campaign was conducted. The methodological approach included geographical field methods, such as percussion drillings and the recording of soil profiles, as well as laboratory analysis.

Figure 28: Panoramic photographs of study sites A (above) and B (below) and the drilling locations (© T. Klein).

Six sediment cores were obtained from the two study sites (Fig. 28 and Table 3). The cores were extracted using a percussion system (Wacker BHF 30 S) 5 cm in diameter. Drillings Aya 01, Aya 02, Aya 03, Aya 06 and Aya 12 were conducted with open probes, while drilling Aya 11 was extracted in closed PVC tubes. The open cores were described on-site and the sediment samples were properly kept in air-tight plastic bags. The closed plastic tubes of Aya 11 were sealed light-proof and stored frozen after the return transport for subsequent laboratory work. Subsequently the tubes were opened and described in the Laboratory of Physical Geography of the Freie Universität Berlin. Sampling of the open cores took place in 10 cm intervals and accordingly immediately above and below layer boundaries. Positions of the cores were determined using a handheld GPS (Garmin 60 CS, 5 m accuracy; vertical accuracy: +/- 3 m). Guidelines from the German manual of soil mapping (Ad-Hoc-AG Boden, 2005) were followed to describe the grain size composition of the sediments.

Table 3: Drilling sites and drilling characteristics.

Study Site	Drilling Core	Latitude	Longitude	Elevation	Drilling Depth	Drilling Character
A	Aya 01	37°13'40.20" N	7°24'16.22" W	13.6 m	1.25 m	open tube
A	Aya 02	37°13'41.65" N	7°24'16.74" W	9.6 m	2.46 m	open tube
A	Aya 03	37°13'42.72" N	7°24'19.18" W	8.9 m	2.77 m	open tube
B	Aya 12	37°13'36.03" N	7°23'41.01" W	29.1 m	2.00 m	open tube
B	Aya 06	37°13'27.80" N	7°23'40.75" W	21.3 m	4.00 m	open tube
B	Aya 11	37°13'25.10" N	7°23'39.60" W	20.2 m	5.00 m	closed tube

After the samples were dried at 50 °C and organic content was removed by hydrogen peroxide. Grain size composition of Aya 11 was determined using a laser particle sizer (Beckman Coulter LS 13320). For further sediment analysis samples were homogenized in an agate swing-sledge mill. Total inorganic carbon contents (TIC) were determined using a Wösthoff carmhograph (detection limit = 0.02 mass-% C). Total carbon (TC) content was determined using the Leco TruSpec CHN 1000 analyzer (detection limit=0.01 mass-%). Total organic carbon contents were calculated as the difference of both values. Electrical conductivity of the sediment solutes was measured with the Hanna handheld device (HI 98301) with a ±2 % accuracy in a solution with a sediment-distilled water ratio of 1:2. Sediment's pH value was determined with a Hanna handheld device (HI 98127) in 0.01 M KCl suspension with 0.1 pH resolution with a sediment-solution ratio of 1:2. Determination of lead concentrations in the sediments of cores Aya 01, 02, 03, 06 and 11 was performed using inductively coupled plasma atomic emission spectroscopy (ICP-OES, Optima 3000, Perkin Elmer). The values of Pb-concentrations exceeded in all samples the detection limit of 5.1 $\mu g*kg^{-1}$. For the assessment of soil heavy metal burden, the German legislation was used (BBodSchG, 1998). The German and Finnish standard values for contaminated soil are similar in many areas, and thus represent a good approximation of the mean values of different

national systems in Europe (Tóth et al., 2016). Magnetic susceptibility (MS) at low frequency (0.46 kHz) was measured on air-dried weighted samples using the MS2B sensor (Bartington Instruments) with 10 cm^3 sample containers (Dearing, 1994).

Age control is provided by fourteen radiocarbon datings (AMS), exclusively grit-sized charcoal analyzed at the Poznan Radiocarbon Laboratory (Table 4). Calibration of radiocarbon dates was done with OxCal 4.1 software (Ramsey, 2009) using the "IntCal09" calibration curve of Reimer et al. (2009).

4.2.4 Results

In the course of the investigations of the sediment cores from the two transects, it has been found that the core architectures of the individual cores are very similar. For this reason, first the individual sedimentary units are described and classified briefly (chapter 4.2.4.1) and a typical sediment core of each transect is presented (chapter 4.2.4.2 and 4.2.4.3). Subsequently, the geochronology of the sequences is summarized in chapter 4.2.4.4.

4.2.4.1 Sedimentary Units

The sediment cores in transect A have a comparable architecture, and each can be subdivided into three units by means of geochemical parameters and their age. Apart from the chronological affiliation of the individual units, especially the three parameters total organic carbon (TOC), magnetic susceptibility and lead concentrations allow an assignment of the single units. The basal units in the sediment cores of transect A (units I) are characterized by the highest magnetic susceptibilities ($\mu = 775*10^{-8}$ m^3*kg^{-1}, std. = 130, n = 7), as well as lowest TOC contents (μ = 0.05 mass-%, std. = 0.07, n = 7) and lead concentrations (μ = 0.7 $mg*kg^{-1}$, std. = 0.2, n = 9). Within the overlying sediments (units II) TOC contents (μ = 0.8 mass-%, std. = 0.5, n = 20) and lead concentrations rise steadily with decreasing depth (μ = 3.8 $mg*kg^{-1}$, std. = 1.9, n = 20), while values of magnetic susceptibility decrease slowly towards the top ($\mu = 720*10^{-8}$ m^3*kg^{-1}, std. = 150, n = 19). The lowest values of magnetic susceptibility

occur in the uppermost units III (μ = 545*10^{-8} m^3*kg^{-1}, std. = 140, n = 16). On the other hand, lead concentrations (μ = 17.3 mg*kg^{-1}, std. = 4.2, n = 34) and TOC contents (μ = 1.4 mass-%, std. = 0.6, n = 280) reach maximum values in the uppermost unit.

A clear distinction between sedimentary units and classification, as conducted for transect A, is not easily possible in transect B. The reasons are the strong sedimentary heterogeneities and marginal geochemical differences between the individual sedimentary units. Based on the parameters mentioned, general trends in the sediment cores can be seen. The lowest areas of the cores that reached the weathered bedrock (units I of Aya 12 and Aya 06; see Fig. A.5 and Fig. A.6) showed the lowest values of magnetic susceptibility (μ = 10*10^{-8} m^3*kg^{-1}, std. = 0.5, n = 31), TOC contents (μ = 0.35 mass-%, std. = 0.2, n = 13) and lead concentrations (μ = 13.1 mg*kg^{-1}, std. = 1.2, n = 7). Weathered bedrock could not be drilled at the foot slope of the transect. At this position, the lowest unit of the core at this position (unit I of Aya 11) is characterized by the highest magnetic susceptibility (μ = 20*10 $^{-8}$ m^3*kg^{-1}, std. = 1.5, n = 24). As in transect A, the top layers are characterized by the high lead (μ = 26.5 mg*kg^{-1}, std. = 28.8, n = 21) and TOC contents (μ = 2.25 mass-%, std. = 1.2, n = 21). The layers between the lower- and uppermost units are distinguished by medium TOC values and a geochemical heterogeneity. A particular feature of these interposing layers is an area of darker coloration and slightly increased TOC values and magnetic susceptibility within core Aya 06 at intermediate slope position.

4.2.4.2 Transect A

The chronological framework of transect A is accomplished by seven radiocarbon dates derived from remains of charcoal. It covers the period between the Bronze Age c. 3000 ±140 BP (2010-1300 cal BCE) and the modern Era (1450-1945 cal CE) (see Table 4). A chronological inversion as caused by alternating cycles of sediment storage and remobilization has been observed at the two uppermost datings of Aya 03 (Fig. 29;

Table 4: Poz#2-59738, 80 cm depth b.s. and Poz#2-59749, 152 cm depth b.s.). In summary, Transect A is characterized by a clear geochemically and geochronologically distinctable structure.

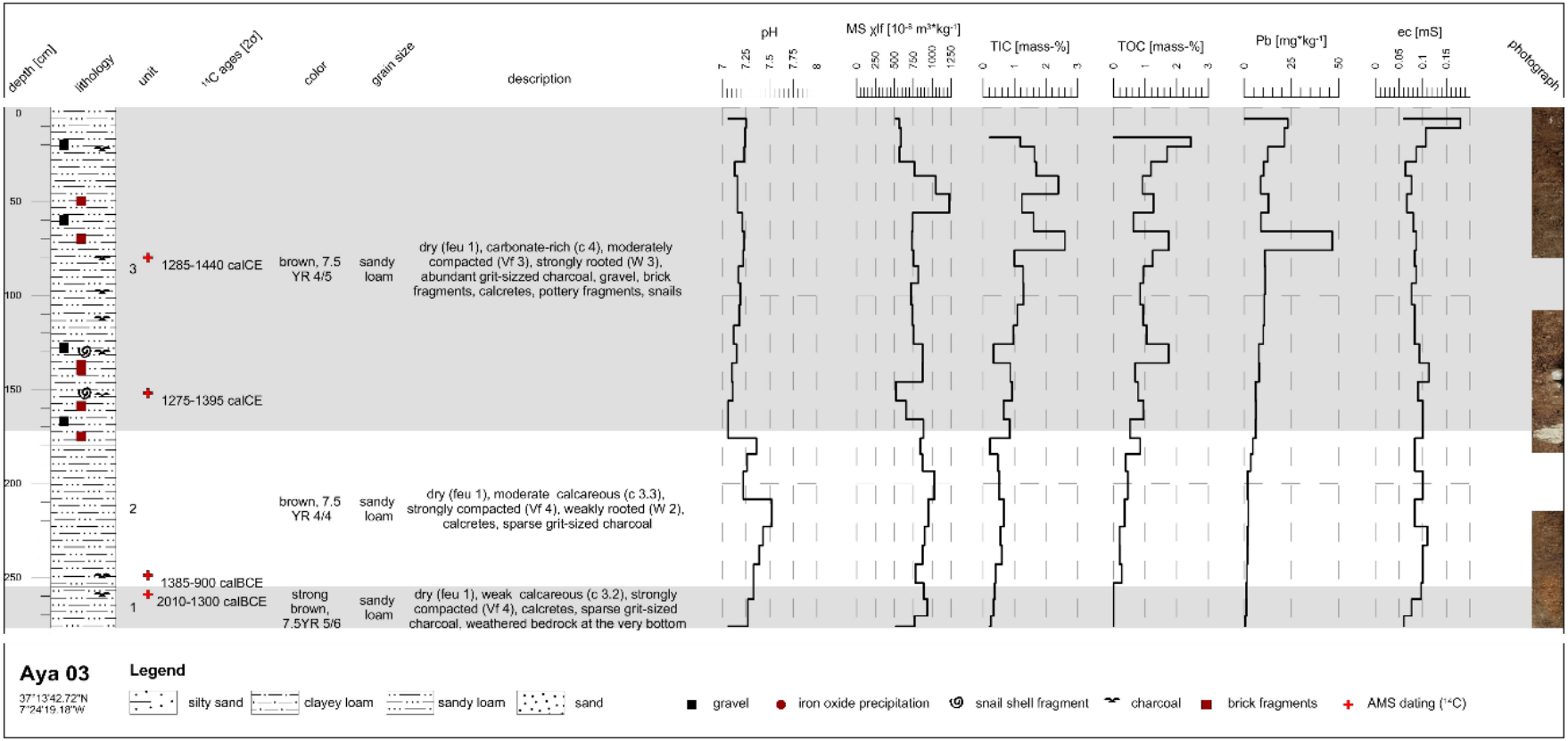

Figure 29: Stratigraphy and geochemical parameters of sediment core Aya 03. Unit 1 - 3: colluvial deposits.

4.2.4.3 Transect B

Transect B covers the time span between the Roman Warm Period around 35 cal BCE - 130 cal CE and the Modern Era (1645-1940 cal CE). Charcoal fragments dating into the Roman period occurred in Aya 11, extracted from the foot slope. The further available charcoal datings show ages assigned to the (Late) Medieval and the Early Modern Period (Fig. 30). A chronological inversion in drilling Aya 06, 132 and 150 cm depth illustrates the occurrence of temporary deposition of sediments and their remobilization along a sediment cascade (Lang and Hönscheidt, 1999). Transect B shows more heterogeneities than transect A (see Fig. 30)

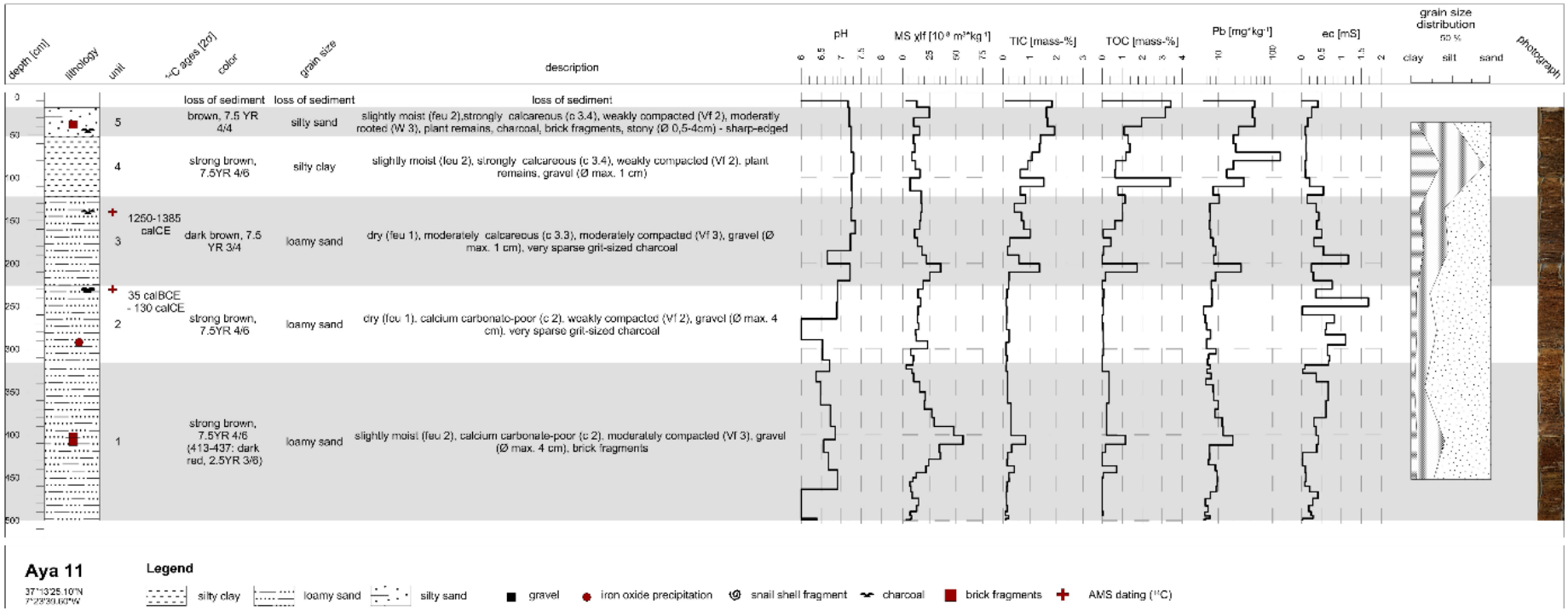

Figure 30: Stratigraphy, grain size distribution and geochemical parameters of sediment core Aya 11. Unit 1-5: colluvial deposits.

Table 4: Radiocarbon dates of samples from both studied slopes. (*calibration with OxCal 4.1 (Ramsey, 2009) and the IntCal09 calibration curve (Reimer et al., 2009)).

Sample depth [m]	Sample elevation [m a.s.l.]	Lab. Code	^{14}C age (BP)
Aya 01			
0.30	13.30	Poz#2-59748	260 ± 100 BP
Aya 02			
0.46	9.18	Poz#2-59739	410 ± 70 BP
0.60	9.04	Poz#2-59736	680 ± 35 BP
Aya 03			
0.80	8.09	Poz#2-59738	580 ± 70 BP
1.52	7.37	Poz#2-59749	660 ± 40 BP
2.49	6.40	Poz#2-59746	2910 ± 90 BP
2.59	6.30	Poz#2-59744	3320 ± 140 BP
Aya 12			
0.75	28.37	Poz#2-74205	565 ± 30 BP
Aya 06			
0.51	20.76	Poz#2-59740	130 ± 30 BP
0.76	20.51	Poz#2-59745	200 ± 40 BP
1.32	19.95	Poz#2-59742	1140 ± 90 BP
1.50	19.77	Poz#2-59747	825 ± 30 BP
Aya 11			
1.40	18.78	Poz#2-74206	715 ± 30 BP
2.30	17.88	Poz#2-72991	1940 ± 35 BP

4.2.4.4 Geochronology

The radiocarbon dates are mostly in chronological order and can be assigned to several climatic periods and cultural epochs (Fig. 31, Fig. 32 and Fig. 33): (I) the Modern Era/Little Ice Age, represented by ages in all dated sediment cores, (II) the Bronze Age, represented by samples of Aya 03 (transect A), (III) High Medieval Times/Medieval Warm Period represented by samples from Aya 06 (transect B) and (IV) the Roman Era/Roman Warm Period, represented by a single sample originating from Aya 11 (transect B).

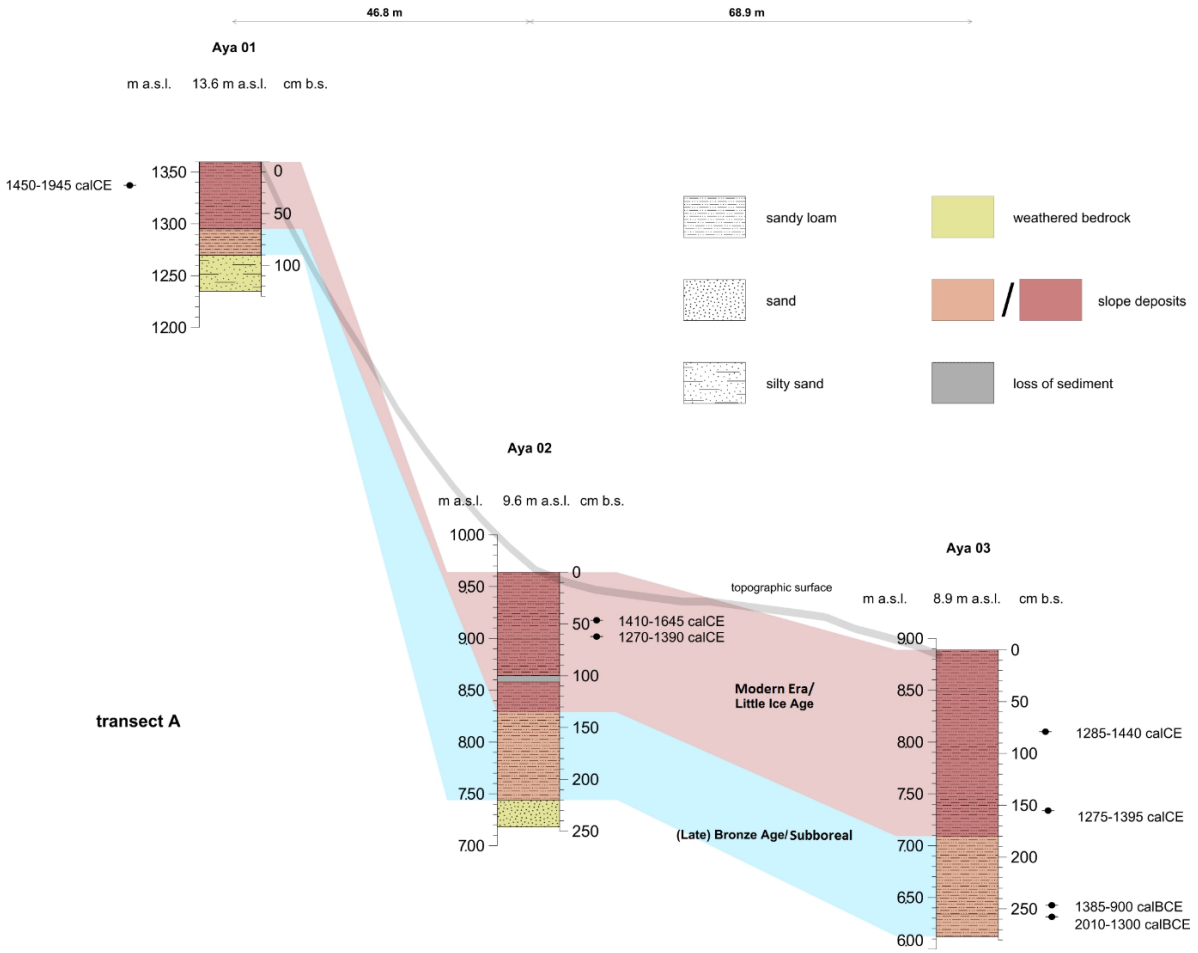

Figure 31: Conceptual Cross-sections of transect A showing the topographic surface, the estimated distribution of chronological units and the lithology.

Taking the period between the oldest and the most recent sample as a reference frame, two major hiatuses occur: The first occurs roughly between 750 cal BCE and the beginning of the Common Era covering the period of the expansion of the Celtic culture in SW-Iberia (Dinis et al., 2006). The second hiatus occurs between 250-750 cal CE, covering the decline of the Roman Empire and the subsequent Migration Period with the invasion of the Visigoths.

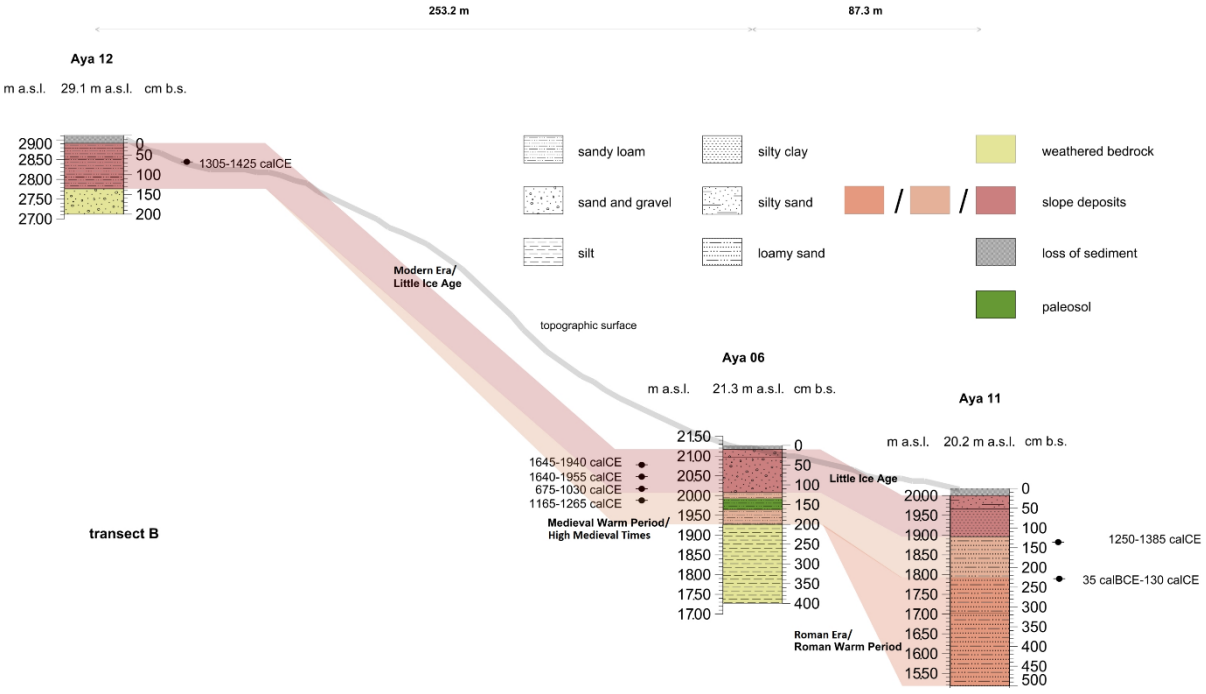

Figure 32: Conceptual Cross-sections of transect B showing the topographic surface, the estimated distribution of chronological units and the lithology.

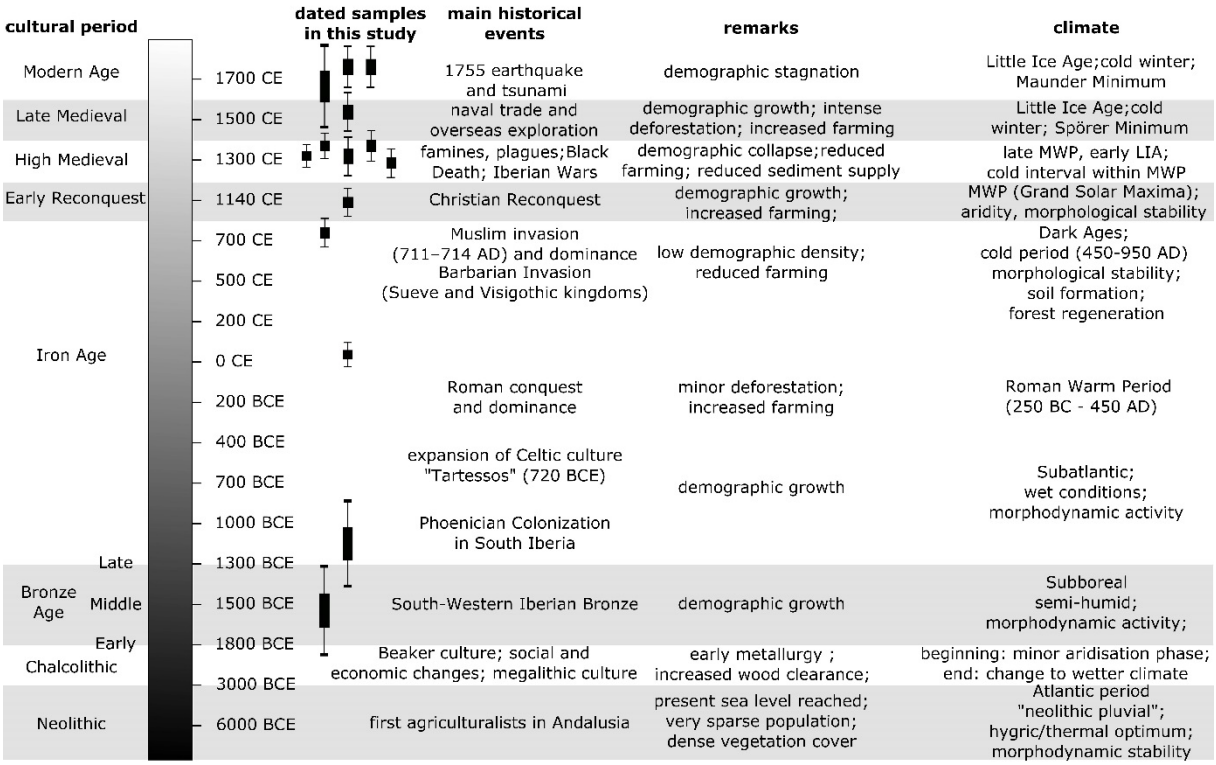

Figure 33: Synthesis of dated samples within this study, cultural epochs and main historical events with large landscape impacts based on Bellin et al. (2013) and Dinis et al. (2006).

4.2.5 Discussion

4.2.5.1 Sediment Characteristics

The stratigraphies of the two transects investigated give a brief look into the sedimentological evolution of the slopes surrounding the Phoenician settlement of Ayamonte. In both transects, colluvial deposits characterize the sedimentary record. It is likely that the colluvial deposits, inter alia characterized by angular clasts, originate from the adjacent slopes and cover the weathered bedrock reached by the drillings in various depths.

Transect A

At the bases of drillings Aya 01 and Aya 02 parent material was exposed, corresponding to the volcanic bedrock (see Fig. A3 and Fig. A4). Magnetic susceptibility (χ_{lf}) values within these bedrock-units average at c. $715*10^{-8}$ m^3*kg^{-1}, indicating volcanic bedrock material (Evans and Heller, 2003; Hunt et al., 2013; Pandarinath et al., 2014). These high χ_{lf} values in the bedrock originate from dolerite, which contains comparatively high contents of both ferromagnetic minerals (biotite, olivine, augite and hypersthene) and magnetic minerals (mainly magnetite and ilmenite). Hunt et al. (2013) compiled the magnetic data of different rocks and materials and reported the magnetic susceptibility of dolerites as between 35 and $5600*10^{-8}$ m^3*kg^{-1}.

The lower magnetic susceptibility values of the slope deposits overlying the parent material is most likely affected by weathering and redeposition as the predominant synsedimentary processes (Mullins, 1977), coinciding with changing mineralogical characters due to soil forming processes (Dearing, 1994; Evans and Heller, 2003). Fires as they appear frequently within the Mediterranean, induce an increase of the magnetic susceptibility of the topsoil (Evans and Heller, 2003; Le Borgne, 1955). Based on this complex pattern of processes affecting the magnetic susceptibility of slope deposits in sediment cores Aya 01, 02 and 03 the slight increase of magnetic susceptibility values

with depth is most likely attributed to a blending of poorly weathered parent material (which has high magnetic susceptibility values) with colluvial deposits.

Organic carbon in colluvial deposits might be due to in-situ soil forming processes (Zádorová et al., 2011; Zádorová et al., 2015) or to the accumulation of soil sediments resulting from soil erosion processes (Dunne et al., 1991; Kuhn et al., 2012; Lal, 2005; Polyakov and Lal, 2004; Quinton et al., 2006). High organic carbon contents in the uppermost layers correspond to the current soil formation. The decreasing contents of organic carbon with depth may originate from various processes. It can be conceived that the early diagenetic decomposition of organic matter in a depositional environment led to a depletion of organic matter (Rheinheimer, 1974). In addition, soil turbation processes, which may lead to a biogenic turnover, cannot be excluded (Hemelryck et al., 2009). These systematic changes of organic carbon in the sediments occur in all extracted cores, but become particularly apparent in core Aya 01, the topographically uppermost core along the transect. In this sediment core increased organic carbon contents in deeper sediment layers lack. Sediments of cores Aya 02 and Aya 03 show peaks of organic carbon contents also in deeper sediment sections which are unaffected from present day soil forming processes. Due to the findings, that increased organic carbon contents in deeper strata occurs exclusively in the sediments extracted from mid-slope and foot-slope positions, there is the possibility that the process of impeded decomposition of organic material after covering by sediments can be identified as a possible cause (Lerman, 1979; Schütt, 2006). However, frequency dependent susceptibility measurements revealed no values indicative for buried soil material and thus it cannot be excluded that the increased organic carbon contents result from other causes, such as integration of charred matter by root glow or incorporation by turbation (Carcaillet, 2000; Schaetzl, 1986). Therefore, the precise nature of the findings cannot be clarified completely by the available methodical means. The charcoal fragments incorporated into the sediments date back to the late Medieval times.

The observed carbonates in the colluvial deposits largely correspond to redeposited weathering products of Triassic limy dolomitic marls outcropping in the headwater area of the site. The local occurrence of calcareous concretions (Aya 01, 77-89 cm depth, Aya 02, 84-100 cm depth and Aya 03 75-277 cm depth) underlines the secondary precipitation of carbonates from ascending soil water under semi-arid environmental conditions (Goudie, 1983; Michael, 2007). It is assumed that dissolved calcium carbonate in the soil water originates from solution of upslope outcropping Triassic carbonate bedrock (IGME, 1983).

The lead concentrations in all three sediment cores show comparable curves. The close correlation of Pb contents to TOC contents points to the importance of organic matter as absorbent. This positive correlation between organic matter contents and lead concentrations has been recorded within previous studies and is mainly associated with adsorption processes of fine-grained organic-rich sediment fractions (Syvitski, 1991; Wang, 2008). Lowest lead concentrations are observed within the weathered bedrock, documenting the geological background concentrations. Deposits immediately overlying (each marked as unit 2), show lead contents up to fivefold higher than the underlying bedrock. These stepwise increasing lead concentrations most likely indicate regional pre-industrial mining and smelting activities during which lead was atmospherically emitted and accumulated during the smelting process as a by-product (Hunt Ortiz, 2003; Nocete et al., 2005). Early lead production in SW-Iberia started about five millennia before present (Leblanc et al., 2000) with the discovery of new techniques for smelting lead-silver alloys from lead sulfide ores and cupeling silver from the alloys (Hong et al., 1994; National Research Council US Geodynamics Committee, 1980; Nriagu, 1983a). Metal production within the Mediterranean increased constantly since the Chalcolithic period as a result of silver coinage (García-Alix et al., 2013; Nriagu, 1983a; Nriagu, 1983b). Lead is a 300-to-one by-product of silver production (Hong et al., 1994) and has thus the potential to accumulate in a significant amount in terrestrial

archives and, therefore, is a valid indicator for silver mining and smelting processes. In all three cores extracted along transect A the highest lead concentrations occur in the most recent deposits, accumulated during the Modern Era. Compared to the weathered bedrock these deposits show concentrations increased by the factor fifteen (max. 46.6 $mg*kg^{-1}$) and reach precautionary values of the german soil protection ordinance of 40 $mg*kg^{-1}$ (BBodSchG, 1998). These high values of elemental lead most likely originate from atmospherical deposition, which arise during industrialization processes (e.g. traffic, industrial pollution) detectable all around the world (Candelone et al., 1995; Goudie, 2001). However, it has to be taken into account that these Pb-concentrations within the uppermost sediment units could be superimposed by a strong regional signal, resulting from the reactivation of mines in the lower catchment area of the Guadiana River during the last centuries (Delgado et al., 2012b; Strauss et al., 1977). After the flourishing period of Roman mining operations, mining recommenced in the first half of the 18^{th} century and released significant amounts of atmospheric heavy metals, being the largest load in the mining history of the region (Delgado et al., 2012a). These in most cases open-pit mining operations were large in scale and aimed mainly for the exploitation of copper and sulphuric acid (van Geen et al., 1997). The São Domingos mine, located 50 km north of Ayamonte was exploited particularly intensively, exposing the Guadiana Estuary and its surroundings to serious contaminations (Delgado et al., 2011; Delgado et al., 2012a; Delgado et al., 2010; Delgado et al., 2012b).

Transect B

Similar to transect A, the captured sediments correspond to colluvial deposits or valley fills respectively, which overlie Triassic carbonates (IGME, 1983). Bedrock material recovered from the lowermost units of cores Aya 12 (Fig. A.5) and Aya 06 (Fig. A.6) shows low magnetic susceptibility values corresponding to the carbonate-rich bedrock (Evans and Heller, 2003; IGME, 1983). Magnetic susceptibility (χ_{lf}) values within these bedrock-units average at c. $10*10^{-8}$ m^3*kg^{-1}. These exceptionally low values of magnetic

susceptibility most likely originate from diamagnetic components of the dolomitic bedrock. Hunt et al. (2013) reported the magnetic susceptibility of dolomite between -1 and $41*10^{-8}$ m^3*kg^{-1}.

Similar to sediments of transect A, the magnetic susceptibility values in the unconsolidated units overlying the bedrock material, most likely reflect the different synsedimentary processes. It is assumed that relatively high, oscillating magnetic susceptibility within the colluvial deposits predominantly result from the alternating influence of soil forming processes or forest fires (de Jong et al., 1998; Evans and Heller, 2003; Le Borgne, 1955). High levels of magnetic susceptibility are particular evident within units 3 and 4 of Aya 06 (Fig. A.6). It is assumed that these increased values originate from soil forming processes, indicating the occurrence of relict topsoil material (Dearing et al., 1996). The high contents of organic carbon within the units 3 and 4 of sediment core Aya 06 most likely confirm the findings of a relict topsoil (Retallack, 2001). The charcoal incorporated into these sediments dates back to High Medieval times.

Similar to transect A highest organic carbon contents are found within the uppermost sediment layers, resulting from soil forming and pedoturbation processes including organic detritus, soil biota and charcoal fragments (Scheffer et al., 2010). In all cores extracted along transect B high organic carbon contents in the uppermost sediments continuously decrease with depth. Comparable to sediments extracted along transect A, this most likely points to early diagenetic decomposition of organic matter (Rheinheimer, 1974) and soil turbation as an effect of soil formation (Hemelryck et al., 2009; Scheffer et al., 2010). In all the three cores extracted along transect B also in the sediments found between 120-160 cm depth, TOC contents are slightly (Aya 06, Aya 11) to distinctly (Aya 12) increased. Radiocarbon ages from charcoal fragments show ages dating back to the Late Medieval Period (Table 4 and Fig. 32). It is assumed that these increased TOC contents in the near-subsurface sediments indicate soil forming

processes in a phase of landscape stability during Moorish settlement in SW Iberia (Roth et al., 2016). The recurring peaks of TOC in 100 cm intervals of Aya 11 are interpreted as topsoil sediments dropping during the core extraction. Low amounts of organic carbon within the sediment cores originating from the footslope (Aya 11, unit 2 of Aya 06) most likely reflect the deposition of material originating from sources poor in soil formation (Kuhn et al., 2012; Lal, 2005; Polyakov and Lal, 2004).

TIC curves show high values within the bedrock units of Aya 12 (Fig. A.5) and Aya 06 (Fig. A.6) and reflect the weathered carbonaceous parent material (IGME, 1983). Correspondingly, solutes in the soil water within transect B contain increased amounts of carbonates. As depletion of inorganic carbon is directly related to pH values and as pH values in topsoils are usually slightly acid due to humic acids resulting from decay processes, decreased TIC values of inorganic carbon contents coincide with the increased organic carbon contents in the fossil soils (Suarez, 2002). On the other hand altogether low electric conductivity of sediment solution points accordingly to transect A to the terrestrial origin of the extracted sediments (Rhoades, 1999).

The high contents of inorganic carbon within the uppermost units of all three cores is most likely caused by secondary precipitation resulting from evaporation and initial formation of calcareous concretions under altogether dry-subhumid climatic conditions (Goudie, 1972). The pseudomycel-like occurrence documents the precipitation of secondary carbonates in and along root traces (Schaetzl and Anderson, 2007). The recurring peaks of increased TIC in 100 cm intervals of Aya 11 are interpreted as droppings during the core extraction.

Lead concentrations in the sediments extracted along transect B show high values in the topmost meter of the respective sediment column exceeding clearly the precautionary values of the german soil protection ordinance of 40 $mg*kg^{-1}$ (BBodSchG, 1998). In one case (140 $mg*kg^{-1}$ in core Aya 11 in 75 cm depth), the limit of lead

concentration in soil used for recreational purposes in the US and Germany is reached, documenting the emergence of a harmful soil change (BBodSchG, 1998). These observations document predominantly increased lead pollutions since the onset of industrialization and the occurrence of organic carbon acting as absorbent (Candelone et al., 1995; Goudie, 2001). In contrast, low concentrations of lead in the sediments with incorporated charcoal fragments dating back to the Medieval age, most likely document the temporary abandonment of mining activities (Currás et al., 2012; Davis Jr et al., 2000). Like in the sediments extracted along transect A, the results most likely represent a global signal, overlain by a regional signal originating from the reactivation of ore mines in the Huelva, Algarve and Alentejo provinces since the 18th century AD (Delgado et al., 2012a; Strauss et al., 1977). Corresponding to the high importance of the Roman mining industry in today's Spanish provinces of Seville and Huelva (Delgado et al., 2012a) lead concentrations in the sediments assigned to the Roman period are expected to be high. The Roman period is one of the main pre-industrialization lead pollution periods recorded in the Northern Hemisphere. Tinto River sediments, 40 km east of Ayamonte, show extraordinary high levels of ancient lead concentrations and other elements indicative for mining contamination (Davis Jr et al., 2000; Galán et al., 2003; Rufo et al., 2007). However, for unknown reasons, the sedimentological evidences for Roman period mining and smelting activities lack in the sediments of transects A and B. The recurring peaks of increased lead concentrations in 100 cm intervals of Aya 11 are interpreted as topsoil sediments enriched with elemental lead dropping during the core extraction.

4.2.5.2 Evaluation of Slope Dynamics

Colluvial processes require local disturbances of the soil cover (and subsequent erosion) which can be triggered by natural causes (e.g. opening of the vegetation by desiccation and cooling) (Jalut et al., 2000) or human impact (e.g. forest clearing, agriculture). For the SW-Iberian margin, most of the studies on climate development have concluded

relative stable climatic and environmental conditions during the period 3150 cal BCE to 500-800 cal CE (Mendes et al. 2010). After 800 cal CE benthic foraminifera in sediment cores from the continental shelf indicate the establishment of environmental conditions tending towards a wetter and colder climate that culminated in the Little Ice Age (Mendes et al., 2010). However, there are records which expand this conclusion, pointing to a complex pattern of climatic and human-induced geomorphic responses in the landscape (Chester, 2012; Chester and James, 1991; Schneider et al., 2016).

The recorded datings of charred matter within the colluvial layers fall into the Late Holocene and reveal most likely local soil erosion. Due to methodological limitations, the data cannot be understood as synsedimentary process ages, but represent an approximation to the colluvial depositional age. So far, the paleoclimatic, geomorphological and archaeological records available, allow no proper decision as to which cause (climate, geomorphological random, anthropogenic) triggered erosion and produced colluvial layers at the study sites. Nevertheless, due to the findings discussed in section 4.2.4.1 it can be assumed that humans have impacted the landscape budget significantly since prehistoric times.

Allowing the assumption, that colluvial accumulation can be approximately chronologically framed by AMS-dating of charcoal particles and the dating of secondary redeposition can be excluded due to charcoal preservation only feasible on the basis of fast coverage by minerogenic material (Niller, 1998), the obtained radiocarbon ages suggest prehistoric beginning and development of local colluviation. The stratigraphy and chronology of the sediment profiles investigated along both transects, suggest pronounced colluviation occurring during the last c. 4000 years (Fig. 34 and Fig. 35). The colluvial deposition is indicated by charcoal embedded in the sediments, resulting from hillwash, a constantly increasing thickness of the units towards the footslope line, embedded debris and the badly sorted character of the deposits (Leopold and Völkel, 2007). The contact to weathered bedrock surface is in each case reached at the mid-

slope positions of the drillings, while sediments extracted from the foot-slope positions are completely composed of colluvial deposits. The sedimentological characters (e.g. sediment thickness, geochronology) of the sediment profiles extracted along both transects may indicate strong slope dynamics during Late Bronze Age and the Little Ice Age. An intercalated phase characterized by soil formation processes may indicate a reduced phase of geomorphodynamic activities.

The earliest radiocarbon dating incorporated in colluvial sediments dates back to the Subboreal period and coincides with the cultural epoch of Bronze Age to Late Bronze Age (Schubart, 1975). Radiocarbon dated charcoal of this age could only be found in sediment core Aya 03. Prior research results identified this time period of South-Western Iberian Bronze as a morphodynamic active phase and culturally characterized by demographic growth (Bellin et al., 2013; Chester, 2012; García-Alix et al., 2013; García-Ruiz et al., 2013; Martín-Puertas et al., 2008).

According to the temporal assignment of the greater portion of dated charcoal in the colluvial layers, a second phase of increased slope dynamics is suggested. The majority of dated charcoal particles found in both transects dates from 14th - 19th century CE and coincide with the Reconquest/ Early Modern Period, corresponding to the climatic period of the Little Ice Age (LIA) (Grove, 2001). The erosional processes are conclusively shown by cultural debris (brick fragments) which is embedded in the sediments of this period in all sediment profiles. The loose, non-stratified and poorly sorted texture of the material suggests a young process of colluviation (Leopold and Völkel, 2007). To the bottom decreasing TOC contents are prone to syn- and post-sedimentary decay processes (Beckers et al., 2013; Schütt, 1998). Locally, near-surface sediments feature increased inorganic carbon contents (TIC) coinciding with increased occurrence of carbonate precipitations (concretions). This points to secondary carbonate precipitation in consequence of ascendant soil water movement during dry phases, resulting in the formation of initial calcareous concretions (Einsele, 1992).

For Medieval times, in-between the two supposed erosion phases during Late Bronze Age and the Modern times, a phase of reduced erosion coinciding with soil formation also in slope positions is documented in the sediments. Based on three radiocarbon dates from the sediment cores Aya 06 and Aya 11 a fossil soil with up to 40 cm thickness observed in 130-150 cm depth suggests relative stable environmental conditions during the Moorish occupation.

Due to the methods chosen, the presented data cannot guarantee a complete unambiguously assignment to phases of geomorphic activity. It rather gives a raw framework for colluviation phases, due to probable gaps (hiatuses) between dating material formation and colluvial sedimentation (Kaiser et al., 2007). Radiocarbon dating and the assignment of colluvial processes can raise various difficulties. For instance, younger humic substances carried by groundwater or stagnant water can cause contamination of the radiocarbon sample (Alon et al., 2002; Grootes et al., 1998). Radiocarbon dating on soil organic matter of buried soils (age on humic acids of core Aya 06) could overestimate the true age of burial by as much as the steady-state age of the soil horizon (Grootes et al., 1998; Wang et al., 1996). Moreover, due to remobilization processes and possible pedoturbation processes, radiocarbon data requires careful and critical interpretation (Carcaillet, 2000). The origins and sources of the charcoal fragments, only a few millimeters in size, are unknown. Thus, a chronological connection to depositional processes of a certain time cannot be guaranteed with absolute certainty. Additionally, root systems can, as a result of vegetation fires, glow down slowly and thus incorporate charcoal at depth into much older sediments, distorting the chronological results (Oster et al., 2012; Schaetzl, 1986). Moreover, since TC and TIC are measured and TOC is determined by a simple subtraction, there is a high risk of observing high TOC values due to the integration of charred matter which could be integrated either later through root glowing, or washed together due to turbation (Scharpenseel and Becker-Heidmann, 1992).

4.2.6 Conclusions

Sedimentological results and the dating of charcoal fragments indicate the geomorphic activity at the slopes surrounding the Phoenician settlement of Ayamonte during the Late Holocene. A complete reconstruction, which accurately sketches the chronology of geomorphic events, is hampered by unfavorable findings and methodological circumstances. However, the results illustrate the geomorphic dynamics at the location occurring since prehistoric times. The results are expanded by geochemical findings, indicating prehistoric ecologic burden on the environment by anthropogenic input of lead.

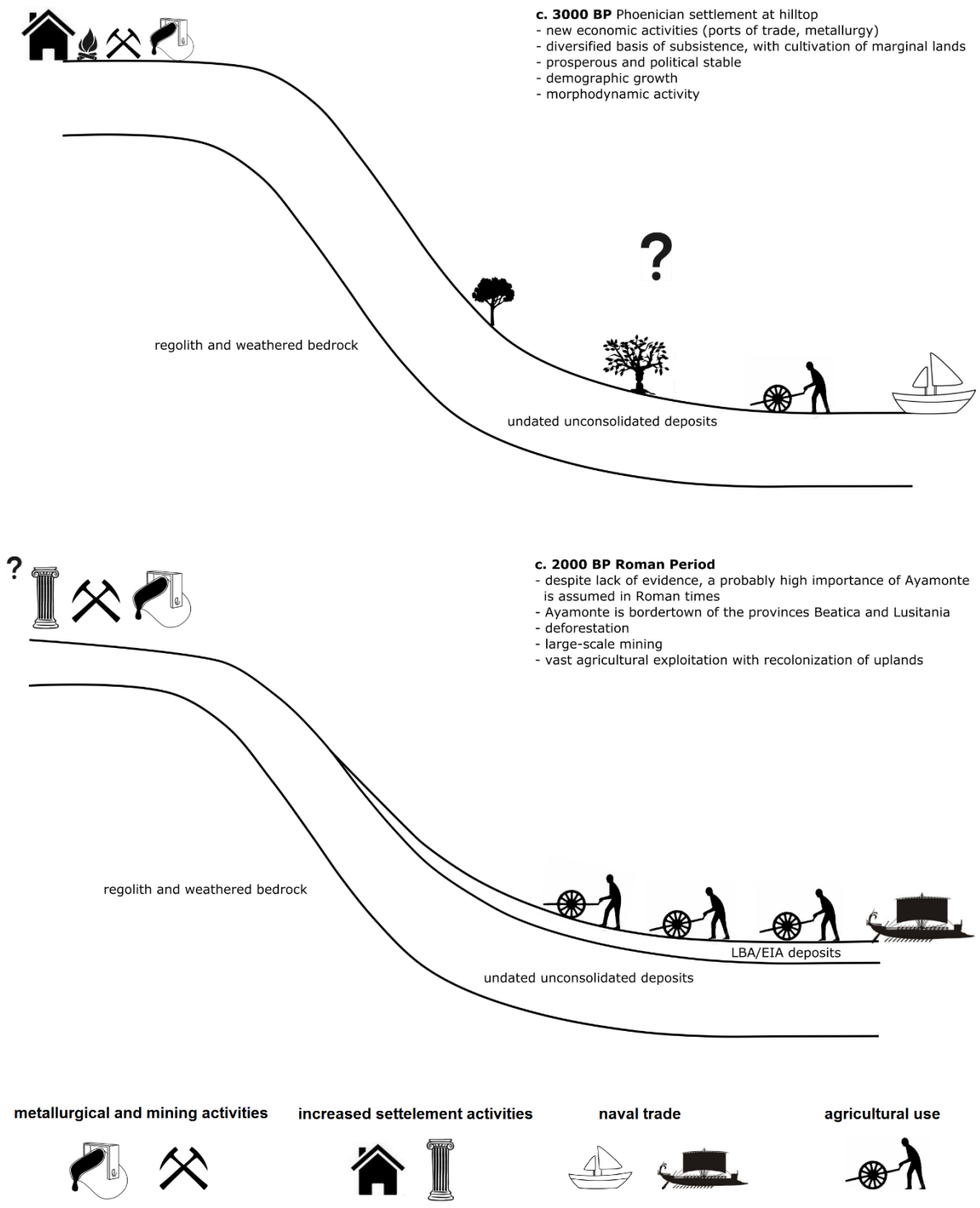

Figure 34: Conceptual model of slope processes during Bronze- and Iron Age occurring at the hillsides surrounding Ayamonte. The model unites the results of both areas of investigation and aims for a general picture (own layout based on based on Bellin et al. (2013) and Dinis et al. (2006)).

Further clarification on the slope activities during distinct times, and their relation to human settlement activity in the environs of Ayamonte is required. The current status of research remains, at this point, incomplete. Especially the establishment of a concise landscape model has not yet been sufficiently achieved. Additional dating techniques (e.g. OSL dating), investigations with large pits and transects, as well as a wider mapping of the area need to be undertaken to sufficiently meet this goal.

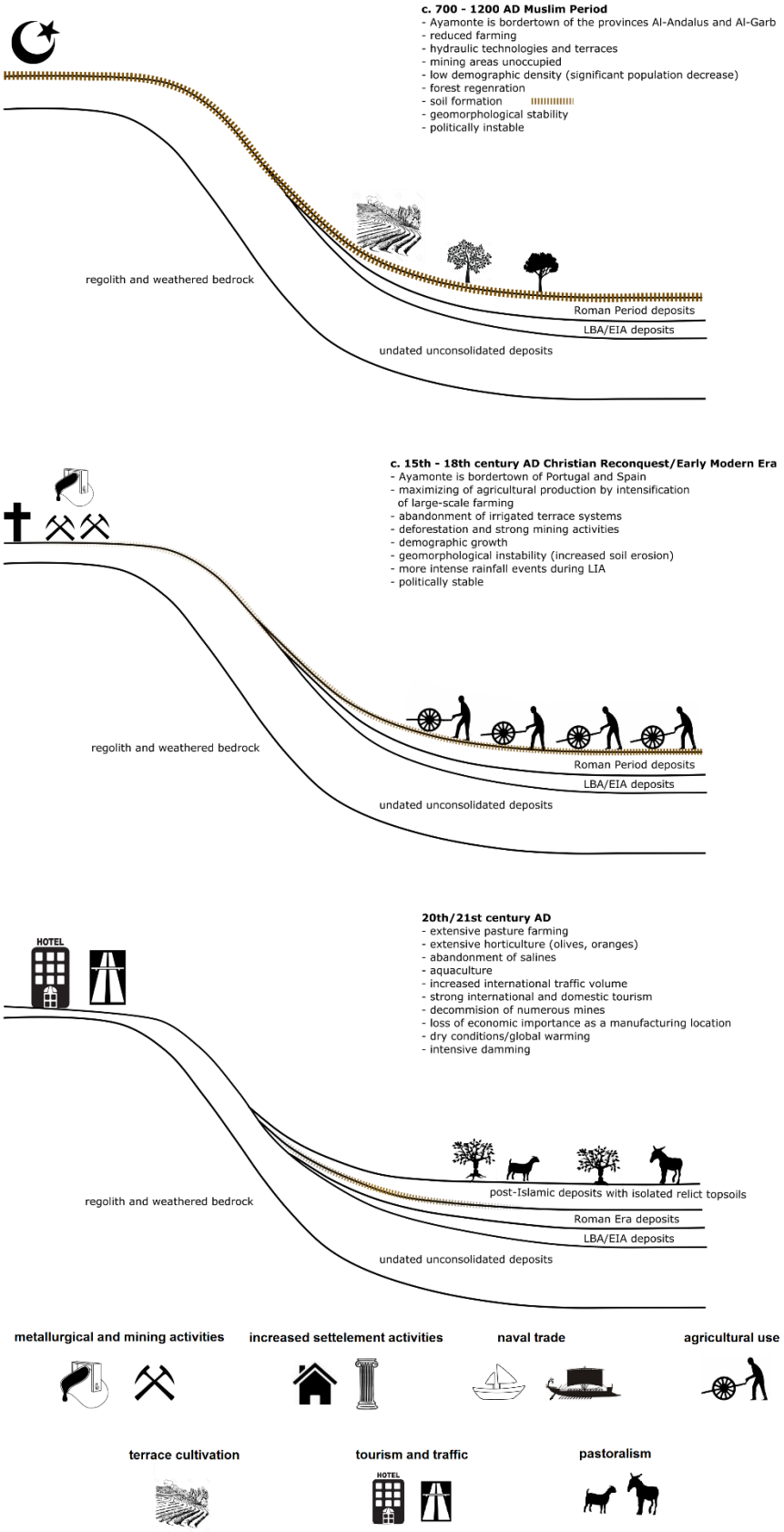

Figure 35: Conceptual model of slope processes since the Islamic Period occurring at the hillsides surrounding Ayamonte. The model unites the results of both areas of investigation and aims for a general picture (own layout based on based on Bellin et al. (2013) and Dinis et al. (2006)).

4.3 Rapid Late Holocene Estuarine Changes and Anthropogenic Activities at the Guadiana Estuary (SW-Spain) Recorded in Sedimentary and Cartographic Archives

Abstract

The study combines sedimentological, geochemical, chronometric and cartographic records providing insights into the Late Holocene coastal evolution of the lower Guadiana Estuary. The focus is on the Isla Cristina marshlands located at the estuary's eastern margin; sediment characteristics recovered from two sediment cores are presented. The data are supplemented by topographical analysis of historical maps and geomorphological mapping. Sedimentological analysis indicates highly dynamic coastal development throughout the Late Holocene in the littoral zone of the lower Guadiana Estuary. Alluvial deposits on top of the marine sequences depict an extensive erosional history in the drainage area since pre-Christian times. Radiocarbon dates from charcoal show maximum marine deposition ages of c. 6000 cal BP. Enrichment of heavy metals within the estuarine/lagoonal deposits since the Bronze Age provides evidence for human activities in the catchment. Historical maps dating from the 16th century AD confirm the highly dynamic development of the lower Guadiana Estuary during the Modern Era, linked to strong anthropogenic interference such as coastal protection.

4.3.1 Introduction

Morphological and environmental developments along the coasts of the Gulf of Cádiz in the Holocene have been controlled by climate and sea-level changes. Sensitive coastal systems, such as estuaries, are highly impacted by changes in seawater penetration, land loss due to flooding and alterations in the flow of nutrients (Dabrio et al., 1998; Dabrio et al., 2000; Fernandez-Salas et al., 1999; González et al., 2004; Lario et al., 2010; Reicherter et al., 2010; Rodríguez-Ramírez et al., 2014a; Rodríguez-Ramírez et al., 2014b; Sá et al., 2006; Vis et al., 2008; Zazo et al., 2005). The filling of estuaries is controlled by highly complex interactions between waves, tidal currents, fluvial runoff,

river sediment supply and sea-level changes (Derbyshire et al., 1979). The Guadiana Estuary in the south-west of the Iberian Peninsula is at an advanced stage of infilling and within a prograding phase (Morales, 1997). Today the outlet of the estuary is characterized by ecologically rich wetland zones with salt marshes, lagoons and tidal creeks (Chícharo et al., 2007). Its lower reach from the city of Azinhal to the river mouth was a cynosure for early cultures (Klein et al., 2016; Kunst, 1988; Teyssandier and Marzoli, 2014; Wachsmann et al., 2009).

The main objective of this paper is to reconstruct the geomorphological development of the coastal marshland at the lower Guadiana Estuary during the Late Holocene period. The reconstruction of processes is predominantly based on two sediment cores from the transitional area between the coastal wetland and the footslopes of an adjacent Pliocene/Pleistocene ridge. Spatial analyses of changes in the coastal structure are based on the study of historical maps, complemented by geomorphological mapping. The coupling of these datasets allows the spatio-temporal reconstruction of the coastal marshland at the lower Guadiana Estuary since 6 ka BP.

4.3.2 Study Area

The Guadiana River is, with a total length of 730 km, the fourth longest stream of the Iberian Peninsula (Boski et al., 2002). Its catchment covers an area of c. 67,000 km² (Boski et al., 2008). The hydrological regime of the Guadiana River is characterized by strong seasonal discharge (Borrego et al., 1995; Borrego et al., 1993; Camacho et al., 2014; González et al., 2004) but since the completion of the Alqueva dam (135 km upstream from the Guadiana mouth) the river discharge and seasonal oscillations have been drastically reduced (Delgado et al., 2010).

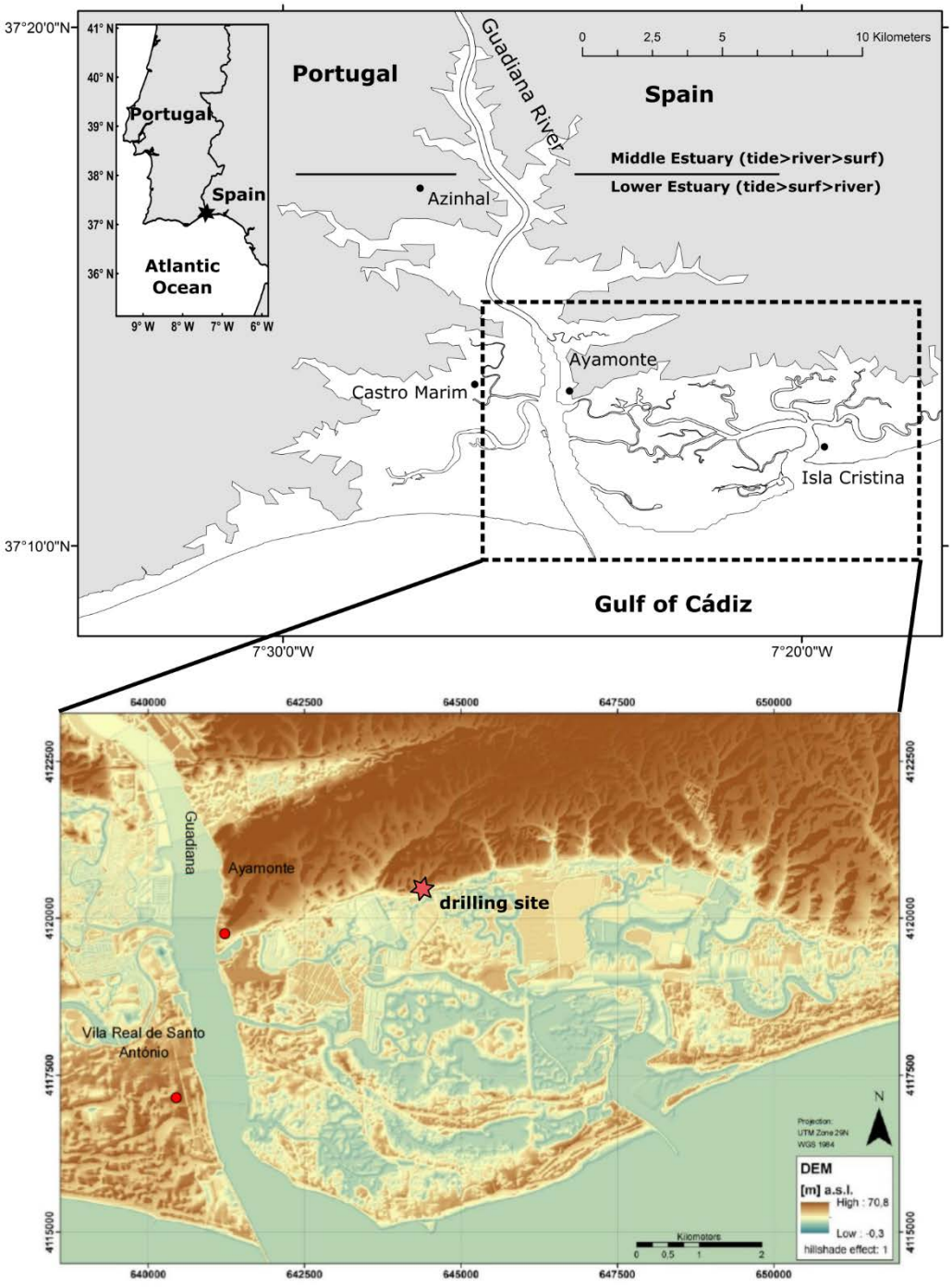

Figure 36: Overview maps of the study area, including the estuarine subareas with their dominant influencing factors (data source: CNIG (2017)).

The study area corresponds to the coastal marshland at the lower Guadiana Estuary. To the south the study area is limited by the shoreline of the Gulf of Cádiz and to the north by a distinctive edge in the terrain where the landscape changes from flat

marshland to a hilly landscape with incised valleys (Fig. 36). To the east, the study area is defined by the town of Isla Cristina. The western boundary corresponds to the Portuguese banks of the Guadiana River.

The tide-affected estuary extends up to 85 km upstream, after the river breaks through the Sierra Pelada (Dias et al., 2004). Downstream of a waterfall called Pulo do Lobo the valley opens in a funnel-like fashion, forming an estuarine area. The estuary can be categorized into three sections according to different driving processes: i) the upper estuary (between Mertola and Foz de Odeleite) is mainly characterized by river discharge, ii) the middle reach (Foz de Odeleite to Azinahl) is dominated by tidal processes and iii) the lower estuary (Azinhal to the river mouth) represents the most dynamic section and is influenced by tide, surf and river discharge (Morales, 1997). This semidiurnal mesotidal regime is characterized by a mean tidal range of 2.5 m (Borrego et al., 1995; Morales, 1997; Perillo, 1995). The mean neap tidal range is 1.22 m and the mean spring tidal range is 2.82 m (Garel et al., 2009). The Guadiana Estuary is deeply incised and is experiencing the final stages of infilling (Boski et al., 2008).

At the outlet of the river, the estuary is characterized by a sequence of former barrier islands which have been aggregated to elongated spits because of longshore drift. In the Gulf of Cádiz longshore drift is affected by the movement of the tidal wave, which appears from west to east, coming from the open Atlantic Ocean with a speed of 0.40 m/s during high tide and withdrawing with 0.30 m/s during ebb (measured at mean spring tide) (Morales, 1997). Consequently, the tidal waves hit the estuary laterally, causing a higher intensity of the eastward littoral drift. Moreover, the coastal region at the lower estuary is also strongly influenced by local sea waves. Between the spits and the former coastline wide wave-dominated marsh areas have developed (Morales et al., 2006). These salt marshes are pervaded by a complex system of tidal channels (*Span.* caños). Part of these marshlands, the so-called “Marisma de Isla Cristina” is a protected natural wetland area of high ecological value (Chícharo et al., 2007).

In its lower course, along its break through the Sierra Pelada, as the local part of the Iberian Pyrite belt, the Guadiana Riverbed is carved deeply into the carboniferous schists and graywackes which constitute the Hercynian basement, shaping a gorge (Boski et al., 2002). The Iberian Pyrite belt is globally one of the most important metallogenetic sulphide provinces. Mining in this area dates back to the 3rd millennium BCE (Delgado et al., 2012a; Nocete et al., 2005). Downstream of the breakthrough, where the estuary begins, the geology is dominated by Quaternary deposits. The dune formations at the shoreline consist of white sands and loam and are mainly caused by the deflation of sand-sized sediments from the beach (Morales et al., 2006). The geology north of the marshland mainly consists of material that can be dated to the Neogene and Quaternary. Sands and reddish gravels can be found in the hilly hinterland, and conglomerates and red clays in the upper regions. To the northeast of Ayamonte a distinctive spot of volcanic rocks occurs (IGME, 1983).

4.3.3 Methods

During the field campaign in October 2013, the present-day geomorphological conditions were recorded according to Leser and Stäblein (1980). Additionally, LiDAR data was used to outline geomorphological units within the study area.

4.3.3.1 Fieldwork

To gain information on the sedimentary processes during estuary development, two drillings were conducted in the transitional zone between marshland and mainland. The coring sites are located in the eastern lower estuary on an alluvial fan associated with a first-order valley incised in the Pliocene/Pleistocene ridge, bounding the marshland to the north (core Aya 14). Core Aya 15 is located at the fringe of the salt marsh area and mainland, c. 40 m south of Aya 14 (Table A.1, Appendix A.2).

The cores were extracted using a vibracore device (BHF 30 S), 5 cm in diameter. A handheld GPS Garmin 60c (5 m accuracy) was used for the geocoding of the drilling

sites. Sediment descriptions were implemented according to Ad-Hoc-AG Boden (2005). The sampling interval was 10 cm and at layer boundaries.

4.3.3.2 Sediment Analyses

Samples were dried at 105°C and homogenized in an agate swing-disc mill. To determine the sum of volatile substances, loss on ignition (LOI) was applied to oven-dried samples at 550 °C and 900 °C following the procedure of Dean (1974). Total inorganic carbon contents (TIC) were determined using a Wösthoff carmhograph (detection limit = 0.02 mass-% C). Total carbon (TC) content was determined using the Leco TruSpec CHN 1000 analyzer (detection limit=0.01 mass-%). Total organic carbon contents were calculated as the difference of TC and TIC. Electrical conductivity (mS) of the sediment solutes was measured using the Hanna handheld device (HI 98301) with a ± 2 % accuracy in a solution with a sediment-distilled water ratio of 1:2. The sediment's pH value was determined using a Hanna handheld device (HI 98127) in 0.01 M KCl solution and a solution ration of 1:2. The chemical composition for cores Aya 14 and Aya 15 was determined on the dried and bisected sediment cores using the portable XRF spectrometer Niton Xl3t 900 GOLDD applying a vertical resolution of 1 cm and a main filter 50 kV. The calibration procedure followed the description in Thelemann (2016), with the exception that standard river sediments and soils were used as reference material (stream sediment: GBW 07309-07312, soils: NCS DC 73325 & NCS DC 73389). Iron, calcium and silicon concentrations were measured in mass-%. In order to enhance accuracy each measurement was conducted with an exposure interval of 120 seconds (for detailed information see Hoelzmann et al., 2016). Aqua regia extractable metal and metalloids (Cr, Ni, Pb and Zn) from core Aya 15 were additionally determined by digestion of 0.5 g of sample with aqua regia extracts (3:1 HCl-HNO3) at 95 °C for 1 h, followed by ICP-OES analysis. Magnetic susceptibility (MS) at low frequency (0.46 kHz) was measured on air-dried weighted

samples using the MS2B sensor (Bartington Instruments) with 10 cm^3 sample containers (Dearing, 1994).

Age control is provided by seven radiocarbon datings (AMS) from charcoal fragments processed at the Poznan Radiocarbon Laboratory. The AMS data were calibrated using OxCal 4.1 (Ramsey, 2009) and the IntCal09 (Reimer et al., 2009) calibration curve.

4.3.3.3 Spatial Analyses of Historical Maps and Orthophotos

Five historical maps were selected, based on the characteristics scale and information content for a change detection analysis of geomorphological features in the study area (Table 5). Maps from the 16th to mid-17th century CE were only used for visual interpretation of former shoreline characteristics, as their accuracy was not sufficient for a GIS-based approach. For an overview of available maps of the study area see Table A.3 in the Appendix A.2. All historical maps were facilitated by the Centro Nacional de Información Geográfica, the Museo Naval de Madrid, Archivo General Militar de Madrid (Cartoteca) and the Berlin State Library. Maps were scanned at 300 dpi and the resulting raster data were georeferenced applying the software ArcMap 10.1 with Universal Transverse Mercator (UTM) Zone 29S as coordinate reference system. Georeferencing is based on five unchangeable ground control points like the church named "Iglesia de Nuestra Señora de las Angustias" in Ayamonte or the Torre de Isla Cristina. At least four ground control points were available for each map. The resulting RMS errors vary between 13.82 for the year 1861 and 850.13 for the year 1748. Including information from orthophotos of the years 1956, 1998 and 2010 (see Table A.2 in the Appendix A.2 for resolution information), shoreline changes of the last centuries were reconstructed. For the time slices 1956 and 1998 orthophotos are only available for the Spanish part of the study area.

Table 5: Historical maps used for change detection analyses.

Map Title	Author/Publisher	Year	RMSE
Terra e costas de Portugal	Llobet, D.F.	1748	850.13
Plano de la barra y puerto de la ciudad de Ayamonte que divide los reinos de España y Portugal	Hurtado, A.	1776	316.32
Plano de la isla de la Canela y sus inmediaciones	Capitán con José Ibáñez	1811	411.52
unknown (Map no. 1988000003)	unknown	1861	13.82
unknown (Map no. 1988000604)	unknown (Consejería de economía y hacienda, Junta de Andalucía)	1872	199.36

4.3.4 Results

4.3.4.1 Geomorphological Mapping

The marshland is subdivided into four major geomorphological process areas. At the shore line, coastal processes characterize a relatively thin strip, mapped as beach. Land inward, irregular inactive spits, partly carrying longitudinal dunes on top, are today characterized by predominantly eolian processes. These spits follow the Guadiana River mouth upwards, until the outer city areas of Ayamonte (Fig. 37). Another area characterized by eolian processes is located in the center of the eastern marshland. North of the spits fluvial processes influenced by the tide prevail. This area is drained by a highly dynamic and very finely divided channel network which can be classified into two major classes of channels: (a) the wide major channels continuously carry water even during low tide. In contrast, (b) the tidal channels, which have a much smaller cross-profile, only periodically carry water when saltwater intrudes into the marshland during high tide. The channel network is directly connected to the Atlantic Ocean. Further in its western section three major channels are linked to the Guadiana River. The northern boundary of the estuarine area is well defined by a sharp terrain edge, showing a strong change in geomorphology (Fig. A.7 d, Appendix A.3). Active

and inactive salt fields and aqua culture areas document the anthropogenic utilization of the marshland. In contrast, west of the Guadiana River mouth the geomorphology is mainly characterized by sand deposits. The mouth of the Guadiana River and the main tidal channel east of the nearby town of Isla Cristina are protected by jetties.

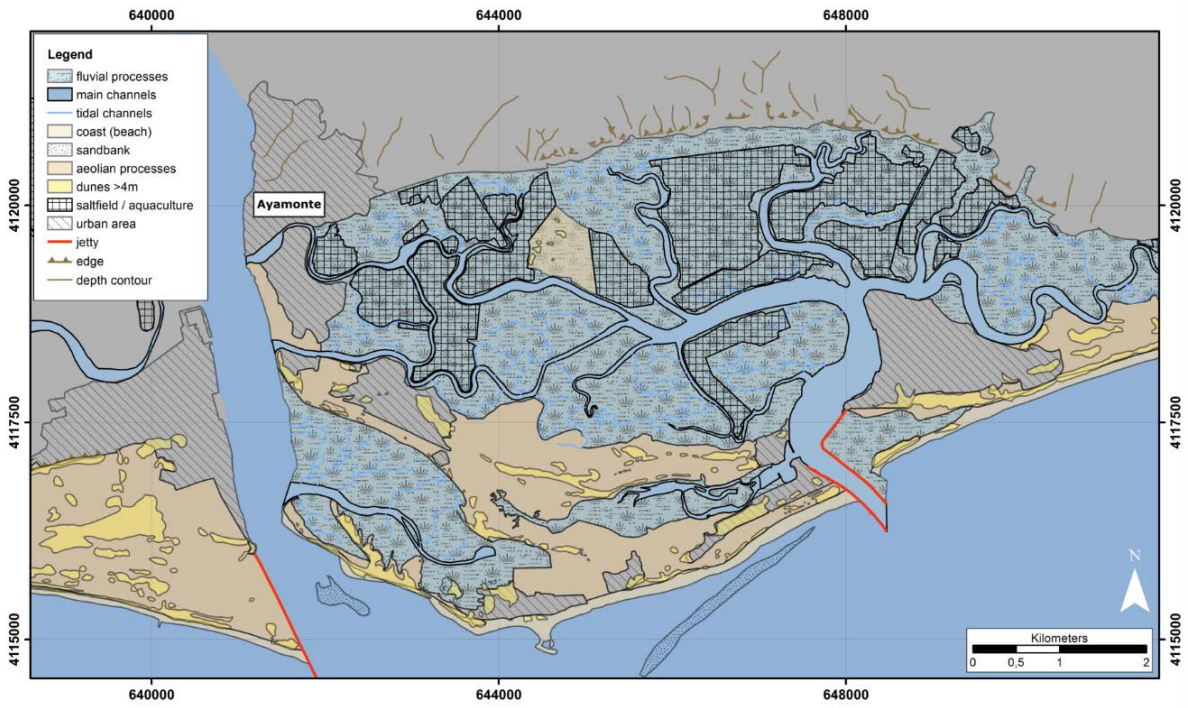

Figure 37: Geomorphological map of the lower Guadiana Estuary (Ißelhorst, 2014).

4.3.4.2 Reconstruction of the Former Shorelines

The results of the shoreline reconstruction are presented for eight time slices between 1748 and 2010 (Fig. 38). To enable a better illustration of certain shorelines the DEM is used as a base map layer.

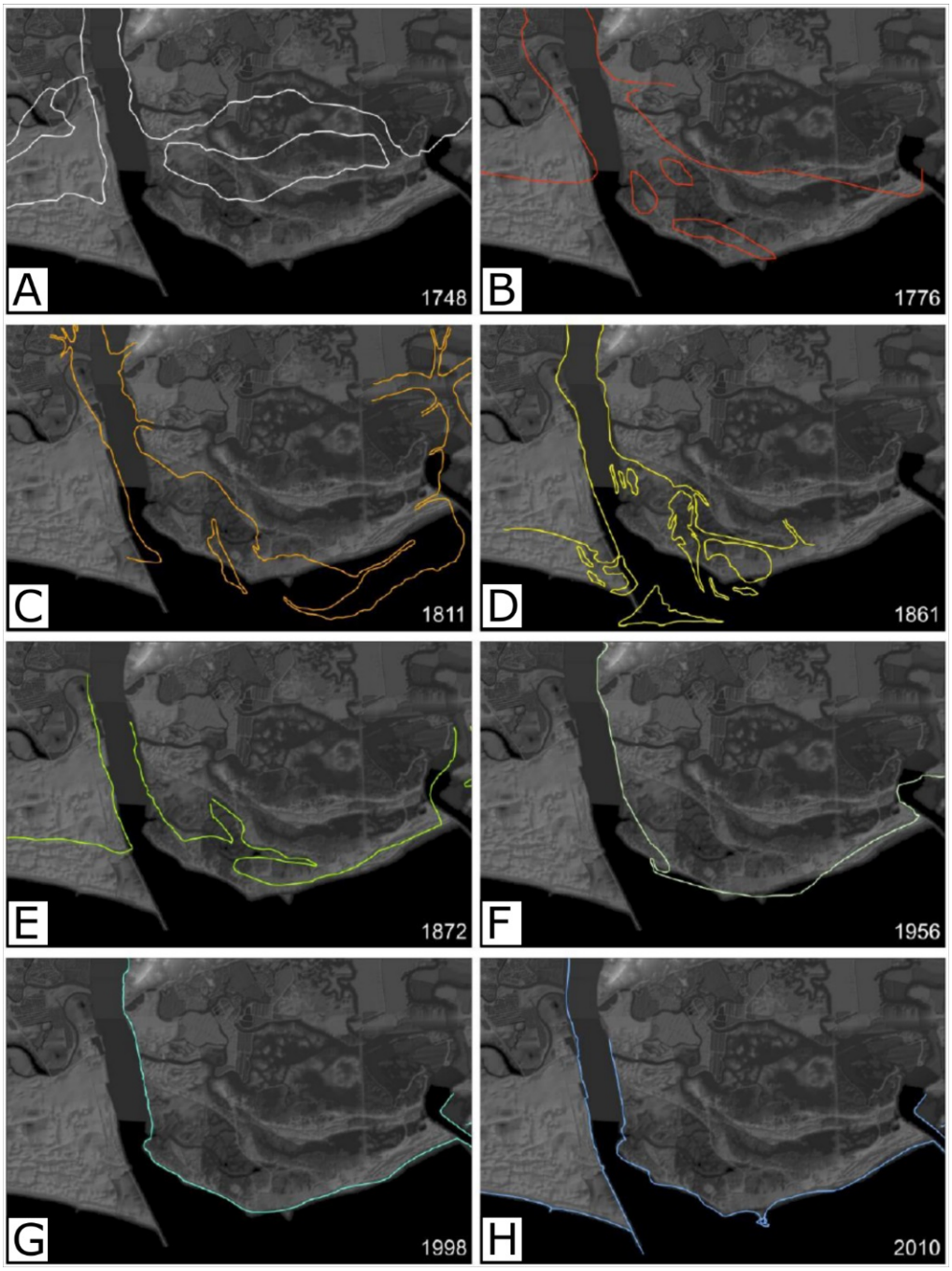

Figure 38: Shoreline reconstruction of distinctive time slices from 1748 to 2010 (Ißelhorst, 2014).

In 1748 a distinctive barrier island is situated in front of the Spanish mainland (Fig. 38 A). Another barrier island is located in front of the Portuguese shoreline and appears to be nearly connected to the mainland, as it is just separated by a small channel.

In 1776 the barrier island at the Spanish coast seems to be connected with the mainland (Fig. 38 B). Additionally, three relatively small new islands have developed in front of the new Spanish shoreline in prolongation of the Guadiana River mouth. The

Portuguese section of the study area is only schematically displayed in the map of 1776. Therefore, interpretation of this section is omitted.

The subsequent development of two spits is indicated by the historical map from 1811 (Fig. 38 C). The bigger and more highly developed spit extends from the eastern estuary inlet in a westerly direction. Another spit can be recognized at the eastern edge of the Portuguese coastline to the Guadiana outlet. It is distinctly less developed than the eastern spit and the E-W-orientated spit. Furthermore, the map indicates a change in the former location of the newly developed islands in front of the mainland, as extracted from the map of 1776. Only a single prolate island is left in this area. The further development of the coastal setup is characterized by a much more complex breakdown of the shoreline system. A triangle-shaped island has developed within the center of the estuary's main outlet. This island is called "Isla Isabella" and is recorded in several maps of the period (Fig. 38 D). Sixty years later (1872), the shoreline is nearly identical with the present-day situation (Fig. 38 E). From 1956 to 2010 no significant changes occured along the Spanish shoreline of the Guadiana Estuary; between the years 1956 and 1998 there was only a slight adjustment of the shoreline into today's position.

The Portuguese part of the study area shows a distinctive progradation of the shoreline, probably as a consequence of the construction of a jetty at the western river mouth, which led to the accumulation of sediments in this section (Figures 38 F - H).

4.3.4.3 Sediments

Core Aya 14

The drilling site of Aya 14 is located at an altitude of 3.6 m a.s.l. on an alluvial fan 5 km north of the present-day coastline. The core is 400 cm long. Sediments are carbonate-free and dry to slightly moist. Texture varies only slightly with sand being the predominating grain size. The sediments of Aya 14 can be distinguished into six

lithostratigraphical units according to their macroscopic characteristics including color and texture (Fig. 39). The basal unit 1 (400-380 cm depth b.s.) is characterized by a strongly compacted loamy sand; within this unit sharp-edged detritals (Ø < 3 cm) occur. The color is overall reddish brown changing in intensity from a distinct reddish shade at the top, to ocher in the middle section, to a weak reddish at the bottom. The texture of the overlying unit 2 (380-300 cm depth b.s.) is predominated by weakly compacted loamy sand with intercalations of sharp-edged gravels (Ø < 5 cm). Sediment color is dark brown. Unit 3 (300-280 cm depth b.s.) is composed of weakly compacted silty sand interspersed by coarse debris (Ø < 3 cm). Sediment color is reddish brown. The texture of unit 4 (280-200 cm depth b.s.) is similar to that of unit 3 while the color is slightly more reddish. Rounded quartzites occur between 230-260 cm depth b.s. The sediments are moderately rooted. Unit 5 (200-150 cm depth) consists of weakly silty sand, bright brown in color. Clastic debris occurs throughout this unit, while charcoal fragments (Ø < 0.5 cm) occur at the top. Towards the bottom, the silty sands grade into bleached fine sands, in which edge-rounded stones occur. The uppermost unit 6 (150-0 cm depth b.s.) is composed of silty sand, dark brown in color. The sediments are rooted, weakly compacted and charcoal fragments (Ø < 3 cm) are abundant.

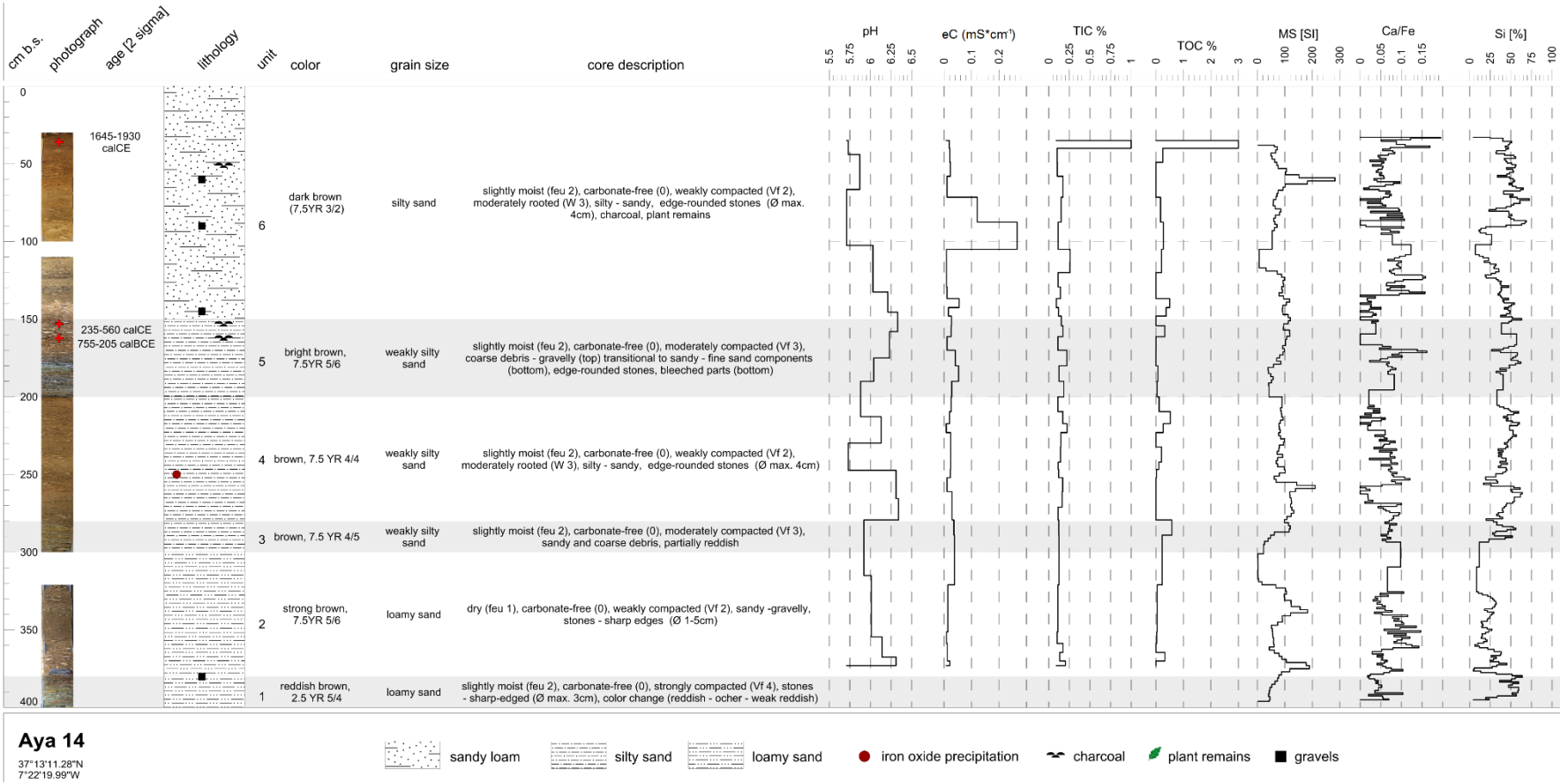

Figure 39: Stratigraphy and geochemical parameters of sediment core Aya 14.

Inorganic carbon contents (TIC) (μ = 0.17 mass-%, std. = 0.15, n = 34) and organic carbon contents (TOC) (μ = 0.15 mass-%, std. = 0.17, n = 34) show low values within all units. Neither trends with depth nor significant changes in concentration between the different units occur (α >0.05). At 40 cm core depth TIC peaks with c. 1 mass-% and parallel TOC shows a maximum value of c. 3 mass-%. Likewise, pH (μ = 6, std. = 0.2, n = 18) and electrical conductivity (eC) (μ = 0.03 mS, std. = 0.04, n = 34) lack any trend with depth and do not allow differentiation between the different lithostratigraphical units. There are no remarkable peaks of either parameter; slightly increased electric conductivity values of the sediments solutes occur in the uppermost unit between 80-95 cm depth b.s., peaking with 0.27 mS and slightly declining to the top. Magnetic susceptibility shows undulating values (μ=83 $*10^{-8}$ m^3*kg^{-1}, std. = 40, n = 161) and peaks at 60 cm (283 $*10^{-8}$ m^3*kg^{-1}), 258 cm (210 $*10^{-8}$ m^3*kg^{-1}), 338 cm (183 $*10^{-8}$ m^3*kg^{-1}) and 374 cm depth b.s. (190 $*10^{-8}$ m^3*kg^{-1}). Ca-Fe-ratios average around μ=0.06 (std.=0.03, n=284) throughout the entire core; significant differences in average Ca-Fe-ratios between the different lithostratigraphical units cannot be confirmed (α > 0.05). In units 1-4 graphs of Ca-Fe-ratio and magnetic susceptibility run inversely, while a linear trend is missing (α > 0.05). Silicon concentrations range between 6 and 72% over all the extracted sediments and show a highly irregular trend throughout the whole sediment core (μ = 39 %, std. = 14.2, n = 284).

Chronological control was achieved by three radiocarbon dates from charcoal fragments originating from 51, 153, and 162 cm depth below surface showing calibrated ages of 1645-1930 cal CE (Aya 14-01-21), 235-560 cal CE (Aya 14-02-53) and 755-205 cal BCE (Aya 14-02-62) (Table 6 and Fig. A.4, Appendix A.2).

Core Aya 15

The drilling site of Aya 15 (Table A.1, Appendix A.2) is located at an altitude of 2.3 m a.s.l. approx. 40 m south of Aya 14. The core was extracted from the distal part of the fan, from its immediate transition zone with the salt marsh of the “Marismas de

Isla Cristina". The core is 500 cm long. The sediments of Aya 15 can be distinguished into three units (Fig. 40). The basal unit 1 (500-350 cm depth b.s.) is characterized by weakly compacted moist sand. While the base of the unit is of dark gray color, it changes to olive brown in the mid-section and dark olive brown at the top of the unit. Hydrochloric acid testing in the field indicated that the sediments are free of calcium carbonate. Shell fragments (Ø < 3 mm; depths: 375, 420, 450 and 480 cm b.s.), plant remains (depth: 474 cm b.s.) and remains of charcoal fragments (Ø < 2 mm; depths: 382 and 493 cm b.s.) occur in the lowermost unit. Layers of shell hash were observed at 370-375 cm depth b.s. and 470-475 cm depth b.s. Two thin bands of rounded gravels (Ø < 2 cm) were recorded for 475-480 cm depth b.s. and 488-493 cm depth b.s. The overlying unit 2 (350-140 cm depth b.s.) is formed by moist silt. The textural transition from unit 1 to unit 2 occurs very gradually showing fining-upwards characteristics. The color of unit 2 is a very dark gray. The sediments are poor in calcium carbonate and weakly compacted. Plant remains, shell fragments (Ø < 1 cm) and charcoal (Ø < 2 mm) occur irregularly throughout this unit. Three thin distinct layers of coarse sand and gravel (Ø < 3 cm) in 235-240 cm, 268-273 cm and 320-330 cm depth b.s are special features of this unit. All three layers show sharp transitions to the fine sediments into which they are intercalated. While the lowermost layers show mainly brown and red gravel, the uppermost layer shows gray gravel with rounded quartzites (Ø < 3 cm). The uppermost unit 3 is composed of dry, brown silty sand. The sediments are strongly compacted, carbonate-free and strongly rooted. In addition, irregularly rounded gravels (Ø < 5 mm), charcoal fragments (Ø < 3 mm), brick fragments (Ø < 3 mm) and iron oxide precipitations occur sporadically in this unit.

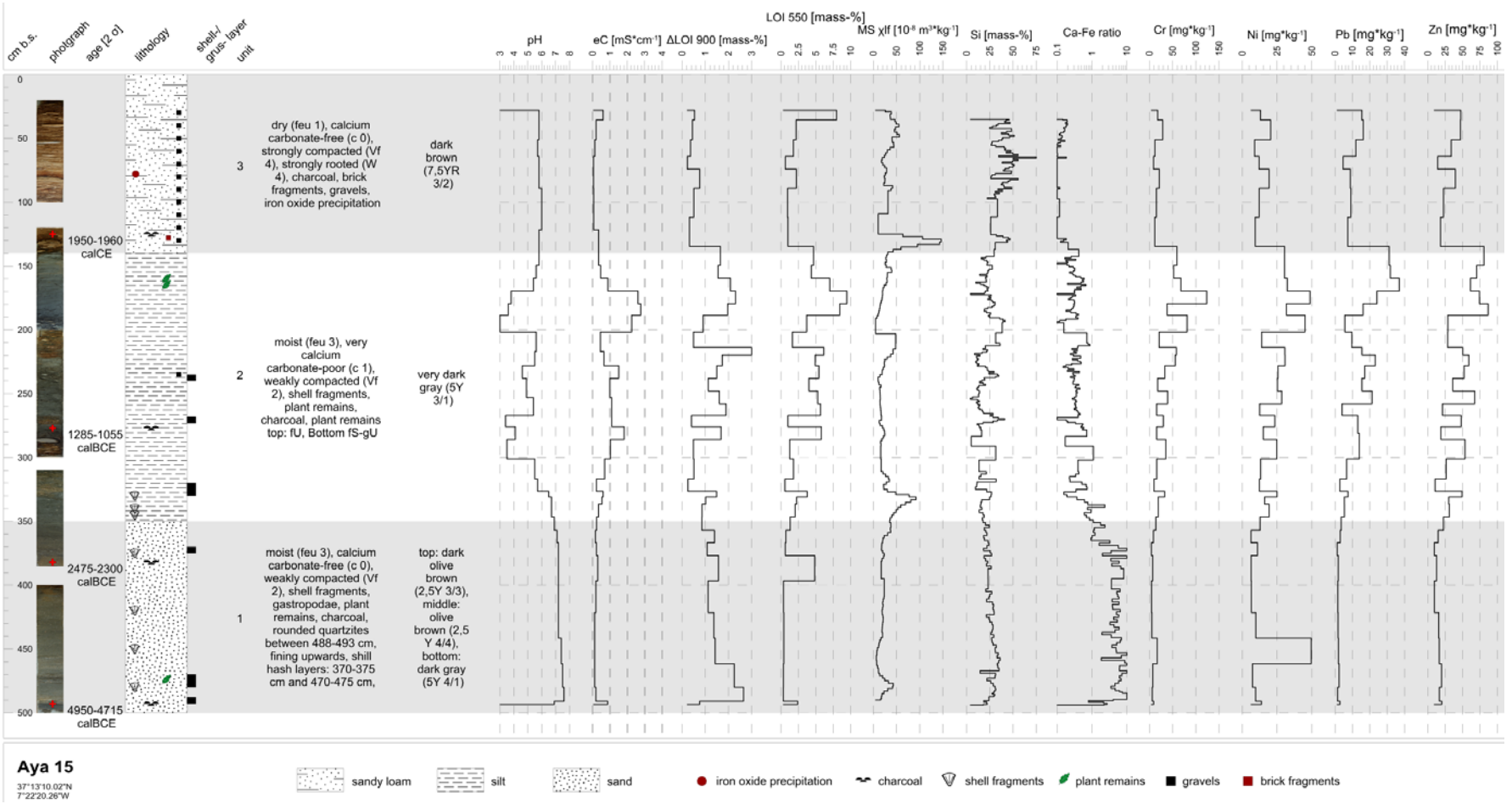

Figure 40: Stratigraphy and geochemical parameters of sediment core Aya 15.

Unlike the sediments in core Aya 14, the subdivision into three units can be confirmed by clear changes in their chemical characteristics. LOI_{900} shows highest average values in unit 2 ($\mu = 1.9$ mass-%, std. = 2.88, n = 21), as reflected by their high standard deviation significantly differing from the average LOI_{900} values in the underlying sediments of unit 1 ($\mu = 1.4$ mass-%, std. = 0.59, n = 10) ($\alpha < 0.05$). Average LOI_{900} values are lowest in the uppermost unit 3 ($\mu = 0.45$ mass-%, std. = 0.17, n = 7), significantly differing from the average LOI_{900} values in unit 2. Average LOI_{500} values in unit 2 ($\mu = 4.3$ mass-%, std. = 2.44, n = 21) are significantly higher than the LOI_{500} values in the overlying unit 3 ($\mu = 2.38$ mass-%, std. = 2.54, n = 7) ($\alpha<0.05$) and the basal unit 1 ($\mu = 1.17$ mass-%, std. = 1.44, n = 10) ($\alpha < 0.05$). Magnetic susceptibility remains low throughout the entire core but peaks notably at 128-134 cm ($\mu=132*10^{-8}$ m^3*kg^{-1}), 330-336 cm ($\mu=80*10^{-8}$ m^3*kg^{-1}) and 476-480 cm ($\mu=39*10^{-8}$ m^3*kg^{-1}) depth b.s. pH values differ significantly along the extracted sediment sequence. While averages of 6.0 and 7.0 are reached within units 1 and 3, reduced average pH values in unit 2 ($\mu = 5.0$, std. = 1.2, n = 19) are caused by two sudden decreases of pH values in 175-195 cm depth b.s. and 270-290 cm depth b.s., reaching minimum values of pH 3.4. The graph of the sediments solutes' electrical conductivity runs inversely to that of the pH value ($\alpha < 0.01$). Correspondingly, electrical conductivity within unit 1 average at 0.18 mS (std. = 0.21, n = 6) and within unit 3 at 0.25 mS (std. = 0.22, n = 9), while they distinctly increase within unit 2 ($\mu = 1.07$ mS, std. = 0.77, n = 19) ($\alpha < 0.01$).

The given results of elemental composition, derived from XRF and ICP-OES measurements, confirm the three-part structure of the sediment core. Ca-Fe-ratios show minimum values in unit 3 ($\mu = 0.1$, std. = 0.05, n = 72), medium values in unit 2 ($\mu = 0.4$, std. = 0.25, n = 147) and the highest values in unit 1 ($\mu = 6.9$, std. = 11.5, n = 72). Conversely, silicon concentrations are highest in unit 3 ($\mu = 40.0$ mass-%, std. = 9.6, n = 72), and decrease in unit 2 ($\mu = 20.3$ mass-%, std. = 7.9, n = 147) and unit

1 (μ = 26.0 mass-%, std. = 4.8, n = 72). Heavy metal concentrations also show a clear three-part pattern. While the lowermost unit 1 shows minimum values (e.g. Pb: μ = 2.1 mg*kg^{-1}, std. = 0.75, n = 10), they increase within unit 2 (e.g. Pb: μ = 15.3 mg*kg^{-1}, std. = 10, n = 20), before reducing again in unit 3 (e.g. Pb: μ = 10.0 mg*kg^{-1}, std. = 4.2, n = 7).

Chronological control was gained by dating four samples of charcoal fragments originating from 125 cm, 277 cm, 382 cm and 493 cm depth b.s. Calibrated ages constitute 1950-1960 cal CE, 1285-1055 cal BCE, 2475-2300 cal BCE and 4950-4715 cal BCE (all ages in 2σ-range) (Table 6 and Fig. A.4, Appendix A.2).

Chronology

The geochronological model covers the period between c. 5000 cal BCE and 1900 cal CE and is based on seven radiocarbon dates from pieces of charcoal fragments (Table 6, Fig. A.4, Appendix A.2). Five samples contained less than 1 mg of carbon (Aya 14-02-53: 153 cm, Aya 14-02-62: 162 cm, Aya 15-02.25: 125 cm and Aya 15-05-93: 493 cm depth b.s.). But as all ages are in stratigraphic order they are considered to provide a reliable chronostratigraphy. The ages are distributed over several periods from the Bronze Age to the Modern Era.

Table 6: Radiocarbon dates from drillings Aya 14 and Aya 15.

Lab. Code	Core/ Sample depth	Elevation	^{14}C age (BP)	Calibrated age (cal BCE/CE; 2σ)	^{13}C (ppm)	C (mg)
Aya 14						
Aya 14-01-51	0.51	3.39 m a.s.l.	215 ± 30 BP	1645-1930 cal CE	-16.2	1.2
Aya 14-02-53	1.53	2.07 m a.s.l.	1650 ± 70 BP	235-560 cal CE	-23.2	0.10
Aya 14-02-62	1.62	1.98 m a.s.l.	2340 ± 80 BP	755-205 cal BCE	-24.4	0.05

Aya 15						
Aya 15-02-25	1.25	1.05 m a.s.l.	220 ± 30 BP	1950-1960 cal CE	-23.2	0.84
Aya 15-03-77	2.77	0.47 m a.s.l.	2970 ± 35 BP	1285-1055 cal BCE	-23.9	1.32
Aya 15-04-82	3.82	1.52 m b.s.l.	3915 ± 30 BP	2475-2300 cal BCE	-19.3	2.64
Aya 15-05-93	4.93	2.63 m b.s.l.	5950 ± 50 BP	4950-4715 cal BCE	-35.4	0.27

4.3.5 Discussion

4.3.5.1 Sediments Characteristics

The sedimentological data from cores Aya 14 and Aya 15 are used to draw conclusions on the geomorphological processes controlling the development of the marshland. The sequence of Aya 14 corresponds to the alluvial fan deposits of a small valley, intersecting the Pliocene/Pleistocene ridge. Immediately downslope of Aya 14, sediments of Aya 15 were extracted providing information for the reconstruction of the littoral development (Fig. 41).

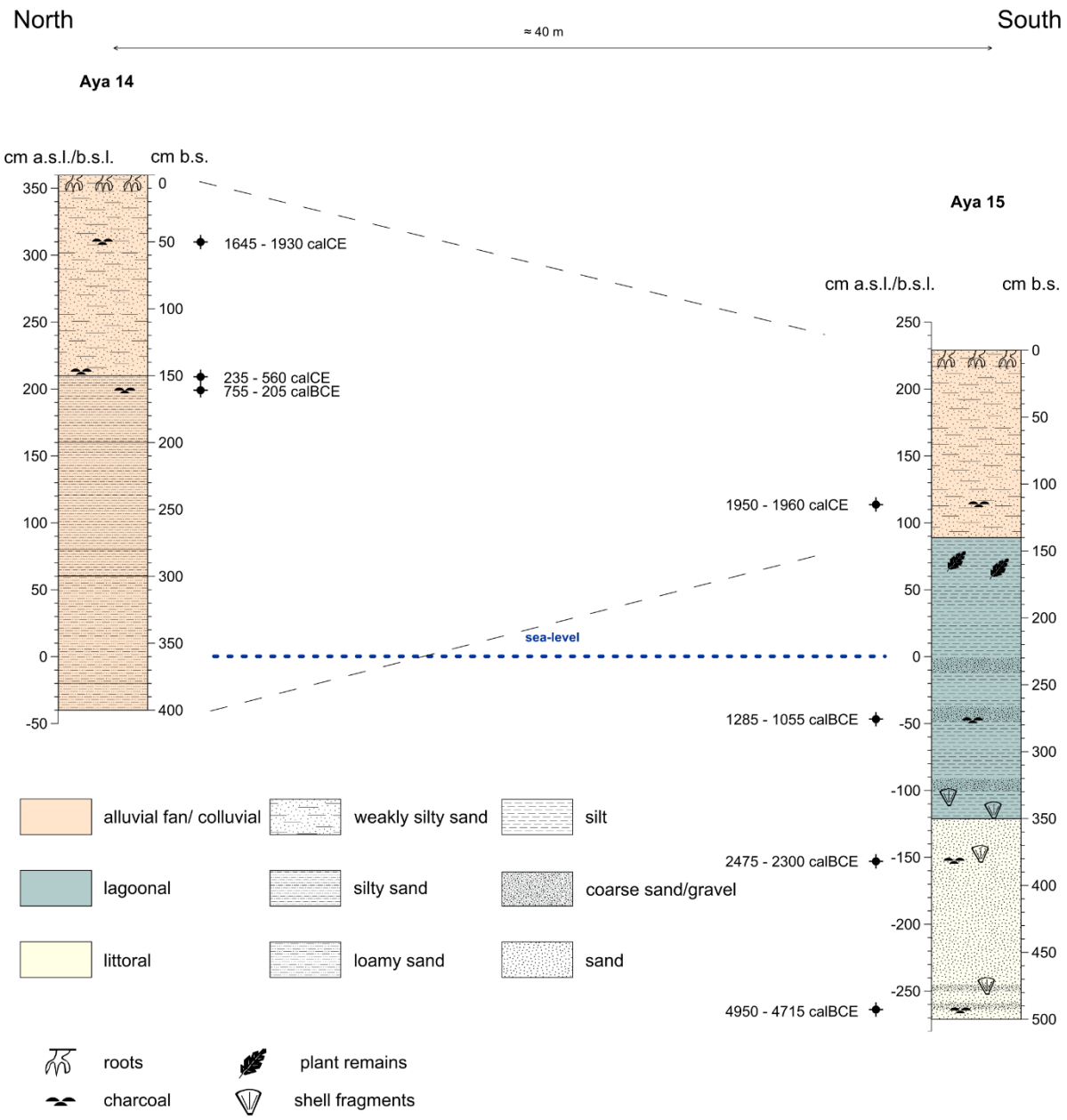

Figure 41: Cross-section and facies distribution of the studied cores.

Core Aya 14

Sediments exposed in core Aya 14 are entirely composed of terrestrial material originating from the adjacent slopes of the Plio-/Pleistocene ridge. The occurrence of reddish-brown sandy deposits together with edge-rounded gravels within units 4 to 6 is interpreted as alluvial-fan deposits (Miall, 2006). The development of alluvial fans is closely related to stages of erosion processes, many of which correspond to Quaternary environmental changes (García-Ruiz et al., 2013). Other erosion processes have been

related to land-use changes and deforestation in historical times (Gómez-Villar et al. 2006). The rounded quartzites found in 230-260 cm b.s. (corresponding to 130-100 cm a.s.l.) are most probably reworked from older fluvial deposits of the "Paleo-Guadiana" which frequently crop out along the eroded shores and on top of the plateaus (González et al., 2004; Zazo et al., 2005). The rounded quartzites recorded in Aya 14 are unconsolidated heterogeneous deposits embedded in a sandy matrix. In this unit TIC values remain below detection limit, possibly indicating intercalated colluvial deposits as correlative sediments to soil erosion (Kuhn et al., 2012; Lal, 2005; Leopold and Völkel, 2007; Polyakov and Lal, 2004). Relatively high organic carbon contents in the uppermost layer (upper part of unit 6) correspond to the current soil forming. The abruptly decreasing organic carbon contents indicate the early diagenetic decomposition of organic matter or pedoturbation (Hemelryck et al., 2009). The correspondingly low organic carbon contents throughout the extracted sediments can be explained by the gradual decomposition of organic matter in the soil sediments under the influence of light and oxygen (Schütt, 2004). The lack of carbonates in the deposits of Aya 14 corresponds to the lack of calcareous bedrock in the drainage basin. The overall low values of electrical conductivity of sediment solutes point to terrestrial depositional processes (Rhoades, 1999). Sediment Ca-Fe-ratios usually are suitable as a tool to differentiate between stratigraphical units deposited under predominantly terrestrial or marine conditions (Hadler, 2013). The exclusively terrestrial origin of the material is documented by extremely low Ca-Fe-ratios and high portions of quartz – here seen in high contents of elemental silicon.

The absolute chronology based on radiocarbon dates suggests that the uppermost sediments (c. 50 cm b.s.) of unit 6 were deposited between the 17th and 20th centuries CE. As reported by several authors, the past four centuries have witnessed substantial soil deterioration and deterioration of arboreal vegetation resulting from strong

population growth, land reform and the mechanization of agriculture (Carrión et al., 2010; Delano-Smith, 1981; Grove and Rackham, 2003; Grove, 1988).

In contrast, during the rise of metallurgic activities the population also increased, while overall remaining just a fraction of the present-day population (Bellin et al., 2013). The two radiocarbon ages in unit 5 range from 755 cal BCE to 250 cal CE and span the Tartessian/Phoenician to the Roman period in SW-Iberia. The older of the radiocarbon ages falls into a period of sparse population and dense vegetation cover (Dinis et al., 2006). During this period the mining of sulfide deposits by the Tartessian culture emerged (Borrego et al., 2004; Borrego et al., 2005). The Tartessian culture of SW-Iberia collapsed around 500 BCE and was succeeded by the Iberian and Roman civilizations in the area (Schüle, 1960). During the Roman Era mining activities intensified, resulting in deforestation and increased erosion rates (García-Alix et al., 2013). Over all, at least since the Roman period aridization and continuing deforestation shifted the ecosystem over a threshold to a condition of extreme degradation coinciding with soil erosion and the deposition of colluvials, as is the case today (Campo et al., 2006; Carrión et al., 2001; García-Ruiz, 2010)

Although the significance of two radiocarbon ages is limited, the data suggest repeated phases of geomorphological activities since the Bronze Age. The four peaks of magnetic susceptibility along the sediment profile are interpreted as indicating the relocation and sequential deposition of sediments rich in magnetically active minerals, e.g. relocated topsoil (Dearing, 1994; Evans and Heller, 2003; Le Borgne, 1955). However, these features could not be confirmed by the lithostratigraphical and chemical sediment characteristics. In addition, it also has to be considered that soils as distinct features of stability phases might have been eroded during successive phases of geomorphic activity (Costantini et al., 2002; Schaetzl and Anderson, 2007).

Core Aya 15

Sediments exposed in core Aya 15 are composed of three strongly differing units which clearly divide the sediment core into distinct facies sequences: the lowermost sandy littoral facies, the interposed silty lagoonal facies and the uppermost lithological heterogeneous terrestrial deposits. LOI_{550} is used to deduce the contents of organic carbon of core Aya 15 (Dean, 1974). Low LOI_{550} values within the sandy sediments of unit 1 are interpreted as indicating a highly dynamic barrier island formation with reduced input and poor conservation conditions for organic matter (Lerman, 1979; Rheinheimer, 1974). High LOI_{550} values in the underlying unit 2 (350-140 cm depth b.s.) correspond to deposition in an aquiferous, low-energy estuarine environment rich in organic matter (Bordovskiy, 1965; Meyers, 1997). Similar to Aya 14, the uppermost unit 3 reveals high LOI_{550} contents indicating soil forming processes (Wainwright, 2009). Comparable to core Aya 14 these values decrease rapidly with depth, pointing to the early diagenetic decomposition of organic matter (Rheinheimer, 1974). LOI_{900} is used to deduce the contents of inorganic carbon (TIC) of core Aya 15 (Dean, 1974). High LOI_{900} values within the two underlying units 1 and 2 as well as high Ca-Fe-ratios clearly document littoral influences on the depositional environment by the increased input of calcareous skeletal remains of marine organisms (e.g. the shell hash layer at various depths) (Engel et al., 2010; Perillo, 1995b; Pozo et al., 2010). Similar to Aya 14, contents of inorganic carbon show low values of LOI_{900} in the uppermost unit 3 indicating a non-calcareous origin of the overlying terrestrial deposits. Correspondingly, the low Ca-Fe-ratios within the uppermost unit 3 confirm the terrestrial origin of the sediments (Hadler, 2014). Additionally, the estuarine facies of units 1 and 2 is furthermore confirmed by relatively high values of electrical conductivity, documenting a marine to brackish depositional environment (Ernst, 1970).

Three samples of charcoal fragments revealed depositional ages between 4950-4715 cal BCE and 1285-1055 cal BCE. The third and uppermost radiocarbon age originating

from 125 cm b.s. is most likely influenced by disturbances occurring during the drilling process (e.g. downfall). As a consequence, this sample is disregarded in the following analysis. Due to its topographical position, littoral processes, including the Late Holocene sea-level rise, and fluvial processes have to be considered as the major forces that deposited the sediments of core Aya 15. The lowermost absolute age of 4950-4715 cal BCE in 493 cm b.a. marks the transition from rapid postglacial sea-level rise documented by fluvial deposits at the base of unit I to a phase of minor sea-level oscillations characterized by littoral drift and eolian dynamics (Boski et al., 2008; Boski et al., 2002; Rosa et al., 2011; Zazo et al., 2008a)

The increased heavy metal concentrations, especially within the marine sediments of unit 2, allow conclusions to be drawn about the historical metallogenic use of the catchment area of the Guadiana River. The lowest heavy metal concentrations are observed within the sandy deposits of the lowermost unit 1, which are assumed to document the geological background values of the sediments' source region (IGME, 1983). In the deposits of the overlying unit 2 the stepwise increase of heavy metal concentrations most likely indicates the regional emergence of mining and smelting activities during Late Bronze Age (Hunt Ortiz, 2003). It is assumed that the high concentrations of heavy metals originate from mining wastes and slurries situated at the upstream drainage basin of the Guadiana River (Delgado et al., 2010). In any case, a close correlation of heavy metal contents to LOI_{550} contents indicates the importance of organic matter as an absorbent and is mainly associated with adsorption processes of fine-grained organic-rich sediment fractions (Syvitski, 1991; Wang, 2008).

4.3.5.2 Landscape Development Derived from Sedimentological Data (6000 BP – 3000 BP)

An estuary consists of a highly complex network of landscape-shaping processes. With the inclusion of two cores, only a selective section of this interaction can be provided. Nevertheless, the results of the core Aya 15 can be discussed to the extent that they

allow statements on the general design of the energetic milieu at the considered time period. The results from the core drillings are not intended to give the impression that a partial section of the estuarine process area will cover the entire estuary, but rather that it will be able to fit into the current state of knowledge of the development of the Guadiana River. Figure 42 is intended to provide a new way of visualizing this dynamic natural space.

Sediments from cores Aya 14 and Aya 15 give evidence of a dynamic geomorphological evolution throughout the Late Holocene in a coastal borderarea dominated by littoral, fluvial and colluvial processes interfingering since antiquity. The mid to Late Holocene marine sediments indicate different phases of littoral dynamics. Samples of dated charcoal fragments from sediment core Aya 15 show a maximum age of c. 6000 cal BP (Fig. A.4, Appendix A.2), marking the transition from rapid postglacial sea-level rise (until c. 7000 cal BP) to a phase of near sea-level stability with only minor oscillations of metric magnitude until the present (Boski et al., 2008; Rosa et al., 2011; Zazo et al., 2008b). The sediments exposed in Aya 15 correspond to this time period; they are grayish-brown medium-grained sands with abundant remains of marine fauna (unit 1) and give clear evidence of the decelerating sea-level rise (Vis et al., 2016). Thus, the deposits most likely indicate increased fluvial sediment output to the shelf with subsequent aggradational filling into the estuarine accommodation space (Boski et al., 2002; Dabrio et al., 2000; Fletcher, 2005; Lario et al., 2002). The aggradational character of sedimentation during this period did not allow the establishment of a beach-barrier system with spits (Fig. 42A).

After c. 3000 cal BP, sedimentation in the estuary changed from vertical to lateral (progradation) (Dabrio et al., 2000), resulting in the accelerated expansion of tidal flats and the rapid growth of sandy barriers (Fig. 42B). With rising sea levels, the Guadiana paleo-estuary became semi-closed (Rodríguez-Ramírez et al., 2014b). During this period, the ongoing expansion of sandy barriers in the paleo-estuary caused the silting-

up of fines in an amphibious environment behind the barrier islands, turning it into a restricted lagoon-like environment with brackish-to-fresh water (Boski et al., 2008; Zazo et al., 2008b) (Fig. 42C). This development is represented by the sediments of unit 2 in core Aya 15 with a grain-size distribution indicative for a low energy environment (Watson et al., 2013). This finding is confirmed by the occurrence of aquatic plant detritals and corroded bivalve shells. The grayish sediment color indicates reducing conditions, allowing the formation of iron sulfides in a long-term sub-aqueous environment (Bordovskiy, 1965; Meyers, 1997). The high calcium carbonate contents as indicated by the high LOI_{900} values are a characteristic feature of estuarine sediments and are predominantly caused by the deposition of corroded shell material (Allen, 2003). Additionally, high contents of organic matter and high electrical conductivity of the sediment's solutes clearly point to sub-aqueous quiescent depositional conditions in a lagoonal-like environment (Bordovskiy, 1965; Meyers, 1997). From the fining-upward character of the sediments in Aya 15, unit 2 it can be concluded that this confinement occurred gradually within the Guadiana Estuary. Written sources indicate that during antiquity the progressive growth of tidal flats resulted in the rapid filling of the Guadiana Estuary basin. Around 2000 yrs BP Strabo (Geographica, III, 1, 9) describes the Guadiana Estuary as a *"delta with two mouths"*. This description indicates that at the turn of the ages the eastern distributary of the Guadiana Estuary was temporarily active (Rosa et al., 2011), forming the prominent prodeltaic wedge described by Mendes et al. (2010). Within this phase of gradual sedimentary infill of the salt-marsh areas located between the mainland and the barrier islands, three relatively siliciclastic bands of 5-10 cm thickness were deposited. The two lower layers consist of gravel as well as allochthonous lithoclasts and show erosive bases. The sedimentological features themselves make it impossible to determine whether these layers were deposited by high-energy wave dynamics or originally as fluvio-lacustrine

deposits resulting from a flood event (Benito et al., 2015; Benito et al., 2008; Lario et al., 2011).

Heavy metal concentrations in the fine-grained sediments of unit 2, Aya 15 reveal metal ore processing in the Guadiana drainage basin. Delgado et al. (2011) studied surficial sediment samples in the marine domain of the Guadiana Estuary and emphasize that the lower Guadiana Estuary contains metal concentrations higher than the natural background values. Together with sedimentological data from drillings, the timing, levels and sources of trace minerals were analyzed, indicating that the sediments contain reactive compounds capable of retaining metals. High heavy metal concentrations of anthropogenic origin within the lagoonal sediments of the Guadiana Estuary (e.g. Pb, Ni and Zn) confirm the existence of notably diffuse pollution. This excess of trace and heavy metals is most likely produced by acid mine drainage generated in the internal zones of the basin, the Iberian Pyrite Belt (Delgado et al., 2011; Delgado et al., 2010). Metalworking activities in the Guadiana basin have been recorded since the beginning of the Copper Age, resulting in increased metal concentrations within the correlate sediments. Metal processing has been particularly intensive between the late Bronze Age and the Roman period (Hürkamp et al., 2009).

4.3.5.3 Landscape Development Derived from Historical Maps and Orthophotos (17th century until today)

To enable an evaluation of the cartographic results, a brief discussion of the quality of the georeferencing procedure should precede the discussion of landscape development based on the derived shoreline reconstruction. Historical maps are usually based on none, old or indefinable projections, ellipsoids and dates (Moore, 2000). Furthermore, historical maps are often affected by uneven map shrinkage, leading to irregular distortions of the original map scale (Crowell et al., 1991). Both characteristics influence the results of the georeferencing process. Due to a scarcity of ground control points for the georeferencing of the maps analyzed, the minimum number of four ground

control points is used for georeferencing. Resulting root mean squares errors represent "the magnitude of relative control point displacement" (Crowell et al., 1991) and thus reflect the sum of errors referring to distortion and/or inaccuracies by manually setting the ground control points (Crowell et al., 1991). In this study the root mean square error increases with the age of the maps, pointing to the stronger effects of distortion in the maps dating from the 18th century. In any case, data derived from the maps can be correlated with present-day geomorphological features, like the inactive spits in the salt marshland of the study area and is therefore considered as adequate for an interpretation of shoreline changes (Fig. 42D-G). The consolidation of the complex of small barrier islands in front of the Spanish mainland into one large barrier island during the 17th century is clearly documented in early maps, open to visual interpretation. Until the 18th century, an asymmetric development and the preservation of the Guadiana Estuary with a very large western swash shelf on the lagoonal salt marshes at the eastern margin, caused by flood- and ebb-tidal currents and associated wave activities can be observed (Morales, 1997) (Fig. 42D). Morphological development at this time was dominated by an eastward littoral drift that mainly transported sediments along the shoreline, causing the formation of an estuarine lagoon around the Guadiana River mouth (Dias et al., 2004).

The ongoing development of the Guadiana Estuary to its present form can be observed in the maps from the 18th century onwards (Fig. 42E). The fusion of active sandbars and barrier islands resulted in the formation of an island complex (Morales, 1997). The sheltered zones between the minor and major barriers acted as sediment traps, leading to the development of the present-day marshlands which are strongly influenced by tidal currents.

Maps from the 19th century show that the Guadiana Estuary had almost attained its present shape. Three distinct features distinguish the morphological setup from earlier situations. The first clearly different characteristic is the formation of a large spit at

the southernmost western margin. The growth of the spit was mainly influenced by eastward littoral drift, leading to the accretion of swash bars (Dias et al., 2004). Land reclamation in this phase was measured at approximately 24,000 $m^{2}*year^{-1}$ (González et al., 2001). The second feature of geomorphological character evident from the historical maps of this period is the progressive narrowing of the final Guadiana River mouth as a result of active sedimentation at the lateral tidal bars (Morales et al., 2006; Wachsmann et al., 2009). The material which accumulated at the mouth of the Guadiana River is transported by various forces such as tidal waves, wave-dominated sediment transport and the discharge of the river itself (Chícharo et al., 2007; Garel et al., 2009). The third major feature is the blockage of the main Guadiana River mouth by the growth and landward migration of shoals (Garel et al., 2014). To counteract and stabilize the outlet, as well as to protect the mouth from further sedimentation by the predominant eastward littoral drift, two jetties were constructed between 1972 and 1976, creating an erosion hot-spot associated with temporally persistent and divergent longshore transport providing sand to the adjacent areas (Garel et al., 2014; Portela, 2006).

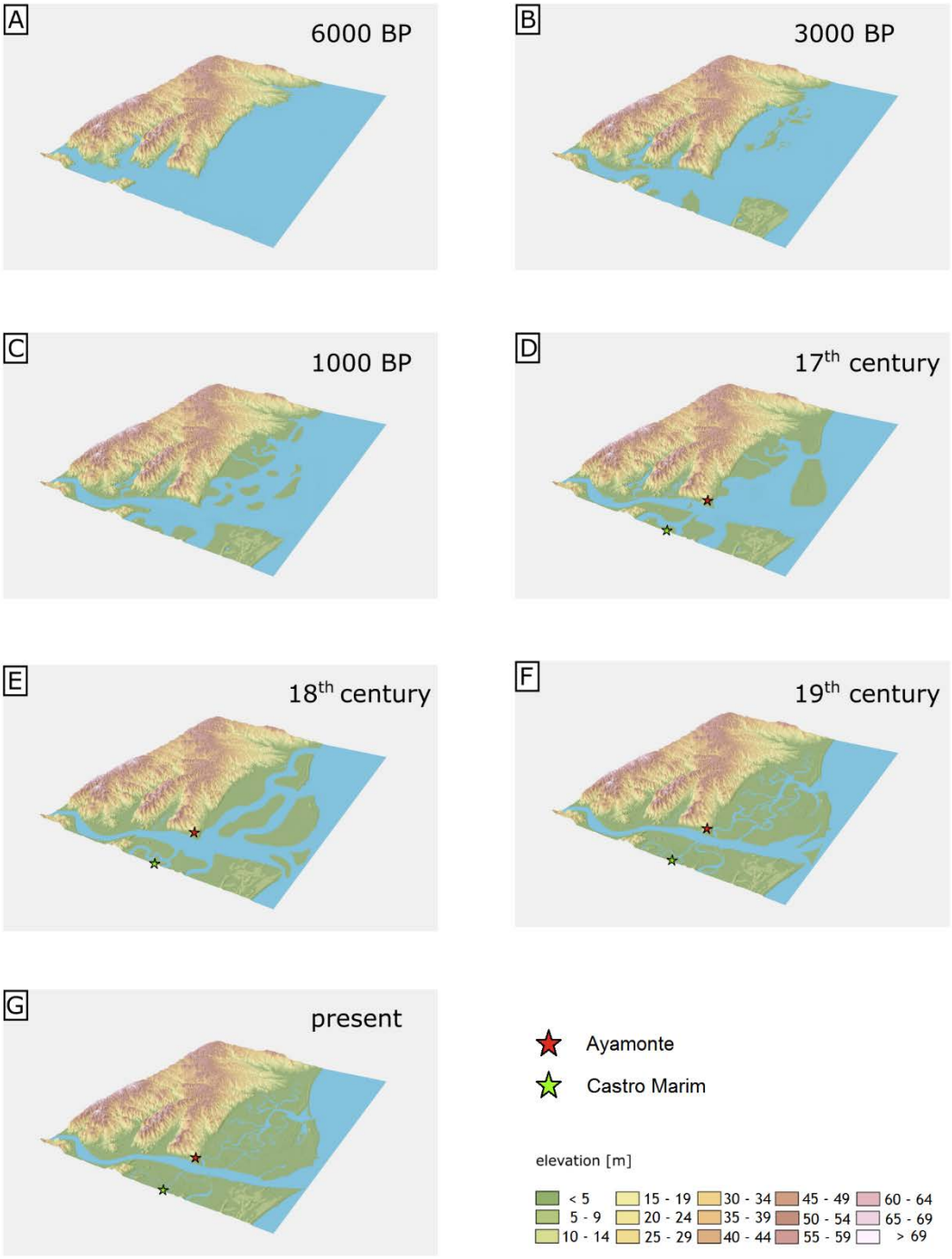

Figure 42: Schematic Mid- to Late Holocene evolution of the Guadiana Estuary mouth, based on reviewed data (Morales, 1997), sedimentological data (presented in this study) and spatial analysis of historical maps. A – maximum flooding and open estuary conditions, B – increasing sediment export to the shelf, forming initial spits and barrier islands, C – sedimentary infilling by fluvial input and initial marsh development; D - very large western swash shelf on the Portuguese part and lagoonal salt marshes at the eastern margin; E - fusion of active sandbars and barrier islands results in the formation of an island complex; F - formation of a large spit at the southernmost western margin, progressive narrowing of the final Guadiana River mouth and blockage of the main Guadiana River mouth by the growth and landward migration of shoals; G – present situation with extensive marsh areas and narrow tidal channels (visualization layout: own design; data source: Centro Nacional de Información Geográfica [http://centrodedescargas.cnig.es/CentroDescargas/index.jsp], access: 23.01.2018]).

4.3.6 Conclusions

Based on the sedimentological, geochronological, geochemical, cartographical and geomorphological data presented, the study reveals information about 6000 years of coastal change at the lower Guadiana Estuary. Sedimentological evidences show the development from an open to a closed estuary. Sediments exposed by two drillings extracted from the area where the salt marsh interfingers with the footslopes of the mainland allow the definition of three Mid- to Late Holocene sedimentary facies for the Guadiana Estuary. Several Mid- to Late Holocene changes in geomorphological processes are indicated. The basal sediments exposed document the phase when the Holocene eustatic sea-level rise stagnated in the Mid-Holocene and littoral processes were increasingly influenced by fluvio-lacustrine processes and coastline evolution. At this time (c. 6000 cal BP) maximum flooding occurred and most of the sandy fluvial sediments were trapped in the bay-head delta (Fig. 42A). These nearly open-estuary conditions prevailed until about 4000 cal BP, with a gradual transition towards lagoonal deposition. During this time the fluvial input into the estuary exceeded the rate of sea-level rise, favoring the accelerated expansion of marsh areas behind sand spits and barrier islands. After approximately 3000 cal BP, the expansion of sandy barriers in the paleo-estuary caused by littoral drift resulted in the deposition of silty to clayey sediments. The previously open area turned into a restricted brackish to fresh water lagoon-like environment (Fig. 42B). Progradation of new barrier islands from active sand bars continued, generating a large shallow shelf area (Fig. 42C). Due to proximity to the slopes of the adjacent coastal mainland, the lagoonal and littoral facies were covered by terrestrial material, which shows distinct phases of increased denudation and slope wash during prehistoric times.

Since the onset of the Modern times, during the last five centuries, historical and cartographical data document the interplay of littoral drift and large fluvial input. High

sediment yields of the Guadiana River accelerated by soil erosion have favored the accumulation of large sand bodies at the lower estuary area (Fig. 42D–G). This development has resulted in a constantly decreasing lagoonal water body as indicated by the historical maps.

The findings also show the ecological imprint of heavy metal concentrations within the lagoonal deposits. Prehistorical and historical mining activities within the areas of the Iberian Pyrite Belt most likely caused this “diffuse historical” contamination.

5. Concluding Remarks

5.1 Conclusions from the Individual Case Studies

This geoarchaeological study in the surroundings of the Phoenician settlement in Ayamonte provides new insights into the ongoing discussions about an assumed Phoenician harbor site, local landscape changes, coastal development and human-environment interactions since the beginning of the Late Holocene. Sediment cores as well as cartographic material have been analyzed using a multiproxy approach. Approximately 8000 years of landscape development in the Guadiana Estuary and its surroundings were investigated in this study.

The case studies allow the reconstruction of the Late Holocene landscape development of the three sub environs: I) Estero de la Nao wetlands, II) the slopes of the Cerro del Castillo and the Las Quintana dry valleys, as well as III) the Isla Cristina wetlands. The studies imply a very dynamic landscape during Late Holocene.

5.1.1 The Importance of Ayamontes Lagoons During Phoenician Times

Within the urban area of Ayamonte, a former coastal city in southwest Andalusia, located at the international border between the Republic of Portugal and the Kingdom of Spain, well-preserved archaeological remains of Phoenician Times such as tombs and metallurgic workshops have been discovered (Teyssandier and Marzoli, 2014). The main research questions that arose during field discussions are: How was the coastal landscape characterized at the time of the Phoenician period, and what changes occurred during the following centuries? One particular focus is set on coastal changes of a lagoon-like environment, which is believed to be navigable at Phoenician times enabling the establishment of a prehistoric anchorage.

The results of this study in the wetlands of the “Estero de la Nao” attest to marine transgression since at least 8000 years ago. Five ^{14}C-ages of plant remains and bulk material give maximum ages and indicate marine conditions since approx. 6000 cal

BCE. The marine sequences are composed of organic-rich silt sediments containing marine fauna and macro-botanical remains. High calcium carbonate content from shell material, high contents of organic matter, low contents of inorganic carbon, low Si concentrations, low Ca-Fe ratios, high electrical conductivity together with a very low and steady course of magnetic susceptibility indicate sub-aqueous quiescent depositional conditions in a landward lagoonal-like environment (Klein et al., 2016, cf chapter 4.1). Chronological and geochemical data of three sediment cores, forming a longitudinal profile through the lagoonal-like environment, suggest beginning siltation of the embayment during the Early Bronze Age, c. 3rd millennium BCE. Brown silty sediments poor in vegetal remains with low contents of total organic carbon, Calcium and low values of electrical conductivity reflect phases of silting-up and the colonization of marsh vegetation within an amphibian environment (Klein et al., 2016). These observations are in general agreement with sedimentological records from Boski et al. (2002), stating that the sea level close to the present was attained at about 5000 cal BP after a period of slower rise (below 0.5 m/century). The complete siltation of the entire eastern embayment occurred around 1000 cal CE.

Considering the age of the Phoenician settlement ($8^{th}/7^{th}$ Century BCE) the eastern part of the Estero de la Nao can be regarded as not usable for Phoenician maritime purposes. However, it cannot be ruled out that water carrying streams ensured a transport of ships into the eastern parts of the lagoon. Although strong changes in the coastline of the coastal areas already occurred during Bronze Age, the landscape that the Phoenicians found in Ayamonte was characterized by a larger area of navigable regions compared to the present situation.

Assuming the position of the prehistoric anchorage in the western areas of the lagoonal-like environment of the “Estero de la Nao”, important insights into this specific question have been achieved. It has been demonstrated by the analysis of sediments, that marine conditions prevailed at the assumed site until the 1st millennium CE.

Thus, the assumption of a potential port location for the local prehistoric community, such as the Phoenicians, is strengthened by these findings. Not only the facies analysis indicates that the site may have been used as a landing point. A stratigraphic gap within the still water facies spanning from the 4th millennium BCE to the 1st millennium CE was discovered within the sedimentary column. This diagnostic finding is likely caused by dredging and has been repeatedly discovered in sediments around populated ports and coastlines of many formerly Phoenician settlements in the Mediterranean area. For the first time, these tentative evidences are given at the Atlantic coastline of the Iberian Peninsula.

Looking at the change between marine and terrestrial deposition another geoscientific aspect could be examined more closely. A prominent, badly sorted debris layer framed by two radiocarbon ages has been correlated to a tsunami-event caused by the 1755 Great Lisbon Earthquake.

5.1.2 The Intensive Utilization of Ayamontes Landscapes

The investigation of slope sediments surrounding the Phoenician settlement provides evidence on the onset of settlement pressure on the landscape during ancient times, revealing high erosion rates during antiquity. Designated phases of increased erosion have been assigned to phases of increased landscape utilization. These phases comprise a) the Late Bronze Age, which spans the period of Phoenician colonization during the Roman Era b) a phase of agrarian and mining intensification, and the Little Ice Age resp. the Modern Era, characterized by recommenced mining activities and industrialization. Furthermore, the findings show low erosion rates during the Moorish domination of the area, indicating relatively stable geomorphic conditions.

The economic importance of the location since ancient times, is confirmed by the detection of increased concentrations of elemental lead within the slope sediments. It is believed that these findings represent an evidence of prehistoric mining activity.

The results of the third case study, investigating the landscape changes at the Guadiana River mouth and its barrier systems and wetlands, confirm the findings of previous results and show that the Guadiana Estuary is geomorphologically a very dynamic space. The multiproxy approach made it possible to record older and younger geomorphological changes. Earlier developments have been recorded by sedimentological data from two corings and show 6000 years of rapid coastal change at the lower Guadiana Estuary. Sandy deposits, dated to c. 6000 cal BP, document that fluvial sediments have been trapped in the bay-head delta and non-eustatic changes determined the coastline of the estuary and its surroundings. Overlying lagoonal deposits document progressive aggradation and the decrease of accommodation space resulting in the expansion of shallow marsh areas, enclosing the estuary gradually towards lagoonal conditions. Subsequent progradation of new barrier islands from active sand bars continued, generating a large shallow shelf area and narrowing of the tidal channels. The analysis of historical maps allowed a reconstruction of the changes of the barrier islands, sand spits and tidal channels during the last 200 years. It has been observed, that the fusion of active sandbars and barriers islands resulted in the formation of an established island complex. Furthermore, active sedimentation takes place on tidal bars, narrowing the tidal channels as well as the entire Guadiana River mouth.

Geochemical results show an ecological imprint of heavy metal concentrations within the lagoonal deposits, indicating a noticeable diffuse historical mining pollution associated with the acid mine drainage generated in the internal zones of the basin. These signs of historical pollution of the estuary may superimpose additional local inputs from other human activities.

5.2 Human-Environmental Interactions in the Surroundings of Ayamonte – a Synoptical Assessment

This doctoral thesis aims to investigate aspects of landscape development and human-environment interactions in the surroundings of Ayamonte (SW-Andalusia) since the phase of intense settlement during the Bronze Age. The project is based in the Topoi Research Group A-1 "Ancient Colonizations of Marginal Habitats". The three case studies presented investigate settlement-related landscape changes in different scales. First, the role of the conceptual approach of marginality within the superordinate research project is expounded. Secondly, the integration of the results is delineated with special focus on the importance of scales. Finally, it is concluded that the post-Phoenician emerging production of metallurgic goods and the subsequent naval trade went along with large-scale landscape disturbances in the study area, showing that the landscape around Ayamonte seems not resilient enough, to sustain the anthropogenic pressure.

5.2.1 The Role of Marginality

Applying the concepts of spatial and ecological marginality from Bebermeier et al. (2016), where marginality is defined with "regard to spatial distribution, be it in relation to 'core' settlement areas i.e. 'centers', or in relation to more favorable habitats which have been defined geographically", the presented case studies provide examples of site-specific studies that help to understand how past societies engaged with their landscapes considered by some as marginal (Ménanteau, 2005).

A lot of geoarchaeological studies regard the evolution of Mediterranean landscapes as characterized by degradation and the development of marginal environments (Butzer, 2005; Grove and Rackham, 2003). In the attempt to understand some societies and their motivation, it might be that 'marginality' is not a helpful term. One is tended to follow the theory of Walsh (2008), where marginality is defined "as a term […] largely a product of totalising histories or archaeologies that attempt to interpret processes

over large geographical spaces". For quite a few authors, many Mediterranean landscapes can be characterized as ruined or marginal (most likely including the landscapes of the presented case studies), but recent publications attempt to demonstrate how the characterization of Mediterranean landscapes might be unsuitable (Horden and Purcell, 2000). Some Mediterranean niches may not be very productive at first sight and especially not in isolation. But taking into account the entire production network of various goods, the process of local deterioration ('marginalization') could be exaggerated. For people have always succeeded in making use of niches spread across the Mediterranean by means of adaptive strategies (Horden and Purcell, 2000). Following these thoughts, we might depart from the simplifying cause/effect analysis of landscape processes.

The geoarchaeological work of the assumed anchorage within the "Estero de la Nao-wetlands" (case study 1, chapter 4.1) aimed for an assessment of the site's locational characteristics and determination of the timing and dynamics of silting-up processes. Results show, that much of its past the site has been a wetland of some sort. Dealing with the question of 'marginality', the debate of utilization of wetlands versus the potential danger and risks (diseases, flooding, tsunamis) is of special interest. Sallares (2002) and some other scholars consider wetlands and marshes as ecological niches that are environmentally marginal and therefore unproductive and dangerous because of malaria. However, numerous wetland areas are rich in resources such as fish and fowl, and malaria has not always been present (Walsh, 2008). Furthermore, especially the edges wetlands have been used for agriculture, and many societies made efforts to drain wetlands in order to gain arable land (Rogers, 2013). The supposed on-site dredging works within the past, trying to keep the anchorage usable, reflect the investment in this economic enterprise, ignoring the risks and inconveniences of a wetland that has been environmentally marginal during many periods in the past. The problems associated with Mediterranean marshlands, such as mosquito infestation and malaria,

and the marginality was overcome through exploitation of labor and the use of technologies to manage a drainage system and clear eroded sediment.

The inland anchorage of Ayamonte was the product of very specific socio-economic systems; the Phoenician trade network and the subsequent Roman Empire, both with its desire to cope and control natural processes through complex forms of engineering. The presented case study focuses on a site where the sedimentological record has been reworked, and many earlier sediments have been removed. The geomorphic events occurred in periods of time that cannot be precisely dated. However, one can be sure that the processes were experienced by humans who lived and worked in the surroundings of the site. Despite the temporal economic success of the presumed inland anchorage and its central role in the regional economy, the characteristics that made this landscape marginal during other periods would still have been present to some extent. Therefore, while this landscape was a 'nucleus' and economically productive for the core regions, it may still have been unpleasant and disagreeable environment for the workers.

After the anchorage was abandoned the network of relations in the area must have changed dramatically. Marshland characteristic re-established themselves after the demise of Roman management systems, and layers of eroded sediment covered the former cultural achievements. These processes produced again a very different network of relations, generating an area of economic unproductiveness.

The sediment and affiliated features of the case study are far more than sedimentological and geoarchaeological record of climatic or human impact on geomorphological systems. They are also a reproduction of complex cultural and social relations that existed between humans and their landscapes. In complex societies, attitudes to and constructions of marginality are varied and expressed by "collective pillars of resilience" facing landscape deteriorations (Butzer, 2005). Resilience at

Ayamonte existed at a macro-economic scale, producing a laborious adaptive approach, as part of a need to maintain an efficient piece of supra-regional-trading. In all the presented studies, natural environment acted upon the population in various ways. The dynamic relationship between anthropogenic and non-anthropogenic agents constituted very specific landscapes where concepts of marginality were perhaps insignificant or quite unlike todays' ideas of marginality.

5.2.2 Implications of Human Action – Multi-Scale Considerations

The historical connections and the way in which social and natural changes are intertwined with each other reveal the importance of spatial and temporal multi-scale investigations. This task was carried out based on the implementation of multi - method studies on a supra-regional level (chapter 4.2 and 4.3) and a sediment-based case study at local scale (chapter 4.1). However, the scale of landscape-influencing processes is not determined solely by the geomorphological position. The presumably atmospheric deposits of lead in case study 2 (chapter 4.2) are an illustrative example of the underlying principle. Nevertheless, the outcomes of the studies can be related to each other because of their spatial proximity and diachronic approach. On the supra-regional and long-term scale, climate-controlled processes determined the landscape-shaping processes decisively, while low human impact in the area during the Neolithic is reflected in the sedimentary records (Chester, 2012; Delgado et al., 2012a; Klein et al., 2016; Kunst, 2001). The historical flood record of the Guadiana Delta has been discussed by several authors (Benito et al., 2015; Benito et al., 2003; Benito et al., 2008; Caetano et al., 2006; Ortega and Garzón, 2003; Ortega and Garzón, 2009; Thorndycraft and Benito, 2006) and must be interpreted as a gauge for macro-scale sediment supply flux. Around 3000 cal BP increased slope activities appear to be related to human impact. In accordance, the analysis of estuarine deposits and the analysis of published pollen data indicates increased anthropogenic factors, such as contents of heavy metals, suggesting mining activities (Camacho et al., 2014; Delgado et al., 2011), as well as

major changes in the vegetation cover with widespread replacement of forest by scrub communities and open ground, suggesting impacts from pastoral activities (grazing and burning) between 4100 and 1400 cal BP (Fletcher, 2005). The timing of human-related impacts on different landscape compartments corresponds to the Phoenician colonization of territories west of the Strait of Gibraltar (Aubet, 2001; Carpenter, 1958; Frankenstein, 1979)

5.3 Synthesis

Synthesizing the project in the Guadiana Estuary, it must be noted that early human-induced landscape changes occurred since the Bronze Age. The actions of the Phoenician colonists had clearly increased impact on geomorphic processes due to interventions in the natural balance. It seems highly probable that the Phoenician settlers, due to their economic commitment, can be considered as a kind of catalyst for landscaping processes. The Phoenician-induced impact is likely to be connected to early ore smelting activities. Direct evidence of early ore smelting activities is provided by the occurrence of Bronze Age metal workshops within the urban area of Ayamonte (Teyssandier and Marzoli, 2014). From an archaeological point of view, with the discovery of the graves and the settlement of Ayamonte we can trace the remnants of people who, from their point of view, lived in a "world-wide" environment and settled on the edge of the ancient world, triggering effective changes within the native milieu. As part of this expansion, the Phoenicians began to build a system of redistribution and the exchange of goods that lasted for more than three centuries (Gras, 1995). This has fostered economic development and technological innovation not only within its own foundations, but also in the hinterland and in the surrounding regions (Matin Hernández, 2013).

As a second, very important step in the development of the landscape and the increasing human impact on the environment, the Roman epoch must be considered. Compared to the pre-Roman sediments, an increased geomorphological activity during

the Roman period could be proven (section 4.2). The Roman strategy in Baetica was largely dictated by the presence of the ore-rich mines in the Sierra Morena area (Sandars, 1905). Before the Roman occupation of Spain, Rome had to buy copper, gold and silver from Phoenician and Carthaginian merchants who, in turn, acted with the Tartessians in whose territory the mines were situated. The intensification of mining activities (García-Alix et al., 2013; Rosman et al., 1997) in the Spanish territories is reflected within the erosive sediments retrieved in case study 2 (chapter 4.2). However, for a conclusive evaluation on settlement- and culture-dependent erosion phases in the surroundings of Ayamonte, further excavations, and investigations on slope deposits with multi-chronometric approaches are needed.

Overall, the presented study supports the assumption of Ayamonte being an important coastal site since the Bronze Age. Moreover, the geoarchives in the surroundings are well suited to study human-environment interactions during the Late Holocene and investigating coastal changes and settlement. This research contributes to a better understanding of sedimentation processes within Ayamontes environment, and their interaction with the development of the coastal site and assumed harbor locations. The tsunami layer presented in case study 1 (chapter 4.1), is the first profoundly dated sedimentological evidence of the tsunami of 1755 within the city of Ayamonte. Furthermore, evidence of historic harbor dredging west of the Strait of Gibraltar has been provided for the first time.

Despite the extensive results presented, many questions remain: Is the favorable geographical location of Ayamonte reflected in the archaeological record? What was the economic importance of Ayamonte in prehistoric times? Are there any other indications that an inland anchorage could have existed? How and by what means could the alleged anchorage have been kept free of sediments? Which agricultural management practices prevailed in Ayamontes environment, and how did they change

over the epochs? And finally: How do the latest developments (dam constructions, tourism) impact the estuarine ecosystem?

Referring to the location of Ayamonte within the network of Phoenician settlements, the results presented give evidence of many favorable geographical factors. Therefore Ayamonte should under no circumstances be regarded as marginal, but represents an important element within the Phoenician trading network.

Bibiography

Acquafredda, P., Muntoni, I.M., Pallara, M., 2018. Reassessment of WD-XRF method for obsidian provenance shareable databases. Quaternary International,Volume 468, Part A, Pages 169-178

Ad-Hoc-AG Boden, B., 2005. Bodenkundliche Kartieranleitung. E. Schweitzerbart'sche Verlagsbuchhandlung, Stuttgart, pp. 438 S.

Allen, H.D., 2003. A transient coastal wetland: from estuarine to supratidal conditions in less than 2000 years—Boca do Rio, Algarve, Portugal. Land Degradation & Development, 14(3), 265-283.

Almagro-Gorbea, M., 2006. La necrópolis de Medellin. I. La excavación y sus hallazgos. Biblioteca Archaeologica Hispana, 26, Madrid.

Almagro-Gorbea, M., 2008a. La necrópolis de Medellin. II. El Estudio de los hallázgos. Biblioteca Archaeologica Hispana, 26, Madrid.

Almagro-Gorbea, M., 2008b. La necrópolis de Medellin. III. Estudios analíticos. IV Interpretación de la necrópolis. V. El marco histórico de Medellín-Conisturgis,. Biblioteca Archaeologica Hispana, 26, Madrid.

Alon, D., Mintz, G., Cohen, I., Weiner, S., Boaretto, E., 2002. The Use of Raman Spectroscopy to Monitor the Removal of Humic Substances from Charcoal: Quality Control for 14C Dating of Charcoal. Radiocarbon, 44(1), 1-11.

Andrade, C., 1992. Tsunami generated forms in the Algarve barrier islands (South Portugal). Science of Tsunami Hazards, 10, 21-34.

Angern, O., Gmelin, L., Meyer, R.J., Gmelin-Institut für Anorganische Chemie und Grenzgebiete (Frankfurt Main), Deutsche Chemische Gesellschaft, 1951. Titan. Gmelins Handbuch der anorganischen Chemie, pp. XXII, 481 S.

Aranbarri, J., 2015. Human–landscape interactions in the Conquezuela–Ambrona Valley (Soria, continental Iberia): From the early Neolithic land use to the origin of the current oak woodland. Palaeogeography, Palaeoclimatology, Palaeoecology 436 (2015) 41–57.

Arruda, A.M., 1997. A cerámica ática do Castelo de Castro Marim, Lisbon.

Arruda, A.M., 2000a. As cerâmicas de importação do Castelo de Castro Marim no âmbito do comércio Ocidental dos séculos V a III a. C., Cádiz 2000, pp. 727-735.

Arruda, A.M. (Ed.), 2000b. Los Fenicios en Portugal: Fenicios y mundo indígena en el centro y sur de Portugal (siglos VIII–VI a.C.). Cuadernos de Arqueologìa Mediterránea, 5-6. Laboratorio de Arqueologìa Universidad Pompeu Fabra de Barcelona.

Arruda, A.M., 2003. A Idade do ferro no Castelo de Castro Marim através das importações cerâmicas. Xelb, 4, 70-88.

Arruda, A.M., 2009. Colonial Encounters in Ancient Iberia - Phoenician, Greek and Indigenous Relations, Chicago.

Arruda, A.M., Teixeira de Freitas, V., 2008. O Castelo de Castro Marim durante os séculos VI e V a. n. e. In: A.M. Arruda, V. Teixeira de Freitas (Eds.), Jiménez Ávila, pp. 429-446.

Arteaga, O., 1988. Zur phönizischen Hafensituation von Toscanos. Madrider Beiträge, 14, 107-141.

Arteaga, O., Hoffmann, G., Schubart, H., Schulz, H.D., 1989. Investigaciones geologicas y arqueologicas sobre los cambios de la linea costera en el litoral de la Andalucia mediterranea. Anuario Arqueologico de Andalucia, 2, 117-122.

Arteaga, O., Kölling, A., Kölling, M., Roos, A.M., Schulz, H., Schulz, H.D., 2001. El puerto de Gadir. Investigación geoarqueológica en el casco antiguo de Cádiz. Revista Atlántica-Mediterránea de Prehistoria y Arqueología Social, 4, 345-415.

Arteaga, O., Roos, A.M., 2002. El puerto fenicio-púnico de Gadir. Una nueva visión desde la Geoarqueología Urbana de Cádiz. Homenaje al Profesor Pellicer II. Spal, 11, 21-39.

Aubet, M.E., 2001. The Phoenicians and the West: politics, colonies and trade. Cambridge Univ. Press, Cambridge.

Avery, D., 1974. Not on Queen Victoria's Birthday - The story of the Rio Tinto mines.

Balsam, W.L., Ellwood, B.B., Ji, J., Williams, E.R., Long, X., El Hassani, A., 2011. Magnetic susceptibility as a proxy for rainfall: Worldwide data from tropical and temperate climate. Quaternary Science Reviews, 30(19–20), 2732-2744.

Baptista, M.A., Miranda, J.M., 2009. Revision of the Portuguese catalog of tsunamis. Nat. Hazards Earth Syst. Sci., 9(1), 25-42.

Bates, R.G., 1973. Determination of pH: theory and practice. A Wiley-Interscience Publication. Wiley, New York.

BBodSchG, 1998. Bundesbodenschutzgesetz - Gesetz zum Schutz vor schädlichen Bodenveränderungen und zur Sanierung von Altlasten. In: B.T. I (Ed.), pp. 502 ff.

Bebermeier, W., Beck, D., Gerlach, I., Klein, T., Knitter, D., Kohlmeyer, K., Krause, J., Marzoli, D., J., M., Müller-Neuhof, B., Näser, C., Rummel, P.v., Sack, D., Schmid, S., Schütt, B., Wulf-Rheidt, U., 2016. Ancient Colonization of Marginal Habitats. A Comparative Analysis of Case Studies from the Old World. In: M.M. Gerd Graßhoff (Ed.), Space and Knowledge. Topoi Research Group Articles. eTopoi, Berlin: Exzellenzcluster 264 Topoi pp. 1–44.

Bebermeier, W., Schütt, B., 2011. Geoarchaeology - A New Discipline? Die Erde, 142(3), 209-212.

Beckers, B., Schütt, B., Tsukamoto, S., Frechen, M., 2013. Age determination of Petra's engineered landscape – optically stimulated luminescence (OSL) and radiocarbon ages of runoff terrace systems in the Eastern Highlands of Jordan. Journal of Archaeological Science, 40(1), 333-348.

Bellin, N., Vanacker, V., De Baets, S., 2013. Anthropogenic and climatic impact on Holocene sediment dynamics in SE Spain: A review. Quaternary International, 308–309, 112-129.

Benito, G., Macklin, M.G., Zielhofer, C., Jones, A.F., Machado, M.J., 2015. Holocene flooding and climate change in the Mediterranean. CATENA, 130, 13-33.

Benito, G., Sopeña, A., Sánchez-Moya, Y., Machado, M.a.J., Pérez-González, A., 2003. Palaeoflood record of the Tagus River (Central Spain) during the Late Pleistocene and Holocene. Quaternary Science Reviews, 22(15–17), 1737-1756.

Benito, G., Thorndycraft, V.R., Rico, M., Sánchez-Moya, Y., Sopeña, A., 2008. Palaeoflood and floodplain records from Spain: Evidence for long-term climate variability and environmental changes. Geomorphology, 101(1–2), 68-77.

Benson, A.K., 1995. Applications of ground penetrating radar in assessing some geological hazards: examples of groundwater contamination, faults, cavities. Journal of Applied Geophysics, 33(1–3), 177-193.

Blättermann, M., Frechen, M., Gass, A., Hoelzmann, P., Parzinger, H., Schütt, B., 2012. Late Holocene landscape reconstruction in the Land of Seven Rivers, Kazakhstan. Quaternary International, 251, 42-51.

Boone, J.L., Worman, F.S., 2007. Rural Settlement and Soil Erosion from the Late Roman Period through the Medieval Islamic Period in the Lower Alentejo of Portugal. Journal of Field Archaeology, 32(2), 115-132.

Bordovskiy, O.K., 1965. Accumulation of organic matter in bottom sediments. Marine Geology, 3(1–2), 33-82.

Borja, F., Zazo, C., Dabrio, C.J., del Olmo, F.D., Goy, J.L., Lario, J., 1999. Holocene aeolian phases and human settlements along the Atlantic coast of southern Spain. The Holocene, 9(3), 333-339.

Borrego, J., López-González, N., Carro, B., 2004. Geochemical signature as paleoenvironmental markers in Holocene sediments of the Tinto River estuary (Southwestern Spain). Estuarine, Coastal and Shelf Science, 61(4), 631-641.

Borrego, J., López-González, N., Carro, B., Lozano-Soria, O., 2005. Geochemistry of rare-earth elements in Holocene sediments of an acidic estuary: Environmental markers (Tinto River Estuary, South-Western Spain). Journal of Geochemical Exploration, 86(3), 119-129.

Borrego, J., Morales, J.A., Pendon, J.G., 1995. Holocene estuarine facies along the mesotidal coast of Huelva, south-western Spain. In: B.W. Flemming, A. Bartholomä (Eds.), Tidal signatures in modern and ancient sediments. Blackwell Science Ltd, London, pp. 151-171.

Borrego, J., Morales, J.A., Pendón, J.G., 1993. Holocene Filling of an Estuarine Lagoon along the Mesotidal Coast of Huelva: The Piedras River Mouth, Southwestern Spain. Journal of Coastal Research, 9(1), 242-254.

Borrego, J., Ruiz, F., Gonzalez-Regalado, M.L., Pendón, J.G., Morales, J.A., 1999. The holocene transgression into the estuarine central basin of the Odiel River mouth (Cadiz gulf, SW, Spain): lithology and faunal assemblages. Quaternary Science Reviews, 18(6), 769-788.

Boski, T., Camacho, S., Moura, D., Fletcher, W., Wilamowski, A., Veiga-Pires, C., Correia, V., Loureiro, C., Santana, P., 2008. Chronology of the sedimentary processes during the postglacial sea level rise in two estuaries of the Algarve coast, Southern Portugal. Estuarine, Coastal and Shelf Science, 77(2), 230-244.

Boski, T., Moura, D., Veiga-Pires, C., Camacho, S., Duarte, D., Scott, D.B., Fernandes, S.G., 2002. Postglacial sea-level rise and sedimentary response in the Guadiana Estuary, Portugal/Spain border. Sedimentary Geology, 150(1–2), 103-122.

Boulter, C.A., 1993. Comparison of Rio-Tinto, Spain, and Guaymas Basin, Gulf of California: An explanation of a supergiant massive sulfide deposit in an ancient sill-sediment complex. Geology 21, 801-804.

Brückner, H., 2011. Geoarchäologie - in Forschung und Lehre, Tagungen des Landesmuseums für Vorgeschichte Halle (Saale), Halle (Saale), pp. 9-20.

Butzer, K.W., 1973. Spring sediments from the Acheulian site of Amanzi (Uitenhage District, South Africa). Quaternaria, 17, 299-319.

Butzer, K.W., 2005. Environmental history in the Mediterranean world: cross-disciplinary investigation of cause-and-effect for degradation and soil erosion. Journal of Archaeological Science, 32(12), 1773-1800.

Cáceres, L.M., Olías, M., de Andrés, J.R., Rodríguez-Vidal, J., Clemente, L., Galván, L., Medina, B., 2013. Geochemistry of Quaternary sediments in terraces of the Tinto River (SW Spain): Paleoenvironmental implications. CATENA, 101(0), 1-10.

Caetano, M., Vale, C., Falcão, M., 2006. Particulate metal distribution in Guadiana estuary punctuated by flood episodes. Estuarine, Coastal and Shelf Science, 70(1–2), 109-116.

Camacho, S., Moura, D., Connor, S., Boski, T., Gomes, A., 2014. Geochemical characteristics of sediments along the margins of an atlantic-mediterranean estuary (the Guadiana, Southeast Portugal): spatial and seasonal variations. Journal of Integrated Coastal Zone Management, 14(1), 129-148.

Campo, J., Andreu, V., Gimeno-García, E., González, O., Rubio, J.L., 2006. Occurrence of soil erosion after repeated experimental fires in a Mediterranean environment. Geomorphology, 82(3–4), 376-387.

Campos, M.L., 1991. Tsunami hazards on the Spanish coasts of the Iberian Peninsula. Science of Tsunami Hazards, 9, 83-90.

Candelone, J.-P., Hong, S., Pellone, C., Boutron, C.F., 1995. Post-Industrial Revolution changes in large-scale atmospheric pollution of the northern hemisphere by heavy metals as documented in central Greenland snow and ice. Journal of Geophysical Research: Atmospheres, 100(D8), 16605-16616.

Capelo, J.H., 1996. Esboço da paisagem vegetal da bacia Portuguesa do Rio Guadiana. Silva Lusitana IV, 13-64.

Carcaillet, C., 2000. Soil particles reworking evidences by AMS ^{14}C dating of charcoal. Earth and Planetary Sciences, 332, 21-28.

Caro Gómez, J.A., Díaz Del Olmo, F., Artigas, R.C., Recio Espejo, J.M., Barrera, C.B., 2011. Geoarchaeological alluvial terrace system in Tarazona: Chronostratigraphical transition of Mode 2 to Mode 3 during the middle-upper pleistocene in the Guadalquivir River valley (Seville, Spain). Quaternary International, 243(1), 143-160.

Carpenter, R., 1958. Phoenicians in the West. American Journal of Archaeology, 62(1), 35-53.

Carretero, M.I., Pozo, M., Ruiz, F., Rodríguez Vidal, J., Cáceres, L.M., Abad, M., Muñoz, J.M., Gómez, F., Campos, J.M., González-Regalado, M.L., Olías, M., 2011. Trace elements in Holocene sediments of the southern Doñana National Park (SW Spain): historical pollution and applications. Environmental Earth Sciences, 64(5), 1215-1223.

Carrión, J.S., Andrade, A., Bennett, K.D., Navarro, C., Munuera, M., 2001. Crossing forest thresholds: inertia and collapse in a Holocene sequence from south-central Spain. The Holocene, 11(6), 635-653.

Carrión, J.S., Fernández, S., Jiménez-Moreno, G., Fauquette, S., Gil-Romera, G., González-Sampériz, P., Finlayson, C., 2010. The historical origins of aridity and vegetation degradation in southeastern Spain. Journal of Arid Environments, 74(7), 731-736.

Cesareo, R., 2000. X-Ray Fluorescence Spectrometry, Ullmann's Encyclopedia of Industrial Chemistry. Wiley-VCH Verlag GmbH & Co.

Chagué-Goff, C., Nichol, S.L., Jenkinson, A.V., Heijnis, H., 2000. Signatures of natural catastrophic events and anthropogenic impact in an estuarine environment, New Zealand. Marine Geology, 167(3–4), 285-301.

Chagué-Goff, C., Szczuciński, W., Shinozaki, T., 2017. Applications of geochemistry in tsunami research: A review. Earth-Science Reviews, 165(Supplement C), 203-244.

Chester, D.K., 2012. Pleistocene and Holocene geomorphological development in the Algarve, southern Portugal. Geomorphology, 153–154(0), 17-28.

Chester, D.K., James, P.A., 1991. Holocene alluviation in the Algarve, southern Portugal: The case for an anthropogenic cause. Journal of Archaeological Science, 18(1), 73-87.

Chícharo, L., Chícharo, A., Ben-Hamadou, R., Morais, P., 2007. The Guadiana Estuary. In: C. King (Ed.), Water and Ecosystems - Managing Water in Diverse Ecosystems To Ensure Human Well-being. The United Nations University, Hamilton, Ontario, pp. 107-117.

CNIG, 2017. Modelos Digitales de Elevaciones. (Centro Nacional de Información Geográfica).

Costa, C., 1994. Final Report of Sub-Project A. Wind Wave Climatology of the Portuguese Coast. Technical Report. In: I.L. Powaves 6/94-A (Ed.).

Costantini, E.A.C., Angelone, M., Damiani, D., 2002. Physical, geochemical and mineralogical indicators of aging in Quaternary soils of Central Italy, 17th World Congress of Soil Science. International Union of Soil Sciences, pp. 1-9.

Crowell, M., Leatherman, S.P., Michael, K.B., 1991. Historical Shoreline Change: Error Analysis and Mapping Accuracy. Journal of Coastal Research, 7(3), 839-852.

CSIC-IARA. (1989). Memoria del Mapa de Suelos de Andalucía a escala 1:400000. C.S.I.C. y Junta de Andalucía, Madrid. 95 pp.

Currás, A., Zamora, L., Reed, J.M., García-Soto, E., Ferrero, S., Armengol, X., Mezquita-Joanes, F., Marqués, M.A., Riera, S., Julià, R., 2012. Climate change and human impact in central Spain during Roman times: High-resolution multi-proxy analysis of a tufa lake record (Somolinos, 1280 m asl). CATENA, 89(1), 31-53.

Cuven, S., Paris, R., Falvard, S., Miot-Noirault, E., Benbakkar, M., Schneider, J.-L., Billy, I., 2013. High-resolution analysis of a tsunami deposit: Case-study from the 1755 Lisbon tsunami in southwestern Spain. Marine Geology, 337(Supplement C), 98-111.

Dabrio, C., Zazo, C., Lario, J., Goy, J., Sierro, F., Borja, F., González, J., Flores, J., 1998. Sequence stratigraphy of Holocene incised-valley fills and coastal evolution in the Gulf of Cádiz (southern Spain). Geologie en Mijnbouw, 77(3-4), 263-281.

Dabrio, C.J., Zazo, C., Goy, J.L., Sierro, F.J., Borja, F., Lario, J., Gonzalez, J.A., Flores, J.A., 2000. Depositional history of estuarine infill during the last postglacial transgression (Gulf of Cadiz, Southern Spain). Marine Geology, 162(2-4), 381-404.

Davis Jr, R.A., Welty, A.T., Borrego, J., Morales, J.A., Pendon, J.G., Ryan, J.G., 2000. Rio Tinto estuary (Spain): 5000 years of pollution. Environmental Geology, 39(10), 1107-1116.

Dawson, A.G., Hindson, R., Andrade, C., Freitas, C., Parish, R., Bateman, M., 1995. Tsunami sedimentation associated with the Lisbon earthquake of 1 November AD 1755: Boca do Rio, Algarve, Portugal. The Holocene, 5(2), 209-215.

De Caro, S., Giampaola, D., 2004. La Metropolitana approda nel porto di Neapolis. Civiltà del Mediterraneo, 4-5, 49-62.

de Jong, E., Nestor, P.A., Pennock, D.J., 1998. The use of magnetic susceptibility to measure long-term soil redistribution. CATENA, 32(1), 23-35.

Dean, W.E., 1974. Determination of carbonate and organic matter in calcareous sediments and sedimentary rocks by loss on ignition; comparison with other methods. Journal of Sedimentary Research, 44(1), 242-248.

Dearing, J., 1994. Environmental magnetic susceptibility: Using the Bartington MS2 System. Chi Publishing, Kenilworth.

Dearing, J.A., Hay, K.L., Baban, S.M.J., Huddleston, A.S., Wellington, E.M.H., Loveland, P.J., 1996. Magnetic susceptibility of soil: an evaluation of conflicting theories using a national data set. Geophysical Journal International, 127(3), 728-734.

Delano-Smith, C., 1981. Consequences of climatic change. Dept. of Geography, Nottingham England.

Delgado, J., Barba-Brioso, C., Nieto, J.M., Boski, T., 2011. Speciation and ecological risk of toxic elements in estuarine sediments affected by multiple anthropogenic contributions (Guadiana saltmarshes, SW Iberian Peninsula): I. Surficial sediments. Science of The Total Environment, 409(19), 3666-3679.

Delgado, J., Boski, T., Nieto, J.M., Pereira, L., Moura, D., Gomes, A., Sousa, C., García-Tenorio, R., 2012a. Sea-level rise and anthropogenic activities recorded in the late Pleistocene/Holocene sedimentary infill of the Guadiana Estuary (SW Iberia). Quaternary Science Reviews, 33(0), 121-141.

Delgado, J., Nieto, J.M., Boski, T., 2010. Analysis of the spatial variation of heavy metals in the Guadiana Estuary sediments (SW Iberian Peninsula) based on GIS-mapping techniques. Estuarine, Coastal and Shelf Science, 88(1), 71-83.

Delgado, J., Pérez-López, R., Galván, L., Nieto, J.M., Boski, T., 2012b. Enrichment of rare earth elements as environmental tracers of contamination by acid mine drainage in salt marshes: A new perspective. Marine Pollution Bulletin, 64(9), 1799-1808.

Derbyshire, E., Gregory, K.J., Hails, J.R., 1979. Geomorphological Processes. Studies in Physical Geography. Westview Press, Inc., Boulder, Colorado.

Dias, J.A., Taborda, R., 1992. Tidal Gauge Data in Deducing Secular Trends of Relative Sea Level and Crustal Movements in Portugal. Journal of Coastal Research, 8(3), 655-659.

Dias, J.M.A., Boski, T., Rodrigues, A., Magalhães, F., 2000. Coast line evolution in Portugal since the Last Glacial Maximum until present — a synthesis. Marine Geology, 170(1–2), 177-186.

Dias, J.M.A., Gonalez, R., Ferreira, O., 2004. Natural versus anthropic causes in variations of sand export from river basins: An example from the Guadiana River Mouth (Southwestern Iberia). Polish Geological Institute Special Papers, 11, 95-102.

Dinis, J.L., Henriques, V., Freitas, M.C., Andrade, C., Costa, P., 2006. Natural to anthropogenic forcing in the Holocene evolution of three coastal lagoons (Caldas da Rainha valley, western Portugal). Quaternary International, 150(1), 41-51.

Dunne, T., Zhang, W., Aubry, B.F., 1991. Effects of Rainfall, Vegetation, and Microtopography on Infiltration and Runoff. Water Resources Research, 27(9), 2271-2285.

Einsele, G., 1992. Sedimentary Basins. Springer, Berlin.

Engel, M., Brückner, H., Wennrich, V., Scheffers, A., Kelletat, D., Vött, A., Schäbitz, F., Daut, G., Willershäuser, T., May, S.M., 2010. Coastal stratigraphies of eastern Bonaire (Netherlands Antilles): New insights into the palaeo-tsunami history of the southern Caribbean. Sedimentary Geology, 231(1–2), 14-30.

Ernst, W., 1970. Geochemical facies analysis. Methods in geochemistry and geophysics. Elsevier, Amsterdam.

Evans, M.E., Heller, F., 2003. Environmental Magnetism. In: E.E. Michael, H. Friedrich (Eds.), International Geophysics. Academic Press, pp. xi-xii.

Fernandez-Salas, L.M., Rey, J., Perez-Vazquez, E., Ramirez, J.L., Hernandez-Molina, F.J., Somoza, L., De Andres, J.R., Lobo, F.J., 1999. Morphology and characterisation of the relict facies on the internal continental shelf in the Gulf of Cadiz, between Ayamonte and Huelva (southern Iberian Peninsula). Boletin - Instituto Espanol de Oceanografia, 15(1-4), 123-132.

Finkler, C., Baika, K., Rigakou, D., Metallinou, G., Fischer, P., Hadler, H., Emde, K., Vött, A., 2017. Geoarchaeological investigations of a prominent quay wall in ancient Corcyra – Implications for harbour development, palaeoenvironmental changes and tectonic geomorphology of Corfu Island (Ionian Islands, Greece). Quaternary International.

Fletcher, W.J., 2005. Holocene Landscape History of Southern Portugal, University of Cambridge, 327 pp.

Fletcher, W.J., Boski, T., Moura, D., 2007. Palynological evidence for environmental and climatic change in the lower Guadiana valley, Portugal, during the last 13 000 years. The Holocene, 17(4), 481-494.

Frahm, E., 2018. Ceramic studies using portable XRF: From experimental tempered ceramics to imports and imitations at Tell Mozan, Syria. Journal of Archaeological Science, Volume 90, Pages 12-38.

Frankenstein, S., 1979. The Phoenicians in the far west: a function of Neo-Assyrian imperialism. In: M.T. Larsen (Ed.), Power and propaganda: a symposium on ancient empires. Akademisk Forlag, Copenhagen, pp. 263-294.

Freitas, M.C., Andrade, C., Cruces, A., 2002. The geological record of environmental changes in southwestern Portuguese coastal lagoons since the Lateglacial. Quaternary International, 93–94(0), 161-170.

Freitas, R.P., Coelho, F.A., Felix, V.S., Pereira, M.O., Souza, M.A.T., Anjos M.J., 2018. Analysis of 19th century ceramic fragments excavated from Pirenópolis (Goiás, Brazil) using FT-IR, Raman, XRF and SEM. Spectrochimica Acta Part A: Molecular and Biomolecular Spectroscopy, Volume 193, Pages 432-439.

French, C., 2003. Geoarchaeology in Action. Routledge.

Galán, E., Gómez-Ariza, J.L., González, I., Fernández-Caliani, J.C., Morales, E., Giráldez, I., 2003. Heavy metal partitioning in river sediments severely polluted by acid mine drainage in the Iberian Pyrite Belt. Applied Geochemistry, 18(3), 409-421.

García-Alix, A., Jimenez-Espejo, F.J., Lozano, J.A., Jiménez-Moreno, G., Martinez-Ruiz, F., García Sanjuán, L., Aranda Jiménez, G., García Alfonso, E., Ruiz-Puertas, G., Anderson, R.S., 2013. Anthropogenic impact and lead pollution throughout the Holocene in Southern Iberia. Science of The Total Environment, 449, 451-460.

García-Ruiz, J.M., 2010. The effects of land uses on soil erosion in Spain: A review. CATENA, 81(1), 1-11.

García-Ruiz, J.M., Nadal-Romero, E., Lana-Renault, N., Beguería, S., 2013. Erosion in Mediterranean landscapes: Changes and future challenges. Geomorphology, 198, 20-36.

Garel, E., Pinto, L., Santos, A., Ferreira, Ó., 2009. Tidal and river discharge forcing upon water and sediment circulation at a rock-bound estuary (Guadiana estuary, Portugal). Estuarine, Coastal and Shelf Science, 84(2), 269-281.

Garel, E., Sousa, C., Ferreira, Ó., Morales, J.A., 2014. Decadal morphological response of an ebb-tidal delta and down-drift beach to artificial breaching and inlet stabilisation. Geomorphology, 216(0), 13-25.

Goiran, J.-P., Salomon, F., Mazzini, I., Bravard, J.-P., Pleuger, E., Vittori, C., Boetto, G., Christiansen, J., Arnaud, P., Pellegrino, A., Pepe, C., Sadori, L., 2014. Geoarchaeology confirms location of the ancient harbour basin of Ostia (Italy). Journal of Archaeological Science, 41(0), 389-398.

Gómez-Villar, A., Álvarez-Martínez, J., García-Ruiz, J.M., 2006. Factors influencing the presence or absence of tributary-junction fans in the Iberian Range, Spain. Geomorphology 81, 252–264.

González de Canales, F., Serrano, L., Lommpart, J., 2004. El Emporio Fenicio-Precolonial de Huelva, (ca. 900-770 a.C.). Biblioteca Nueva, Madrid.

González, R., Araújo, M.F., Burdloff, D., Cachão, M., Cascalho, J., Corredeira, C., Dias, J.M.A., Fradique, C., Ferreira, J., Gomes, C., Machado, A., Mendes, I., Rocha, F., 2007. Sediment and pollutant transport in the Northern Gulf of Cadiz: A multi-proxy approach. Journal of Marine Systems, 68(1–2), 1-23.

González, R., Dias, J.A., Ferreira, Ó., 2001. Recent Rapid Evolution of the Guadiana Estuary Mouth (Southwestern Iberian Peninsula). Journal of Coastal Research, 516-527.

González, R., Dias, J.M.A., Lobo, F., Mendes, I., 2004. Sedimentological and paleoenvironmental characterisation of transgressive sediments on the Guadiana Shelf (Northern Gulf of Cadiz, SW Iberia). Quaternary International, 120(1), 133-144.

Goudie, A., 1983. Chemical sediments and geomorphology: precipitates and residua in the near-surface environment. Acad. Press, London.

Goudie, A., 2001. Encyclopedia of global change: environmental change and human society. Oxford Univ. Press, Oxford.

Goy, J., Zazo, C., Dabrio, C.J., Lario, J., Borja, F., Sierro, F.J., Flores, J., 1996. Global and regional factors controlling changes of coastlines in Southern Iberia (Spain) during the holocene. Quaternary Science Reviews, 15(8–9), 773-780.

Gras, M., 1995. L'univers phénicien. Hachette Littératures, Paris.

Grootes, P.M., Nadeau, M.J., Schleicher, M., 1998. Soil Organic Matter. Mitteilungen der Deutschen Bodenkundlichen Gesellschaft, 87, 191-198.

Grove, A.T., 2001. The “Little Ice Age” and Its Geomorphological Consequences in Mediterranean Europe. In: A.J. Ogilvie, T. Jónsson (Eds.), The Iceberg in the Mist: Northern Research in pursuit of a “Little Ice Age”. Springer Netherlands, pp. 121-136.

Grove, A.T., Rackham, O., 2003. The Nature of Mediterranean Europe. An Ecological History. Yake University Press, New Haven.

Grove, J.M., 1988. The Little Ice Age. Methuen, London.

Gupta, H.K., 2013. Three Great Tsunamis: Lisbon (1755), Sumatra-Andaman (2004) and Japan (2011). SpringerBriefs in Earth Sciences.

Hadler, H., 2013. Ancient Greek harbours used as geo-archives for palaeotsunami research - Case studies from Krane (Cefalonia), Lechaion (Gulf of Corinth) and Kyllini (Peloponnese). Dr. rer. nat. (PhD), Johannes Gutenberg University, Mainz.

Hadler, H., 2014. Ancient Greek harbours used as geo-archives for palaeotsunami research : case studies from Krane (Cefalonia), Lechaion (Gulf of Corinth) and Kyllini (Peloponnese), Johannes Gutenberg-Universität, Dissertationsschrift, Mainz.

Haese, R., 2000. The Reactivity of Iron. In: H. Schulz, M. Zabel (Eds.), Marine Geochemistry. Springer Berlin Heidelberg, pp. 233-261.

Hemelryck, H.v., Fiener, P., Oost, K.v., Govers, G., Merckx, R., 2009. The effect of soil redistribution on soil organic carbon: an experimental study. Biogeosciences, 7, 3971-3986.

Hesnard, A., 1995. Les ports antiques de Marseille, Place Jules-Verne. Journal of Roman Archaeology, 8, 65-77.

Hindson, R., Andrade, C., Parish, R., 1998. A microfaunal and sedimentary record of environmental change within the late Holocene sediments of Boca do Rio (Algarve, Portugal). Geologie en Mijnbouw, 77(3-4), 311-321.

Hoelzmann, P., Klein, T., Kutz, F., Schütt, B., 2016. A new device to mount portable energy dispersive X-ray fluorescence spectrometers (p-ED-XRF) for semi-continuous analyses of split (sediment) cores and solid samples. Geosci. Instrum. Method. Data Syst. Discuss., 2016, 1-12.

Hoffmann, G., Schulz, H.D., 1987. Holocene stratigraphy and changing coastlines at the mediterranean coast of Andalucia (SE-Spain). Trabajos sobre Neogeno-Cuaternario, 10, 153-159.

Hoffmann, G., Schulz, H.D., 1988. Coastline shifts and holocene stratigraphy of the mediterranean coast of Andalucia (SE-Spain). Cities on the sea. , Proceedings BAR Intern., Haifa, pp. 53-70.

Hong, S., Candelone, J.-P., Patterson, C.C., Boutron, C.F., 1994. Greenland Ice Evidence of Hemispheric Lead Pollution Two Millennia Ago by Greek and Roman Civilizations. Science, 265(5180), 1841-1843.

Horden, P., Purcell, N., 2000. The Corrupting Sea: A Study of Mediterranean History. Oxford: Blackwell.

Hou, X., Jones, B.T., 2006. Inductively Coupled Plasma-Optical Emission Spectrometry, Encyclopedia of Analytical Chemistry. John Wiley & Sons, Ltd.

Hunt, C.P., Moskowitz, B.M., Banerjee, S.K., 2013. Magnetic Properties of Rocks and Minerals, Rock Physics & Phase Relations. American Geophysical Union, pp. 189-204.

Hunt Ortiz, M.A., 2003. Prehistoric mining and metallurgy in South West Iberian Peninsula, British archaeological reports : International series 1188. Archaeopress, Oxford.

Hupp, B.N., Donovan, J.J., 2018. Quantitative mineralogy for facies definition in the Marcellus Shale (Appalachian Basin, USA) using XRD-XRF integration. Sedimentary Geology Volume 371, Pages 16-31.

Hürkamp, K., Raab, T., Völkel, J., 2009. Two and three-dimensional quantification of lead contamination in alluvial soils of a historic mining area using field portable X-ray fluorescence (FPXRF) analysis. Geomorphology, 110(1–2), 28-36.

IGME, 1983. Mapa Geologico de España, 998,Ayamonte, 8-41.

IGME, 2017. Servicios de mapas del IGME.

Ißelhorst, S., 2014. A GIS Based Analysis of Historical Maps for the Reconstruction of the Shoreline Development of the Guadiana Estuary, SW Iberian Peninsula (Spain and Portugal). M.Sc., Freie Universität Berlin, Berlin, 77 pp.

Jalut, G., Esteban Amat, A., Bonnet, L., Gauquelin, T., Fontugne, M., 2000. Holocene climatic changes in the Western Mediterranean, from south-east France to south-east Spain. Palaeogeography, Palaeoclimatology, Palaeoecology, 160(3–4), 255-290.

Junta de Andalucia, 2017. Los servicios de mapas en web.

Jurado, J.F., G., S.C., Tomico, P.R., 1997. De Tartessos a Onuba: 15 años de arqueología en Huelva. Diputación de Huelva. Sección de Arqueología.

Kaiser, K., Schoch, W.H., Miehe, G., 2007. Holocene paleosols and colluvial sediments in Northeast Tibet (Qinghai Province, China): Properties, dating and paleoenvironmental implications. CATENA, 69(2), 91-102.

Klein, T., Bebermeier, W., Krause, J., Marzoli, D., Schütt, B., 2016. Sedimentological evidence of an assumed ancient anchorage in the hinterland of a Phoenician settlement (Guadiana estuary/SW-Spain). Quaternary International, 407, Part A, 110-125.

Klein, T., Bebermeier, W., Krause, J., Schütt, B., Marzoli, D., in review. Human-environment interactions at the Phoenician site of Ayamonte (Huelva/Spain): – Findings from terrestrial borehole data. Zeitschrift für Geomorphologie.

Knödel, K., Krummel, H., Lange, G., 2005. Geophysik, Heidelberg.

Koch, M., 2001. Denkmäler der Frühzeit. Hispania Antigua. Philipp von Zabern, Mainz.

Köppen, W., Geiger, G., 1930-1939. Handbuch der Klimatologie. Gebrüder Borntraeger, Berlin.

Kraft, J.C., Bückner, H., Kayan, I., Engelmann, H., 2007. The geographies of ancient ephesus and the Artemision in Anatolia. Geoarchaeology, 22(1), 121-149.

Kuhn, N.J., van Oost, K., Cammeraat, E., 2012. Soil erosion, sedimentation and the carbon cycle. CATENA, 94, 1-2.

Kujau, A., Nürnberg, D., Zielhofer, C., Bahr, A., Röhl, U., 2010. Mississippi River discharge over the last ~560,000 years — Indications from X-ray fluorescence core-scanning. Palaeogeography, Palaeoclimatology, Palaeoecology 298 (2010) 311–318.

Kunst, M., 1988. Zur Besiedlungsgeschichte des Guadiana-Mündungsgebietes - Ergebnisse aus der Küstenforschung. German Archaeological Institute, pp. 1-62.

Kunst, M., 2001. Das Neolithikum der Iberischen Halbinsel. In: D.A.I. (Madrid) (Ed.), Hispania Antiqua - Denkmäler der Frühzeit. von Zabern, Mainz, pp. 37-66.

Lal, R., 2005. Soil erosion and carbon dynamics. Soil and Tillage Research, 81(2), 137-142.

Lang, A., Hönscheidt, S., 1999. Age and source of colluvial sediments at Vaihingen-Enz, Germany. Catena, 38(2), 89-107.

Lario, J., Luque, L., Zazo, C., Goy, J.L., Spencer, C., Cabero, A., Bardají, T., Borja, F., Dabrio, C.J., Civis, J., González-Delgado, J.Á., Borja, C., Alonso-Azcárate, J., 2010. Tsunami vs. storm surge deposits: a review of the sedimentological and geomorphological records of extreme wave events (EWE) during the Holocene in the Gulf of Cadiz, Spain. Zeitschrift für Geomorphologie, Supplementary Issues, 54(3), 301-316.

Lario, J., Zazo, C., Dabrio, C.J., Somoza, L., Goy, J.L., Bardají, T., Silva, P.G., 1995. Record of Recent Holocene Sediment Input on Spit Bars and Deltas of South Spain. Journal of Coastal Research, 241-245.

Lario, J., Zazo, C., Goy, J.L., Dabrio, C.J., Borja, F., Silva, P.G., Sierro, F., González, A., Soler, V., Yll, E., 2002. Changes in sedimentation trends in SW Iberia Holocene estuaries (Spain). Quaternary International, 93–94(0), 171-176.

Lario, J., Zazo, C., Goy, J.L., Silva, P.G., Bardaji, T., Cabero, A., Dabrio, C.J., 2011. Holocene palaeotsunami catalogue of SW Iberia. Quaternary International, 242(1), 196-200.

Le Borgne, E., 1955. Abnormal magnetic susceptibility of the topsoil. Ann. Geophys., 11, 399-419.

Leblanc, M., Morales, J.A., Borrego, J., Elbaz-Poulichet, F., 2000. 4,500-year-old mining pollution in southwestern Spain: Long-term implications for modern mining pollution. Economic Geology, 95(3), 655-662.

Leco, 2011. TruSpecCHN/CHNS Carbon/Hydrogen/Nitrogen/Sulfur Determinators – Instruction Manual, USA.

Leopold, M., Völkel, J., 2007. Colluvium: Definition, differentiation, and possible suitability for reconstructing Holocene climate data. Quaternary International, 162–163, 133-140.

Lerman, A., 1979. Geochemical Processes - Water and Sediment Environments. John Wiley & Sons, New York.

Leser, H., Stäblein, G., 1980. Legende der Geomorphologischen Karte 1:25 000 (GMK). 3. Fassung im GMK-Schwerpunktprogramm. In: D. Barsch, H. Liedtke (Eds.), Methoden und Anwendbarkeit geomorphologischer Detailkarten. Berliner Geographische Abhandlungen, pp. 91-100.

Lobo, F., Hernández-Molina, F., Somoza, L., Díaz del Río, V., Dias, J., 2002. Stratigraphic evidence of an upper Pleistocene TST to HST complex on the Gulf of Cádiz continental shelf (south-west Iberian Peninsula). Geo-Marine Letters, 22(2), 95-107.

Lobo, F.J., Dias, J.M.A., González, R., Hernández-Molina, F.J., Morales, J.A., Díaz del Río, V., 2003. High-resolution seismic stratigraphy of a narrow, bedrock-controlled estuary: The Guadiana estuarine system, SW Iberia. Journal of Sedimentary Research, 73(6), 973-986.

Lobo, F.J., Fernández-Salas, L.M., Hernández-Molina, F.J., González, R., Dias, J.M.A., Díaz Del Río, V., Somoza, L., 2005. Holocene highstand deposits in the Gulf of Cadiz, SW Iberian Peninsula: A high-resolution record of hierarchical environmental changes. Marine Geology, 219(2-3), 109-131.

Loureiro, J.M., 1983. Monografia Hidrológica do Algarve, Universidade do Algarve, Faro.

Lynch, J., 1990. Provisional Elemental values for eight new geochemical lake sediment and stream sediment reference materials LKSD- 1, LKSD-2, LKSD-3, LKSD-4, STSD-1, STSD-2, STSD-3 and STSD-4. Geostandard Newsletter, 14, 153-167.

Magiera, T., Strzyszcz, Z., Kapicka, A., Petrovsky, E., 2006. Discrimination of lithogenic and anthropogenic influences on topsoil magnetic susceptibility in Central Europe. Geoderma, 130(3–4), 299-311.

Maher, B.A., 1986. Characterisation of soils by mineral magnetic measurements. Physics of the Earth and Planetary Interiors, 42(1–2), 76-92.

Marriner, N., Morhange, C., 2005. Under the city centre, the ancient harbour. Tyre and Sidon: heritages to preserve. Journal of Cultural Heritage, 6(2), 183-189.

Marriner, N., Morhange, C., 2006. Geoarchaeological evidence for dredging in Tyre's ancient harbour, Levant. Quaternary Research, 65(1), 164-171.

Marriner, N., Morhange, C., Boudagher-Fadel, M., Bourcier, M., Carbonel, P., 2005. Geoarchaeology of Tyre's ancient northern harbour, Phoenicia. Journal of Archaeological Science, 32(9), 1302-1327.

Marriner, N., Morhange, C., Doumet-Serhal, C., 2006. Geoarchaeology of Sidon's ancient harbours, Phoenicia. Journal of Archaeological Science, 33(11), 1514-1535.

Marriner, N., Morhange, C., Kaniewski, D., Carayon, N., 2014. Ancient harbour infrastructure in the Levant: tracking the birth and rise of new forms of anthropogenic pressure. Sci. Rep., 4.

Martín-Puertas, C., Valero-Garcés, B.L., Pilar Mata, M., González-Sampériz, P., Bao, R., Moreno, A., Stefanova, V., 2008. Arid and humid phases in southern Spain during the last 4000 years: the Zoñar Lake record, Córdoba. The Holocene, 18(6), 907-921.

Matin Hernández, C., 2013. Phoencian trade of raw materials and changes in metal production patterns in SW Iberia during the orientalizing period. Metalla, 20(2), 17-24.

Megía, M.V., Muñoz, A.P., 2006. Geodiversidad y patrimonio geológico de Andalucía - Itinerario geológico por Andalucía. Junta de Andalucía.

Ménanteau, L., 2005. Les marais du Bas-Guadiana (Algarve, Andalousie): emprise, déprise et reprise humaines. 1er colloque international du Groupe d'Histoire des Zones Humides. 1-17.

Mendes, I., Gonzalez, R., Dias, J.M.A., Lobo, F., Martins, V., 2004. Factors influencing recent benthic foraminifera distribution on the Guadiana shelf (Southwestern Iberia). Marine Micropaleontology, 51(1–2), 171-192.

Mendes, I., Rosa, F., Dias, J.A., Schönfeld, J., Ferreira, Ó., Pinheiro, J., 2010. Inner shelf paleoenvironmental evolution as a function of land–ocean interactions in the vicinity of the Guadiana River, SW Iberia. Quaternary International, 221(1–2), 58-67.

Meyers, P.A., 1997. Organic geochemical proxies of paleoceanographic, paleolimnologic, and paleoclimatic processes. Organic Geochemistry, 27(5–6), 213-250.

Miall, A.D., 2006. The Geology of Fluvial Deposits. Springer, Berlin.

Michael, D., 2007. Soil Carbonates and Soil Water, Encyclopedia of Soil Science, Second Edition. Taylor & Francis, pp. 1-4.

Moore, L.J., 2000. Shoreline Mapping Techniques. Journal of Coastal Research, 16(1), 111-124.

Morales, J.A., 1997. Evolution and facies architecture of the mesotidal Guadiana River delta (S.W. Spain-Portugal). Marine Geology, 138(1–2), 127-148.

Morales, J.A., Borrego, J., Jiménez, I., Monterde, J., Gil, N., 2001. Morphostratigraphy of an ebb-tidal delta system associated with a large spit in the Piedras Estuary mouth (Huelva Coast, Southwestern Spain). Marine Geology, 172(3–4), 225-241.

Morales, J.A., Borrego, J., San Miguel, E.G., López-González, N., Carro, B., 2008. Sedimentary record of recent tsunamis in the Huelva Estuary (southwestern Spain). Quaternary Science Reviews, 27(7–8), 734-746.

Morales, J.A., Delgado, I., Gutierrez-Mas, J.M., 2006. Sedimentary characterization of bed types along the Guadiana estuary (SW Europe) before the construction of the Alqueva dam. Estuarine, Coastal and Shelf Science, 70(1–2), 117-131.

Moreira, S., Costa, P.J.M., Andrade, C., Ponte Lira, C., Freitas, M.C., Oliveira, M.A., Reichart, G.-J., 2017. High resolution geochemical and grain-size analysis of the AD 1755 tsunami deposit: Insights into the inland extent and inundation phases. Marine Geology, 390(Supplement C), 94-105.

Morral, F.M., 1990. A mini-history of Rio Tinto. Canadian Mining and Metallurgical Bulletin, 83, 150-154.

Moscati, S., 2001. The Phoenicians. I.B.Tauris, London.

Mulhy, J.D., 1998. Mediterranean Peoples in Transition: Thirteenth to Early Tenth Centuries BCE. Israel Exploration Society, Jerusalem.

Mullins, C.E., 1977. Magnetic susceptibility of the soil and its significance in soil science – A review. Journal of Soil Science, 28(2), 223-246.

National Research Council US Geodynamics Committee, 1980. Lead in the human environment: a report. Nat. Acad. of Sciences, Washington, DC.

Niemeyer, H.G., 1982. Phönizier im Westen, Madrider Beiträge.

Niller, H.-P., 1998. Prähistorische Landschaften im Lößgebiet bei Regensburg.

Kolluvien, Auenlehme und Böden als Archive der Paläoumwelt. PhD, Regensburg.

Nocete, F., Álex, E., Nieto, J.M., Sáez, R., Bayona, M.R., 2005. An archaeological approach to regional environmental pollution in the south-western Iberian Peninsula related to Third millennium BC mining and metallurgy. Journal of Archaeological Science, 32(10), 1566-1576.

Nocete, F., Sáez, R., Bayona, M.R., Peramo, A., Inacio, N., Abril, D., 2011. Direct chronometry (14C AMS) of the earliest copper metallurgy in the Guadalquivir Basin (Spain) during the Third millennium BC: first regional database. Journal of Archaeological Science, 38(12), 3278-3295.

Noureddine, I., 2010. New Light on the Phoenician Harbor at Tyre. Near Eastern Archaeology, 73(2-3), 176-181.

Nriagu, J.O., 1983a. Lead and lead poisoning in antiquity. Environmental science and technology. Wiley, New York.

Nriagu, J.O., 1983b. Occupational exposure to lead in ancient times. Science of The Total Environment, 31(2), 105-116.

Oldfield, F., 2007. Sources of fine-grained magnetic minerals in sediments: A problem revisited. Holocene, 17(8), 1265-1271.

Ortega, J.A., Garzón, G., 2003. Palaeohydrology of the lower Guadiana River Basin, Palaeofloods, historical data and climatic variability: applications in flood risk assessment. Thorndycraft, V.R., Benito, G., Barriendos, M. Llasat, M.C., Madrid, pp. 33-38.

Ortega, J.A., Garzón, G., 2009. A contribution to improved flood magnitude estimation in base of palaeoflood record and climatic implications – Guadiana River (Iberian Peninsula). Natural Hazards Earth System Sciences, 9, 229-239.

Oster, E.A., Ruscavage-Barz, S., Elliott, M.L., 2012. The Effects of Fire on Subsurface Archaeological Materials. In: K.C.J. Ryan, Ann Trinkle; Koerner, Cassandra L.; Lee, Kristine M. (Ed.), Wildland fire in ecosystems: effects of fire on cultural resources and archaeology. U.S. Department of Agriculture, Forest Service, Fort Collins, pp. 143-156.

Pandarinath, K., Shankar, R., Torres-Alvarado, I.S., Warrier, A.K., 2014. Magnetic susceptibility of volcanic rocks in geothermal areas: application potential in geothermal exploration studies for identification of rocks and zones of hydrothermal alteration. Arabian Journal of Geosciences, 7(7), 2851-2860.

Patrice, P., 1995. Les épaves grecques et romaines de la place Jules-Verne à Marseille. Comptes rendus des séances de l'Académie des Inscriptions et Belles-Lettres, 459-484.

Pella, P.A., 1989. X-ray fluorescence spectrometry by Ron Jenkins Published by John Wiley & Sons, New York, 1988; ISBN 0-471-83675-3. X-Ray Spectrometry, 18(4), 187-187.

Pérez Macías, J.A., 1996. Metalurgia extractiva prerromana en Huelva, Huelva.

Perillo, G.M.E., 1995a. Definitions and geomorphological classification of estuaries. In: G.M.E. Perillo (Ed.), Geomorphology and sedimentology of estuaries. Developments in sedimentology. Elsevier, Amsterdam, pp. 17-46.

Perillo, G.M.E. (Ed.), 1995b. Geomorphology and Sedimentology of Estuaries. Developments in Sedimentology. Elsevier.

Pires, H.O., 1998. Project INDIA. Preliminary Report on Wave Climate at Faro, Instituto de Meteorologia technical report, Lisbon.

Polyakov, V.O., Lal, R., 2004. Soil erosion and carbon dynamics under simulated rainfall. Soil Science, 169(8), 590-599.

Portela, L.I., 2006. Calculation of Sediment Delivery from the Guadiana Estuary to the Coastal. Journal of Coastal Research, 1819-1823.

Pozo, M., Ruiz, F., Carretero, M.I., Vidal, J.R., Cáceres, L.M., Abad, M., González-Regalado, M.L., 2010. Mineralogical assemblages, geochemistry and fossil associations of Pleistocene–Holocene complex siliciclastic deposits from the Southwestern Doñana National Park (SW Spain): A palaeoenvironmental approach. Sedimentary Geology, 225(1–2), 1-18.

Quinton, J.N., Catt, J.A., Wood, G.A., Steer, J., 2006. Soil carbon losses by water erosion: Experimentation and modeling at field and national scales in the UK. Agriculture, Ecosystems & Environment, 112(1), 87-102.

Rachwał, M., Kardel, K., Magiera, T., Bens, O., 2017. Application of magnetic susceptibility in assessment of heavy metal contamination of Saxonian soil (Germany) caused by industrial dust deposition. Geoderma, 295(Supplement C), 10-21.

Ramsey, C.B., 2009. Bayesian Analysis of Radiocarbon Dates. 2009.

Ramsey, M.H., Potts, P.J., Webb, P.C., Watkins, P., Watson, J.S., Coles, B.J., 1995. An objective assessment of analytical method precision: comparison of ICP-AES and XRF for the analysis of silicate rocks. Chemical Geology, 124(1), 1-19.

Reicherter, K., Vonberg, D., Koster, B., Fernández-Steeger, T., Grützner, C., Mathes-Schmidt, M., 2010. The sedimentary inventory of tsunamis along the southern Gulf of Cádiz (southwestern Spain). Zeitschrift für Geomorphologie, Supplementary Issues, 54(3), 147-173.

Reimer, P.J., Baillie, M.G.L., Bard, E., Bayliss, A., Beck, J.W., Blackwell, P.G., Ramsey, C.B., Buck, C.E., Burr, G.S., Edwards, R.L., Friedrich, M., Grootes, P.M., Guilderson, T.P., Hajdas, I., Heaton, T.J., Hogg, A.G., Hughen, K.A., Kaiser, K.F., Kromer, B., McCormac, F.G., Manning, S.W., Reimer, R.W., Richards, D.A., Southon, J.R., Talamo, S., Turney, C.S.M., van der Plicht, J., Weyhenmeyer, C.E., 2009. IntCal09 and Marine09 radiocarbon age calibration curves, 0-50,000 years CAL BP. Radiocarbon, 51(4), 1111-1150.

Reimer, P.J., Bard, E., Bayliss, A., Beck, J.W., Blackwell, P.G., Bronk Ramsey, C., Buck, C.E., Cheng, H., Edwards, R.L., Friedrich, M., Grootes, P.M., Guilderson, T.P., Haflidason, H., Hajdas, I., Hatté, C., Heaton, T.J., Hoffmann, D.L., Hogg, A.G., Hughen, K.A., Kaiser, K.F., Kromer, B., Manning, S.W., Niu, M., Reimer, R.W., Richards, D.A., Scott, E.M., Southon, J.R., Staff, R.A., Turney, C.S.M., van der Plicht, J., 2013. IntCal13 and Marine13 Radiocarbon Age Calibration Curves 0-50,000 Years Cal BP. Radiocarbon, 55(4), 1869-1887.

Reineck, H.-E., Singh, I.B., 1986. Depositional sedimentary environments: with reference to terrigenous clastics. Springer study edition. Springer, Berlin.

Retallack, G.J., 2001. Soils of the past: an introduction to paleopedology. Blackwell Science, Oxford.

Rheinheimer, G., 1974. Aquatic Microbiology. John Wiley & Sons, New York.

Rhoades, J.D., 1999. Soil salinity assessment - Methods and interpretation of eleictral conductivity measurements. FAO, Rome.

Ríos, J.M., 1983. Geología de España. Instituto Geológico y Minero de España.

Rivas-Martínez, S., Lousã, M., Díaz González, T.E., Fernández-González, F., Costa, J.C., 1990. La vegetación del sur de Portugal (Sado, Alentejo y Algarve). Iternera Geobotanica, 3, 5-126.

Rodríguez-Ramírez, A., Flores-Hurtado, E., Contreras, C., Villarías-Robles, J.J.R., Jiménez-Moreno, G., Pérez-Asensio, J.N., López-Sáez, J.A., Celestino-Pérez, S., Cerrillo-Cuenca, E., León, Á., 2014a. The role of neo-tectonics in the sedimentary infilling and geomorphological evolution of the Guadalquivir estuary (Gulf of Cadiz, SW Spain) during the Holocene. Geomorphology, 219(0), 126-140.

Rodríguez-Ramírez, A., Pérez-Asensio, J.N., Santos, A., Jiménez-Moreno, G., Villarías-Robles, J.J.R., Mayoral, E., Celestino-Pérez, S., Cerrillo-Cuenca, E., López-Sáez, J.A., León, Á., Contreras, C., 2014b. Atlantic extreme wave events during the last four millennia in the Guadalquivir estuary, SW Spain. Quaternary Research.

Rodríguez-Ramírez, A., Rodríguez-Vidal, J., Cáceres, L., Clemente, L., Belluomini, G., Manfra, L., Improta, S., de Andrés, J., 1996. Recent coastal evolution of the Doñana National Park (SW Spain). Quaternary Science Reviews, 15(8–9), 803-809.

Rodríguez-Ramírez, A., Ruiz, F., Cáceres, L.M., Rodríguez Vidal, J., Pino, R., Muñoz, J.M., 2003. Analysis of the recent storm record in the southwestern Spanish coast: implications for littoral management. Science of The Total Environment, 303(3), 189-201.

Rodríguez-Vidal, J., Ruiz, F., Cáceres, L.M., Abad, M., González-Regalado, M.L., Pozo, M., Carretero, M.I., Monge Soares, A.M., Toscano, F.G., 2011. Geomarkers of the 218–209 BC Atlantic tsunami in the Roman Lacus Ligustinus (SW Spain): A palaeogeographical approach. Quaternary International, 242(1), 201-212.

Rogers, A., 2013. Water and Roman Urbanism. Brill.

Rosa, F., Dias, J.A., Mendes, I., Ferreira, Ó., 2011. Mid to late Holocene constraints for continental shelf mud deposition in association with river input: the Guadiana Mud Patch (SW Iberia). Geo-Marine Letters, 31(2), 109-121.

Rosman, K.J.R., Chisholm, W., Hong, S., Candelone, J.-P., Boutron, C.F., 1997. Lead from Carthaginian and Roman Spanish Mines Isotopically Identified in Greenland Ice Dated from 600 B.C. to 300 A.D. Environmental Science & Technology, 31(12), 3413-3416.

Rossi, V., Sammartino, I., Amorosi, A., Sarti, G., De Luca, S., Lena, A., Morhange, C., 2015. New insights into the palaeoenvironmental evolution of Magdala ancient harbour (Sea of Galilee, Israel) from ostracod assemblages, geochemistry and sedimentology. Journal of Archaeological Science, 54(Supplement C), 356-373.

Roth, D., Beckers, B., Berking, J., Ißelhorst, S., Schütt, B., 2016. A short history of the water and society in the region of Vélez Blanco, East Andalusia. Water History, 8(1), 59-73.

Rothenberg, B., Blanco Freijeiro, A., 1981. Studies in Ancient Mining and Metallurgy in South-West Spain.

Rufo, L., Rodríguez, N., Amils, R., de la Fuente, V., Jiménez-Ballesta, R., 2007. Surface geochemistry of soils associated to the Tinto River (Huelva, Spain). Science of The Total Environment, 378(1–2), 223-227.

Ruiz, F., Abad, M., Vidal, J.R., Cáceres, L.M., Carretero, M.I., Pozo, M., Toscano, F.G., Izquierdo, T., Font, E., 2013. Morpho-Sedimentary Evidence of Holocene Tsunamis in the Southwestern Spanish Estuaries: A Summary, VIII Reunión de Cuaternario Ibérico, La Rinconada, Sevilla, pp. 145-149.

Ruiz, F., Borrego, J., González-Regalado, M.L., López González, N., Carro, B., Abad, M., 2008. Impact of millennial mining activities on sediments and microfauna of the Tinto River estuary (SW Spain). Marine Pollution Bulletin, 56(7), 1258-1264.

Ruiz, F., Borrego, J., López-González, N., Abad, M., González-Regalado, M.L., Carro, B., Pendón, J.G., Rodríguez-Vidal, J., Cáceres, L.M., Prudêncio, M.I., Dias, M.I., 2007. The geological record of a mid-Holocene marine storm in southwestern Spain. Geobios, 40(5), 689-699.

Ruiz, F., Rodríguez-Ramírez, A., Cáceres, L.M., Rodríguez Vidal, J.n., Carretero, M.a.I., Clemente, L., Muñoz, J.M., Yañez, C., Abad, M., 2004. Late Holocene evolution of the southwestern Doñana National Park (Guadalquivir Estuary, SW Spain): a multivariate approach. Palaeogeography, Palaeoclimatology, Palaeoecology, 204(1–2), 47-64.

Sá, R., Bexiga, C., Veiga, P., Vieira, L., Erzini, K., 2006. Feeding ecology and trophic relationships of fish species in the lower Guadiana River Estuary and Castro Marim e Vila Real de Santo António Salt Marsh. Estuarine, Coastal and Shelf Science, 70(1–2), 19-26.

Salkied, L.U., 1987. A Technical History of the Rio Tinto Mines, Some Notes on Exploitation from Pre-Phoenician Times to the 1950's. The Institution of Mining and Metallurgy, London.

Sallares, R., 2002. Malaria and Rome: A History of Malaria in Ancient Italy. Oxford University Press, Oxfrod.

Sampath, D.M.R., 2008. Impact of Shoreline Retreat and Inundation due to Sea Level rise along the Coastline adjacent to the Guadiana Estuary, Portugal/Spain Border. M.Sc., University of Algarve, Faro.

Sampath, D.M.R., Boski, T., Loureiro, C., Sousa, C., 2015. Modelling of estuarine response to sea-level rise during the Holocene: Application to the Guadiana Estuary–SW Iberia. Geomorphology, 232, 47-64.

Sampath, D.M.R., Boski, T., Silva, P.L., Martins, F.A., 2011. Morphological evolution of the Guadiana estuary and intertidal zone in response to projected sea-level rise and sediment supply scenarios. Journal of Quaternary Science, 26(2), 156-170.

Sandars, H., 1905. XVI.—The Linares Bas-Relief and Roman Mining Operations in Baetica. Archaeologia, 59(2), 311-332.

Santos, A., Koshimura, S., Imamura, F., 2009. The 1755 Lisbon Tsunami: Tsunami Source determination and its Validation. Journal of Disaster research, 4(1), 41-52.

Schaetzl, R.J., 1986. Complete soil profile inversion by tree uprooting. Physical Geography, 7(2), 181-189.

Schaetzl, R.J., Anderson, S., 2007. Soils: genesis and geomorphology. Cambridge Univ. Press, Cambridge.

Scharpenseel, H.W., Becker-Heidmann, P., 1992. Twenty-Five years of radiocarbon dating soils: Paradigm of erring and learning. Radiocarbon, 34(3), 541-549.

Schattner, T.G., Zappino, G.O., Pérez Macías, J.A., 2012. Minería y metalurgias antiguas en Munigua. Estado de la cuestión Minería y metalurgia antiguas: visiones y revisiones: homenaje a Claude Domergue.

Scheffer, F., Schachtschabel, P., Blume, H.-P., Thiele, S., 2010. Lehrbuch der Bodenkunde. Spektrum Lehrbuch. Spektrum, Heidelberg.

Schneider, H., Höfer, D., Trog, C., Mäusbacher, R., 2016. Holocene landscape development along the Portuguese Algarve coast – A high resolution palynological approach. Quaternary International, 407, Part A, 47-63.

Schneider, S., 2014. Geoarchaeological Case Studies in the Bakırçay Valley – Paleogeography and Human-environmental Interactions in the Chora of Pergamon in Western Turkey. PhD, Freie Universität Berlin, Berlin.

Schubart, H., 1975. Die Kultur der Bronzezeit im Südwesten der Iberischen Halbinsel. de Gruyter.

Schubart, H., Arteaga, O., Hoffmann, G., Kunst, M., 1988. Investigación geológicaarqueológica sobre la antigua línea de costa en Andalucía. Anuario Arqueológico de Andalucía(2), 185-189.

Schubart, H., Maaß-Lindemann, G., 2004. Hannibal ad portas - Macht und Reichtum Karthagos. Konrad Theiss Stuttgart.

Schubart, H., Schulz, H.D., Arteaga, O., Hoffmann, G., 1989. Investigaciones geologicas y archeologicas sobre la relacion costera de los asentamientos fenicios en la Andalucia Mediterranea. Boletin Asoc. Espanola Am. de la Arqueologia, 27, 61-66.

Schüle, W., 1960. Probleme der Eisenzeit auf der Iberischen Halbinsel. Jahrbuch des Römisch-Germanischen Zentralmuseums Mainz, 7.

Schulz, H.D., 2011. Geoarchäologie an den Küsten von Andalusien. Mitteilungen der Berliner Gesellschaft für Anthropologie, Ethnologie und Urgeschichte, 32, 155-170.

Schütt, B., 1998. Reconstruction of palaeoenvironmental conditions by investigation of Holocene playa sediments in the Ebro Basin, Spain: preliminary results. Geomorphology, 23(2–4), 273-283.

Schütt, B., 2004. The chemistry of playa-lake-sediments as a tool for the reconstruction of Holocene environmental conditions - a case study from the central Ebro basin. In: W. Smykatz-Kloss, P. Felix-Henningsen (Eds.), Paleoecology of Quaternary Drylands. Springer Berlin Heidelberg, Berlin, Heidelberg, pp. 5-30.

Schütt, B., 2006. Rekonstruktion, Abbildung und Modellierung der holozänen Reliefentwicklung der Canada Hermosa, Einzugsgebiet des Rio Guadalentin (SE Iberische Halbinsel). Nova Acta Leopoldina, 83-111.

Schwanghart, W., Bernhardt, A., Stolle, A., Hoelzmann, P., Adhikari, B.R., Andermann, C., Tofelde, S., Merchel, S., Rugel,, G., F., M., and Korup, O., 2016. Repeated catastrophic valley infill following medieval earthquakes in the Nepal Himalaya,. Science, 351, 147-150.

Shackley, M.S., 2011. X-Ray Fluorescence Spectrometry (XRF) in Geoarchaeology. Springer, New York, NY.

Singer, M.J., Verosub, K.L., Fine, P., TenPas, J., 1996. A conceptual model for the enhancement of magnetic susceptibility in soils. Quaternary International, 34–36(0), 243-248.

Siqueira, D.S., Marques, J., Pereira, G.T., Teixeira, D.B., Vasconcelos, V., Carvalho Júnior, O.A., Martins, E.S., 2015. Detailed mapping unit design based on soil–landscape relation and spatial variability of magnetic susceptibility and soil color. CATENA, 135(Supplement C), 149-162.

Smith, J., 1998. An introduction to the magnetic properties of natural matierals. In: Walden J, S.J. Oldfield F (Eds.), Environmental Magnetism: A Practical Guide. Quaternary Research Association, London, pp. 5-25.

Strabo, Geographica, III, 1, 9. The geography of Strabo: in eight volumes. In: H.L. Jones (Ed.), The Loeb classical library. Harvard Univ. Press u.a., Cambridge, Mass.

Strauss, G.K., Madel, J., Alonso, F.F., 1977. Exploration Practice for Strata-Bound Volcanogenic Sulphide Deposits in the Spanish-Portuguese Pyrite Belt: Geology, Geophysics, and Geochemistry. In: D. Klemm, H.-J. Schneider (Eds.), Time- and Strata-Bound Ore Deposits. Springer Berlin Heidelberg, pp. 55-93.

Stucki, B.A.G., U. Schwertmann, 1988. Iron in soils and clay minerals NATO ASI series. Series C, Mathematical and physical sciences ; no. 217. D. Reidel ; Sold and distributed in the U.S.A. and Canada by Kluwer Academic Publishers, Dordrecht ; Boston : Norwell, MA, U.S.A.

Suarez, D., 2002. Inorganic carb. In: R. Lal (Ed.), Encyclopedia of Soil Science. Marcel Dekker, New York, pp. 714-717.

Syvitski, J.P.M., 1991. Principles, methods, and application of particle size analysis. Cambridge Univ. Press, Cambridge.

Teyssandier, E.G., Marzoli, D., 2014. Phönizische Gräber in Ayamonte (Huelva, Spanien). Ein Vorbericht. Deutsches Archäologisches Institut, Madrid.

Thelemann, M., 2016. Human and Environment Interactions in the Environs of Prehistorical Iron Smelting Places in Silesia, Poland, Dissertationsschrift, Freie Universität Berlin.

Landscape Archaeological and Geoarchaeological Investigations in the Context of Early Iron Smelting.

Thorndycraft, V.R., Benito, G., 2006. The Holocene fluvial chronology of Spain: evidence from a newly compiled radiocarbon database. Quaternary Science Reviews, 25(3–4), 223-234.

Tornos, F., 2008. La Geología y Metalogenia de la Faja Pirítica Ibérica. Macla, 10, 13-23.

Tóth, G., Hermann, T., Da Silva, M.R., Montanarella, L., 2016. Heavy metals in agricultural soils of the European Union with implications for food safety. Environment International, 88, 299-309.

Treumann, B., 2009. Colonial Encounters in Ancient Iberia - Phoenician, Greek and Indigenous Relations. In: M. Dietler, C. López-Ruiz (Eds.). The University of Chicago Press, Chicago.

USGS, 2017. USGS Earth Explorer.

Van Geen, A., Adkins, J.F., Boyle, E.A., Nelson, C.H., Palanques, A., 1997. A 120-yr record of widespread contamination from mining of the Iberian pyrite belt. Geology, 25(4), 291-294.

Van Wagoner, J.C., Posamentier, H.W., Mitchum, R.M., Vail, P.R., Sarg, J.F., Loutit, T.S., J. Hardenbol, 1988. An overview of the fundamentals of sequence stratigraphy and key definitions. In: C.K. Wilgus, B.S. Hastings, C.G.S.C. Kendall, H.W. Posamentier, C.A. Ross, J.C.V. Wagoner (Eds.), Sea-level changes: an integrated approach. Society of Economic Paleontologists and Mineralogists Special Publication, pp. 39-45.

Vera, J.A., España, S.G.d., España, I.G.y.M.d., 2004. Geología de España. Sociedad Geológica de España.

Vidal, J.R., Cáceres, L.M., Ramirez, A.R., 1993. Modelo evolutivo da rede fluvial Cuaternaria en el suroeste de la peninsula Iberica, Actas 3a Reunia˜o do Quaternário Ibérico. Universidade de Coimbra, Coimbra, pp. 93-96.

Vis, G.-J., Kasse, C., Kroon, D., Vandenberghe, J., Jung, S., Lebreiro, S.M., Rodrigues, T., 2016. Time-integrated 3D approach of late Quaternary sediment-depocenter migration in the Tagus depositional system: From river valley to abyssal plain. Earth-Science Reviews, 153, 192-211.

Vis, G.-J., Kasse, C., Vandenberghe, J., 2008. Late Pleistocene and Holocene palaeogeography of the Lower Tagus Valley (Portugal): effects of relative sea level, valley morphology and sediment supply. Quaternary Science Reviews, 27(17–18), 1682-1709.

Vita-Finzi, C., 1969. The Mediterranean valleys: geological changes in historical times. Cambridge Univ. Press, London.

Vött, A., Bareth, G., Brückner, H., 2011a. Olympia`s Harbour Site Pheia (Elis, Western Peloponnese, Greece) Destroyed by Tsunami Impact. Erde, 142(3), 259-288.

Vött, A., Lang, F., Brückner, H., Gaki-Papanastassiou, K., Maroukian, H., Papanastassiou, D., Giannikos, A., Hadler, H., Handl, M., Ntageretzis, K., Willershäuser, T., Zander, A., 2011b. Sedimentological and geoarchaeological evidence of multiple tsunamigenic imprint on the Bay of Palairos-Pogonia (Akarnania, NW Greece). Quaternary International, 242(1), 213-239.

Vrebos, B., deVries, J., 2001. Quantification of Infinitely Thick Specimens by XRF Analysis, Handbook of X-Ray Spectrometry, Second Edition. Practical Spectroscopy. CRC Press.

Wachsmann, S., Dunn, R.K., Hale, J.R., Hohlfelder, R.L., Conyers, L.B., Ernenwein, E.G., Sheets, P., Blot, M.L.P., Castro, F., Davis, D., 2009. The Palaeo-Environmental Contexts of Three Possible Phoenician Anchorages in Portugal. International Journal of Nautical Archaeology, 38(2), 221-253.

Wainwright, J., 2009. Weathering, soils and slope processes. In: J.C. Woodward (Ed.), The Physical Geography of the Mediterranean. Oxford University Press, Oxford, pp. 169-202.

Walsh, K., 2008. Mediterranean Landscape Archaeology: Marginality and the Culture–Nature 'Divide'. Landscape Research, 33(5), 547-564.

Wang, X.S., 2008. Correlations between heavy metals and organic carbon extracted by dry oxidation procedure in urban roadside soils. Environmental Geology, 54(2), 269-273.

Wang, Y., Amundson, R., Trumbore, S., 1996. Radiocarbon Dating of Soil Organic Matter. Quaternary Research, 45(3), 282-288.

Watson, E.B., Pasternack, G.B., Gray, A.B., Goñi, M., Woolfolk, A.M., 2013. Particle size characterization of historic sediment deposition from a closed estuarine lagoon, Central California. Estuarine, Coastal and Shelf Science, 126, 23-33.

Werner, V., Baika, K., Fischer, P., Hadler, H., Obrocki, L., Willershäuser, T., Tzigounaki, A., Tsigkou, A., Reicherter, K., Papanikolaou, I., Emde, K., Vött, A., 2017. The sedimentary and geomorphological imprint of the AD 365 tsunami on the coasts of southwestern Crete (Greece) – Examples from Sougia and Palaiochora. Quaternary International.

Zádorová, T., Penížek, V., Šefrna, L., Rohošková, M., Borůvka, L., 2011. Spatial delineation of organic carbon-rich Colluvial soils in Chernozem regions by Terrain analysis and fuzzy classification. CATENA, 85(1), 22-33.

Zádorová, T., Penížek, V., Vašát, R., Žížala, D., Chuman, T., Vaněk, A., 2015. Colluvial soils as a soil organic carbon pool in different soil regions. Geoderma, 253–254, 122-134.

Zazo, C., Dabrio, C.J., Borja, F., Goy, J.L., Lezine, A.M., Lario, J., Polo, M.D., Hoyos, M., Boersma, J.R., 1998. Pleistocene and Holocene aeolian facies along the Huelva coast (southern Spain): climatic and neotectonic implications. Geologie en Mijnbouw, 77(3-4), 209-224.

Zazo, C., Dabrio, C.J., Goy, J.L., Lario, J., Cabero, A., Silva, P.G., Bardají, T., Mercier, N., Borja, F., Roquero, E., 2008a. The coastal archives of the last 15 ka in the Atlantic–Mediterranean Spanish linkage area: Sea level and climate changes. Quaternary International, 181(1), 72-87.

Zazo, C., Goy, J.-L., Somoza, L., Dabrio, C.-J., Belluomini, G., Improta, S., Lario, J., Bardají, T., Silva, P.-G., 1994. Holocene Sequence of Sea-Level Fluctuations in Relation to Climatic Trends in the Atlantic-Mediterranean Linkage Coast. Journal of Coastal Research, 10(4), 933-945.

Zazo, C., Mercier, N., Lario, J., Roquero, E., Goy, J.-L., Silva, P.G., Cabero, A., Borja, F., Dabrio, C.J., Bardají, T., Soler, V., García-Blázquez, A., Luque, L.d., 2008b. Palaeoenvironmental evolution of the Barbate–Trafalgar coast (Cadiz) during the last ~140 ka: Climate, sea-level interactions and tectonics. Geomorphology, 100(1–2), 212-222.

Zazo, C., Mercier, N., Silva, P.G., Dabrio, C.J., Goy, J.L., Roquero, E., Soler, V., Borja, F., Lario, J., Polo, D., de Luque, L., 2005. Landscape evolution and geodynamic controls in the Gulf of Cadiz (Huelva coast, SW Spain) during the Late Quaternary. Geomorphology, 68(3–4), 269-290.

A. Appendices

A.1 Supplementary Information on Chapter 4.1

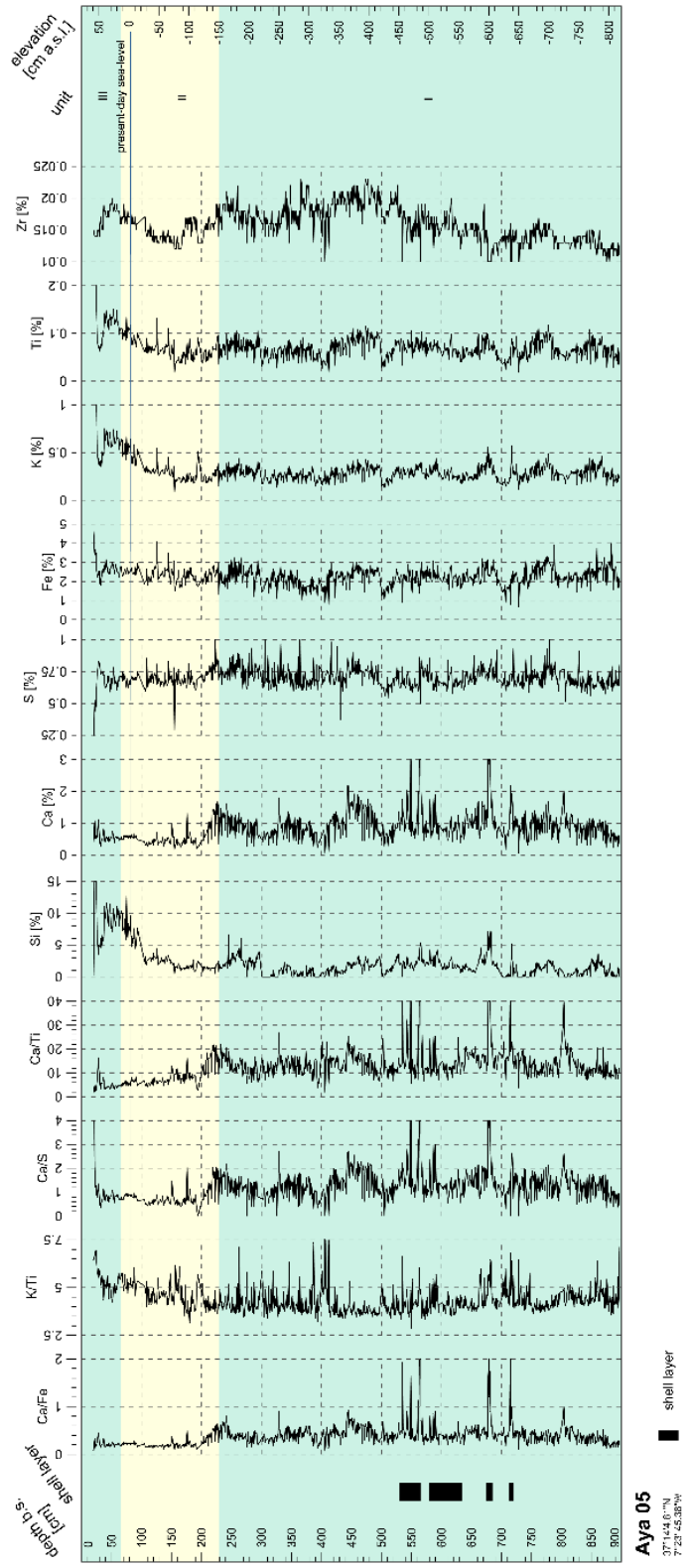

Figure A.1: Elemental composition (XRF) of sediment core Aya 05. Unit I: estuarine/lagoonal facies; Unit II: Salt-marsh facies; Unit III: soil formation and colluvial facies.

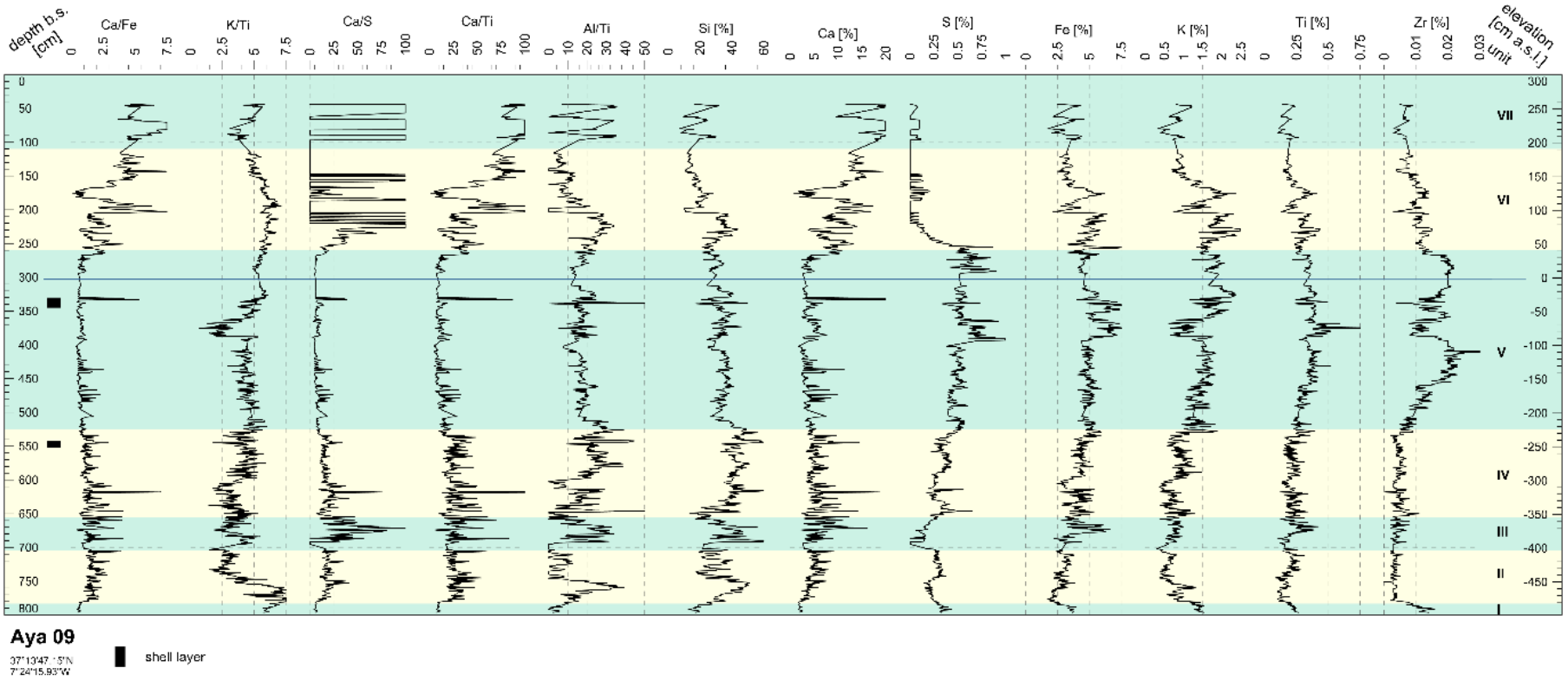

Figure A.2: Elemental composition (XRF) of sediment core Aya 09.

A.2 Supplementary Information on Chapter 4.2

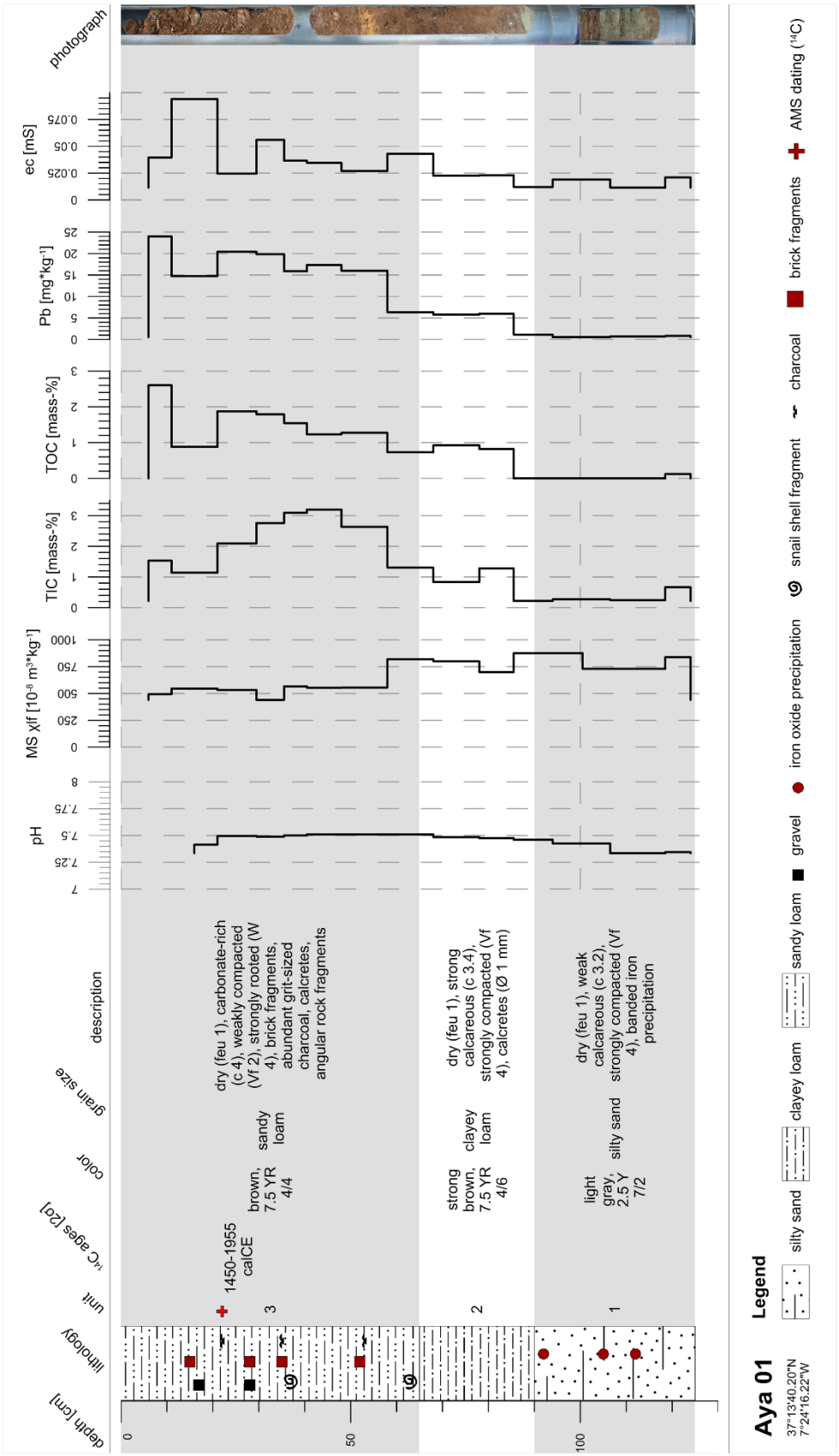

Figure A.3: Stratigraphy and geochemical parameters of sediment core Aya 01.

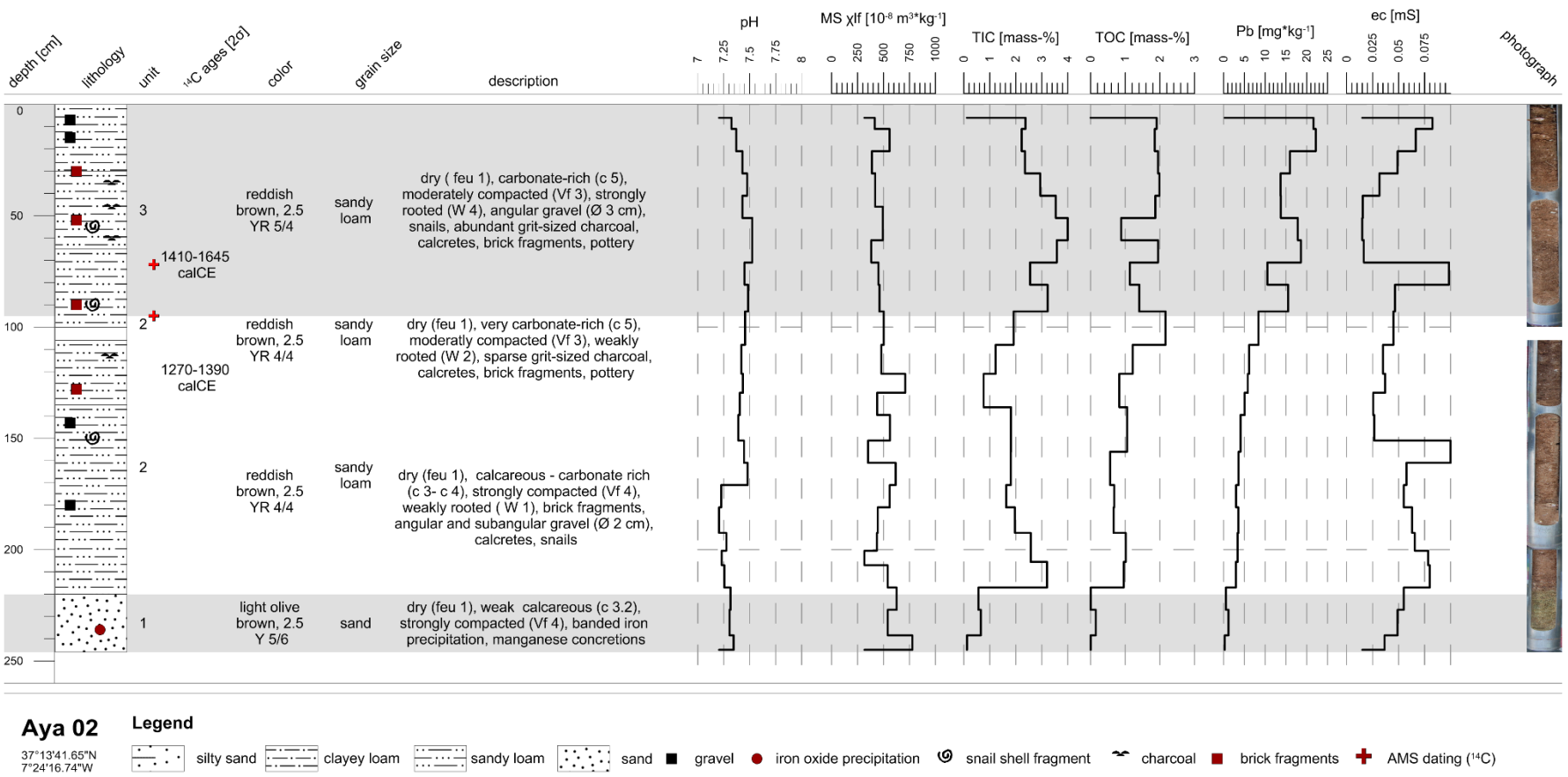

Figure A.4: Stratigraphy and geochemical parameters of sediment core Aya 02.

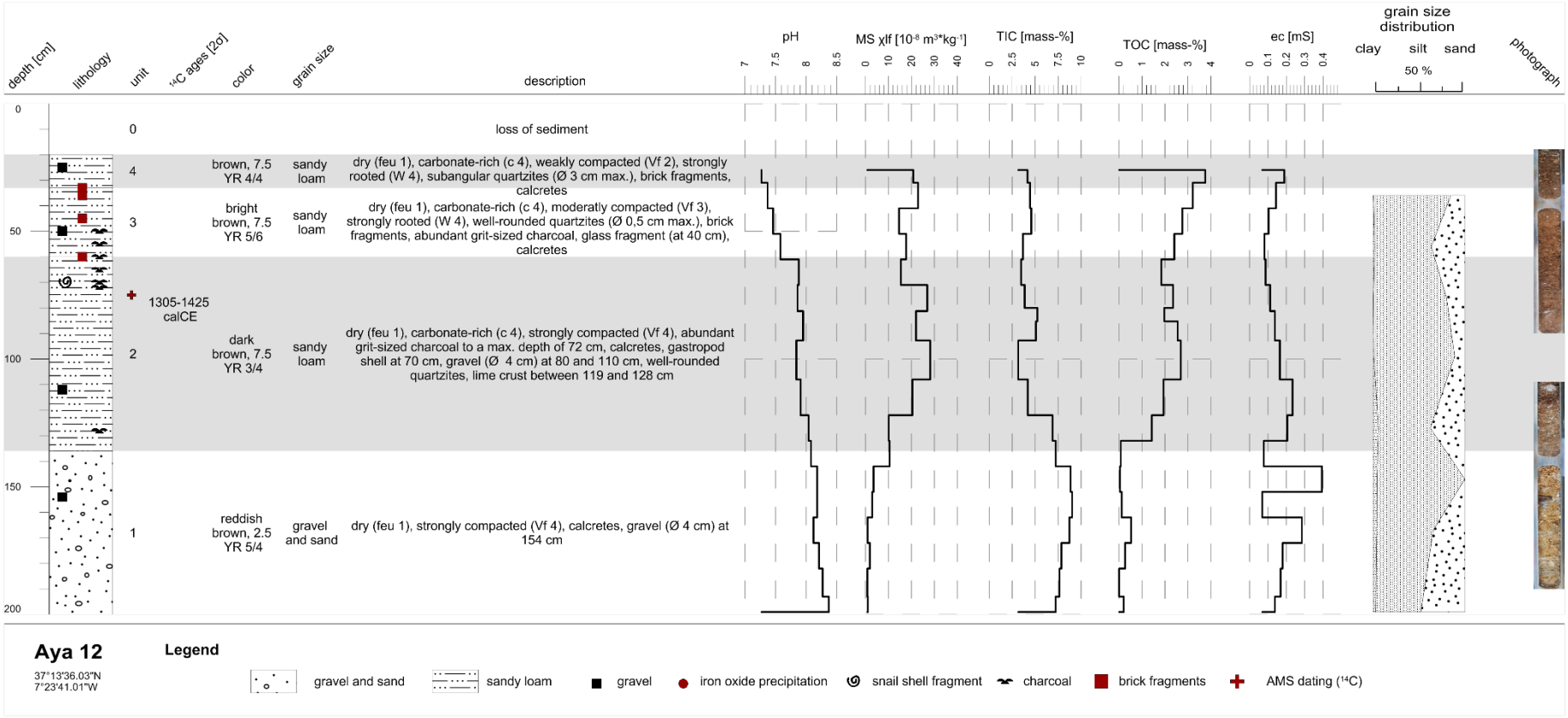

Figure A.5: Stratigraphy and geochemical parameters of sediment core Aya 12.

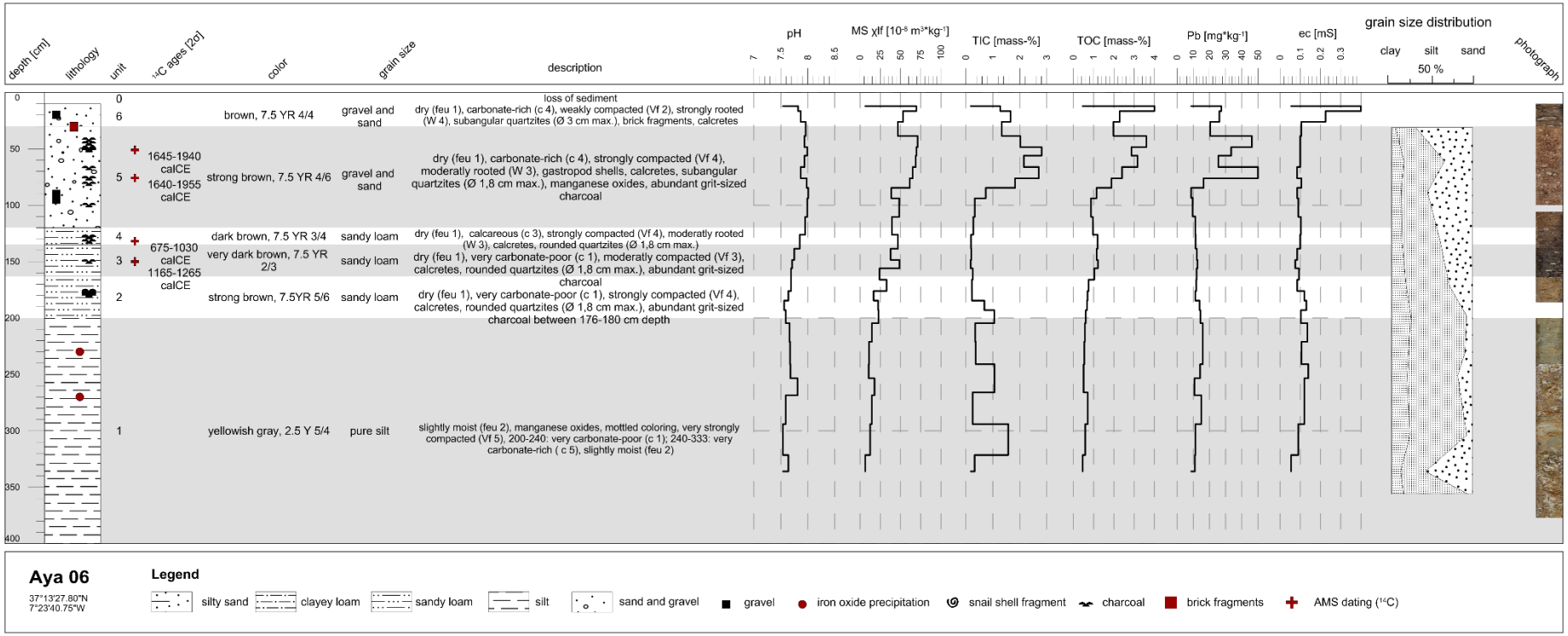

Figure A.6: Stratigraphy and geochemical parameters of sediment core Aya 06.

A.3 Supplementary Information on Chapter 4.3

Table A.1: Drilling characteristics of drilling cores Aya 14 and Aya 15.

Drilling Core	Latitude	Longitude	Elevation [m]	Drilling Depth [m]	Drilling Character
Aya 14	37°13'11.28" N	7°22'20" W	3.6	4.0	closed tube
Aya 15	37° 13' 10.02" N	7° 22' 20.24" W	2.3	5.0	closed tube

Table A.2: Resolutions of the investigated orthophotos.

Year	Resolution [m]
1956	1.32
1998	1.32
2001	0.66
2004	1.32
2007	1.32
2009	0.66
2010	0.66

Table A.3: List of historical maps reviewed in this study.

n	Map Title	Author/Publisher	Year
1	Hispalensis Conventus Deline Atio	Hieronÿmo Chiaues	1579
2	Mapa de Andaluzia	Jodocus Hondius	1606
3	Andaluzia	Petrus Bertius	1618
4	Andaluzia	Petrus Kerius Caelavit	1632

5	Barra del Rio Guadiana	Atlas del Rey Planeta	1634
6	Andaluzia Nova Descript	Jodocus Hondius	1640
7	Plano de la costa del reino del Algarbe en Portugal	unknown	1642
8	Una Carta del mare Oceano, che Comincia con il Capo S. Vincenzio in Portogallo, e Finisce con Io stretto di Gibilterra	Robert Dudley	1661
9	Puerto de Tavila. Discursos y advertencias de la costa de Portugal y de todos puertos, desde Bayona hasta Ayamonte	Acuña y Andrada, Antonio de	1661
10	Andaluzia continens Sevillam et Cordubam	Willem Janszoon Blaeu	1688
11	Castillo de Ayamonte	unknown	1739
12	Plano del Castillo de Ayamonte con su Proyecto	unknown	1741
13	Mapa de la Frontera de Portugal pertenecyente al Condadode Nyebla y Syerra en el Reyno del Andalucya	unknown	1745
14	Terra e costas de Portugal	Llobet, D.F.	1748
15	Puerto de Ayamonte. Plano de Ayamonte con el río Guadiana separando las tierras de Portugal	unknown	1752
16	Plano de Ayamonte con el proyecto de un Fuerte	unknown	1755
17	Plano de la Plaza de Ayamonte la Ciudad situada al margen del Rio Guadiana y segun el Padre Riuicciolio	unknown	1756
18	Plano de la barra y puerto de la ciudad de Ayamonte que divide los reinos de España y Portugal	unknown	1764
19	Plano de parte de la costa y limites de esta Provincia de Andalucia	Antonio de Gaver	1765
20	Mapa de la Costa y territorio desde el río Guadiana hasta la barra del Terrón del río de Piedras	Antonio Hurtado	1776

21	Plano del Proyecto de la pequeña fortaleza que se propone executar en el parage en el que existe el Castillo arrinado de Ayamonte por la poca vtilidad y mucho gasto q[u]e causaría la reedificaz[io]n del antiguo	Antonio Hurtado	1776
22	Carta militar offerecida a S. A. R. o Principe Regente Nosso Senhor, a qual compreende [o] acampamento das tropas nas alturas de S. Bartolomeo e o combate victorioso que tiverão as nossas batarias no Guadiana	unknown	1801
23	Croquis topográfico de Ayamonte	Antonio Ramón del Valle Ayte	1811
24	Plano de la Isla de la Canela y sus inmediaciones	Capitán con José Ibáñez	1811
25	croquis de la parte de frontera de portugal, comprensiva desde del Guadiana	unknown	1827
26	Plano que representa la posicion del islote Cabezo alto a la boca del Rio Guadiana, situado por medio de las marcaciones siguentes	Manuel de Layas Rivero	1839
27	Plano de la desembocadura del río Guadiana, con los fondeaderos de Ayamonte, Villa Real e Isla Cristina	Saturnino Montojo y Antonio Martínez	1840
28	Provincias de Sevilla y Huelva	R. Alabern y E. Mabon	1853
29	unknown (Map no. 1988000003)	unknown	1861
30	Plano de la barra y fondeadero de Isla Cristina	unknown	1862
31	Huelva	D. Francisco Coello	1870
32	Golfo de Huelva	Dirección de Hidrografia	1873
33	Nuevo Mapa Geografico Estadistico de la Provincia de Huelva	D. José Carrasco Padilla	1892

34	Provincia de Huelva	Instituto Geográfico	1936
35	Isla Cristina	Cartografica Militar de Espana	1943

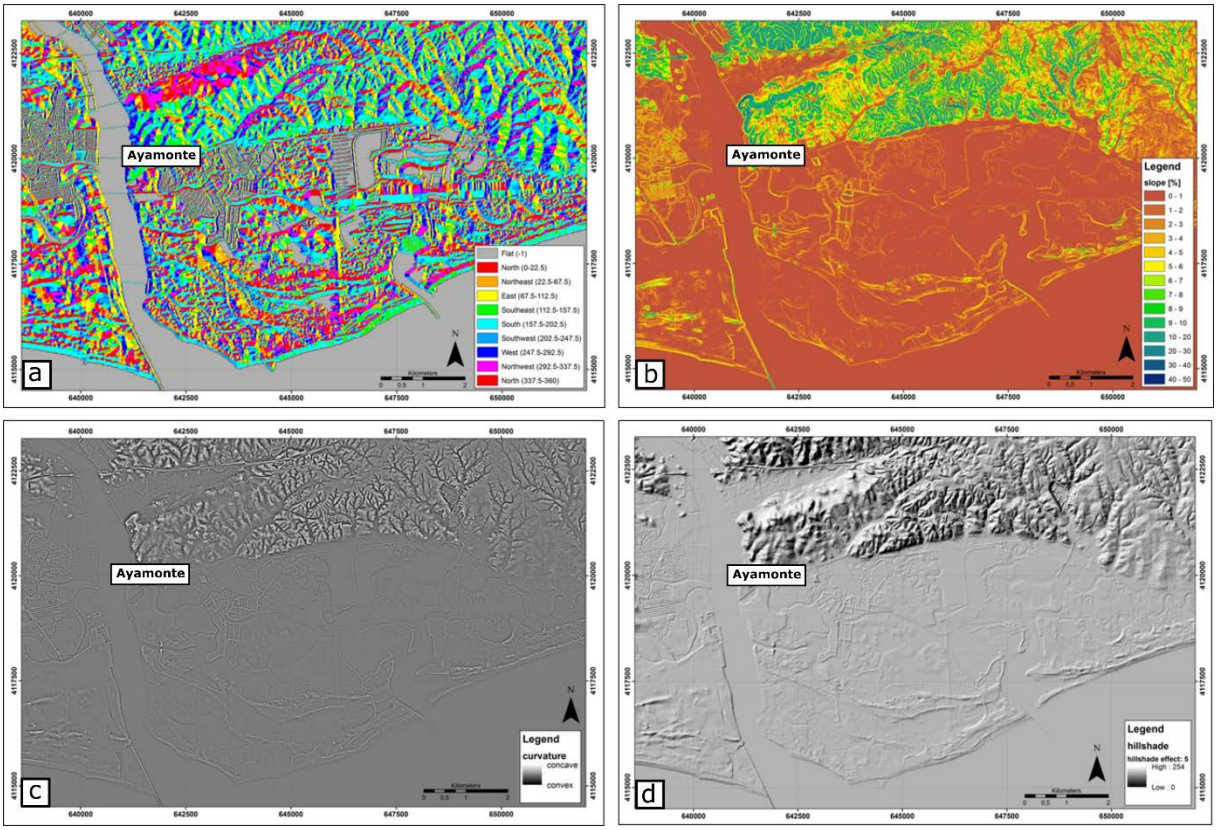

Figure A.7: Maps of the surface analyses, based on the DEM (5 m x 5 m resolution); a) aspect map; b) curvature map; c) slope map; d) hillshade map, displayed with a hillshade effect of 5. (Author: Sarah Ißelhorst).

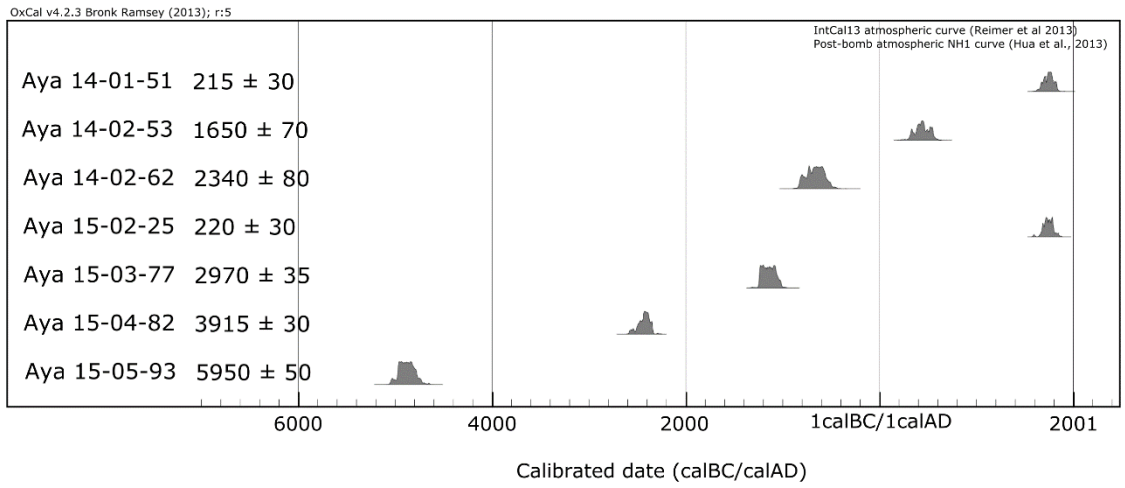

Figure A.4: Age model of the sediments from Aya 14 and Aya 15.

B. Curriculum vitae

For reasons of data protection, the curriculum vitae is not included in the online version.